COMMITTEE CERTIFICATION OF APPROVED VERSION

The committee for Brad Allen Patrick certifies that this is the approved version of the following dissertation:

THE ROLE OF 4-HYDROXYNONENAL IN CELLULAR

SIGNALING MECHANISMS

Committee:

_____
Yogesh C. Awasthi, Ph.D., Supervisor

_____
Piotr Zimniak, Ph.D.

_____
Naseem Ansari, Ph.D.

_____
Cornelis Elferink, Ph.D.

_____
Xiaodong Cheng, Ph.D.

_____
Dean, Graduate School

THE ROLE OF 4-HYDROXYNONENAL IN CELLULAR SIGNALING MECHANISMS

by

Brad Allen Patrick, B.S.

Dissertation

**Presented to the Faculty of The University of Texas Graduate School of
Biomedical Sciences at Galveston
in Partial Fulfillment of the Requirements
for the Degree of**

## Doctor of Philosophy

Approved by the Supervisory Committee

Yogesh C. Awasthi, Ph.D, Chair
Piotr Zimniak, Ph.D.
Naseem Ansari, Ph.D.
Cornelis Elferink, Ph.D.
Xiaodong Cheng, Ph.D.

University of Texas Medical Branch

May 2007

Key words: glutathione s-transferase, lipid peroxidation, cell cycle, signal transduction

To My Father

ACKNOWLEDGEMENTS

THE ROLE OF 4-HYDROXYNONENAL
IN CELLULAR SIGNALING MECHANISMS

Publication No._____

Brad Allen Patrick, Ph.D.
The University of Texas Medical Branch, 2007

Supervisor: Yogesh C. Awasthi

One of the critical steps involved in cellular oxidative stress is the peroxidation of membrane lipids. The downstream effects of the autocatalytic lipid peroxidation (LPO) cycle are widespread and involve several processes. Using lens epithelial cells (HLE B-3) and retinal pigment epithelial cells (RPE28 SV4) as models, in proposed studies we addressed the hypothesis that a physiological level of LPO product 4-hydroxynonenal (HNE) is necessary for maintaining key proliferation, adhesion, and survival signaling by regulating expression of genes involved in these pathways, and that alteration of that level either up or down will result in induction of genes pro-apoptotic or pro-carcinogenic signaling pathways, respectively.

After stable transfection of *hGSTA4* in HLE B-3, cells underwent a morphological transformation becoming smaller and rounded, and lost anchorage dependence. Additionally they were observed to divide much more rapidly and acquired resistance to apoptosis via oxidative stress. In an attempt to provide a mechanistic explanation for this phenotypic set of changes, cells were assayed for changes in expression for a wide set of genes via gene microarray studies. Results showed that over 6900 genes were strongly modulated in *hGSTA4*-transformed cells compared to controls. This prompted further verification in a subset of well-known and important genes involved in cell cycle control, survival, and cell adhesion via quantitative RT-PCR and Western blot studies. In these cells, considerably lower levels of transcription and translation of key genes regulating those affected processes were observed.

Further exploration of HLE B-3 showed that expression of Fas correlated with HNE concentration, an observation found both before and after HNE treatment. This is strengthened by observations that transiently-transfected HLE B-3 overexpress *hGSTA4* along with a depletion of intracellular HNE and depletion of Fas expression and further strengthened in a mouse *mGSTA4* knockout model with high steady-state HNE tissue levels, where Fas expression is found to be elevated in several tissues above WT. Together these studies implicate HNE as an important mediator of expression of several key genes responsible for processes underlying cell cycle regulation, survival, and adhesion, and lay a foundation upon which further investigation can be performed.

TABLE OF CONTENTS

LIST OF TABLES

LIST OF FIGURES

LIST OF ABBREVIATIONS

9-LOOH   9-hydroperoxy linoleic acid

13-LOOH   13-hydroperoxy linoleic acid

ARE   antioxidant response element

BHT   butylated hydroxytoluene

CAT   catalase

CBA   chain breaking antioxidants

CDNB   1-chloro-2,4-dintrobenzene

CU-OOH   cumene hydroperoxide

FA-OOH   fatty acid hydroperoxides

GPx   glutathione peroxidase

GR   glutathione reductase

GSH   glutathione

GST   glutathione S-transferase

hGSTA4-4   human GST A4-4

HLE B-3   human lens epithelial cell line B-3

HNE   4-hydroxynonenal

HPETE   hydroperoxyeicosatetraenoic acid

LOOH   lipid hydroperoxides

LPO   lipid peroxidation

MAPK	mitogen activated protein kinase
MDA	Malondialdehyde
MTT	3-(4,5-dimethylthiazol-2-yl)-2,5-diphenyltetrazolium bromide
ox-LDL	oxidized low-density lipoprotein
PAGE	polyacrylamide gel electrophoresis
PARP	poly(ADP-ribose) polymerase
PBS	phosphate buffered saline
PC-OOH	dilinoleoyl phosphatidylcholine hydroperoxide
PCR	polymerase chain reaction
PE-OOH	dilinoleoyl phosphatidylethanolamine Hydroperoxide
PL-OOH	phospholipid hydroperoxides
PMSF	phenylmethylsulfonyl fluoride
ROS	reactive oxygen species
RPE	retinal pigmented epithelium
SOD	superoxide dismutase

CHAPTER I – Introduction

Background:

  Aerobic organisms are those which have adapted to use oxygen within their systems, as an electron donor for their respiratory and metabolic processes. Because of this, these organisms require means to cope with and counteract the inherent toxic nature of oxygen to attack biological molecules, causing what is generally referred to as oxidative stress. Oxidative stress is one of many types of biological stresses which influence the physiology and pathophysiology of cells. It is characterized by chemical attack of biological systems by reactive oxygen species (ROS), some of which are strong oxidants capable of wrenching electrons from stable compounds, thereby converting them into unstable intermediates (often radicals) and continuing the chain-reaction of 'electron theft', producing toxic species throughout the cell [2].

  Reactive oxygen species are normally found throughout the cellular environment. However, under normal conditions these molecules pose little danger to the cell in terms of toxicity, because cells have adapted various means to detoxify ROS and negate their harmful effects on cellular processes. These detoxification mechanisms consist both of enzymes such as superoxide dismutase, catalase, glutathione peroxidases, glutathione s-transferases, aldose reductase, aldehyde dehydrogenase, thioredoxin, and metallothioneines [3, 4], and also non-enzymatic molecules such as glutathione, ascorbate, tocopherols, urate, cholesterols, and n-acetylcysteine [5].

  Formation of ROS: Examples of ROS include superoxide anion, hydrogen peroxide, singlet oxygen, hydroxyl radical, and peroxynitrite, which is often additionally referred to as a reactive nitrogen species (RNS). The formation of ROS is a multi-step process which occurs throughout tissues in a largely uncontrolled and constitutive manner. Superoxide anion (O_2^-) is formed as a precursor ROS molecule via many

different processes. Superoxide is the progenitor ROS which is metabolized to form the other ROS, and begins the cascade of oxidative stress **(figure 1)**. Via superoxide dismutase (SOD), superoxide is reduced to hydrogen peroxide (H_2O_2), which is much less reactive with biological tissues. Two molecules of H_2O_2 in turn are reduced by catalase (CAT) to form two molecules of water and one of O_2. However, H_2O_2 can escape this detoxification and cycle through the Fenton reaction with ferrous iron, producing a molecule of free hydroxyl anion (-OH) and one of hydroxyl radical ($\cdot$OH) [6]; this cycling reaction also 'recharges' superoxide anion by adding a single electron via ferric iron. Singlet oxygen, a nonradical high-energy state of O_2 produced by both photooxidation and the microsomal NADPH oxidase system [7], is capable of peroxidizing unsaturated phospholipids to form LOOH [8]. In addiditon to oxygen-bearing species, there exist nitrogen-containing compounds which react strongly with intracellular biomolecules. Peroxynitrite (ONOO-) and nitric oxide (NO$\cdot$) are important chemically reactve oxygen-bearing species which interact with ROS and biomolecules during stress. ONOO- is believed to be formed by a reaction between two other ROS, O_2^- and NO$\cdot$.
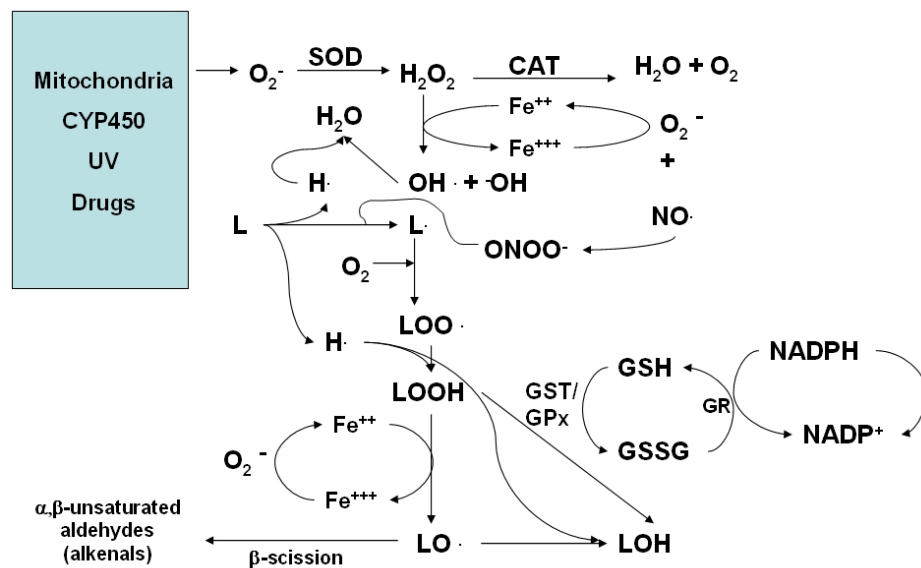
Figure 1: Lipid peroxidation cascade and integration of antioxidant enzymes. Adapted from [9].

Sources of ROS: Sources of ROS can be found both within and outside the cell. Endogenous sources include the mitochondrial oxidative phosphorylation machinery, nitric oxide synthase system, the inflammatory process caused by phagocytosis, and several redox reaction-catalyzing enzymes such as 5-lipoxygenase, cyclooxygenase, xanthine oxidase, and cytochromes P450 [5]. Exogenous sources include various electrophilic xenobiotics, anti-cancer drugs such as doxorubicin and cisplatin, exposure to radiation including blue and ultraviolet light, heat shock, hyperoxia, hyperglycemia, ischemia-reperfusion, etc.

Cytochrome P450: The cytochromes P450 (CYP450) are a large superfamily of membrane-bound Phase I biotransformation enzymes which catalyze a wide variety of reactions, involving both endogenous and exogenous compounds and including the addition, removal, and exposure of small functional groups via numerous reactions (full and stepwise oxidation, reduction, desaturation, aldehyde scission, etc.) [10]. Several isoforms of CYP450 are involved with the microsomal monooxygenase system (MMO), which is active in most animal tissues [11]. This system uses NADPH (and to a lesser extent, cytochrome b5 reductase) as a cofactor to transfer electrons to substrates. However, this electron donor can easily be consumed in the absence of substrates or release its electrons to molecules other than the intended substrate, causing what is known as futile cycling. This cycling causes an uncoupling between electron donation and substrate oxidation reactions, with the degree of such uncoupling averaging higher than 50% [11-13] with various substrates and even as high as 99.5% [14]. This uncoupling allows the constant release of ROS, notably O_2^- but also H_2O_2, into the cell [15, 16], making CYP450 electron leakage a significant source of ROS in many tissues.

Inflammation: Inflammation within the course of natural immune response to foreign bodies within tissue is caused, in part, by massive neutrophil release from bone marrow and migration to infected or injured sites. These neutrophils, along with macrophages found throughout tissues, are phagocytic and engulf any 'non-self' matter that is present. They also release large amounts of superoxide anion via NADPH oxidase (via the reaction of $NADPH + 2e^- + CO_2 \rightarrow NADP^+ + H^+ + 2O_2^-$) and, in the case of neutrophils, hypochlorite anion via myeloperoxidase (with the reaction of $H_2O_2 + Cl^- \rightarrow HOCl + OH^-$; $HOCl \rightarrow H^+ + OCl^-$) as cytotoxic and bacteriotoxic defense mechanisms. Cyclooxygenase (COX) enzymes are capable of producing pro-inflammatory prostaglandins, and their direct contribution to oxidative stress is through the production of O_2^- as a by-product of their conversion of arachidonic acid (AA) to prostaglandins G_2 (PGG_2) and H_2 (PGH_2) (via the reaction of $AA + 2O_2 \rightarrow PGG_2$) [17]. Prolonged inflammation allows for repeated and continuous bombardment with these ROS, thereby increasing oxidative stress on the organism.

Electron transport chain: Electron leakage in the mitochondrial electron transport chain is a continual and unavoidable process whereby electrons traveling along the several steps involved in releasing energy bypass the electron-collecting ubiquinone antioxidants and directly reduce nearby O_2 molecules, forming O_2^- [18]. This process is spontaneous and does not require enzymatic catalysis, and thereby is uncontrolled within all aerobic metabolically active cells, causing a ROS release from approximately 2% of oxygen molecules [19], although quantitation of relative values of uncoupling is not entirely certain and although the value likely fluctuates between species and tissues, the amount is undoubtedly low but biologically significant.

Nitric oxide synthase: Nitric oxide (NO) is a vasodilatory small signaling molecule which is produced by two isoforms of nitric oxide synthase (NOS), endothelial NOS (eNOS) and inducible NOS (iNOS). These enzymes convert O_2 and

4

arginine to citrulline and NO via two successive monooxygenation reactions with a *N*-hydroxylarginine intermediate (via the reaction of L-arginine + 1.5 NADPH + 2 O_2 → L-citrulline + 1.5 $NADP^+$ + 2 NO) where it diffuses into tissues [20]. Like CYP450, eNOS activity can be uncoupled and thereby become a source of ROS [21]. This uncoupling causes the release of superoxide anion in times of oxidative stress due to peroxynitrite (ONOO-) uncoupling [22]. This uncoupling-related ROS release has been associated with lipid peroxidation *in vivo* [23].

Other oxidases as sources of ROS: There several oxidases, such as 5-lipoxygenase and xanthine oxidase, which have disparate biological functions but chemically are similar in that they serve to combine oxygen with various endogenous or exogenous substrates, and as a side-effect release ROS into the cell. 5-lipoxygenase acts in the arachidonic acid (AA) pathway to convert AA first to 5-hydroperoxyeicosatetraenoic acid (5-HPETE) and then to hydrolyse 5-HPETE to leukotriene A_4 (LTA_4), with a concomitant release of water [24]. In the xanthine oxidase pathway, xanthine is converted to hypoxanthine with accompanying activation of water to H_2O_2 or to O_2^- and similarly, hypoxanthine is converted to uric acid with accompanying activation of water to H_2O_2 or to O_2^- [25].

Exogenous sources of ROS: The environment is rich with sources of oxidative stress, as is the variety of drugs used to treat diseases. It has been shown that exposure to blue light [26] is sufficient to cause ROS production in tissues including retinal pigment epithelium. Ultraviolet (UV) light in the UVA range (320-400 nm range) is likewise able to cause oxidative stress in cells, as has been shown in our and other laboratories [27, 28]. Exposure to ionizing radiation either during cancer therapy or during nuclear accidents also leads to the formation of ROS. Ionizing radiation such as X-rays and gamma rays cause oxidative stress and subsequent cell death in several cell types [29, 30] including RPE [31] due to decomposition of water into several ROS [32, 33]. Exposure to high

concentrations of sugar can elicit a response similar to that seen with HNE exposure caused by ROS-induced LPO [34] in eye lenses, assumedly due to xanthine oxidase. Both hyperoxic [35, 36] and hypoxic [37, 38] environments are capable of causing oxidative stress, and transient heat shock of 42°C, merely a 5 degree increase in temperature [27] leads to ROS-induced LPO. Heavy metals such as cadmium, lead, arsenic, and mercury [39] are potent stimulators of ROS generation through depletion of thiol-bearing cellular constituents and the members of the antioxidant pool, thereby increasing LPO [40]. Several xenobiotics are capable of producing ROS in the body via metabolism and due to their ubiquitous nature in the environment these xenobiotics comprise a major exogenous source of ROS. For instance, benzo[a]pyrene, a commonly-found chemical present in auto exhaust, smoke, and industrial waste around the world, can be metabolized to several quinone intermediates which through redox cycling are capable of O_2^- production [41]. Benzene, another aromatic chemical used in industrial processes, is oxidized to a series of hydroquinone/semiquinone radical anion metabolites which at several steps produce superoxide anions [42]. Prescribed and non-prescribed drugs are a class of xenobiotics whose metabolites are capable of producing large amounts of ROS, many of whom are bioactivated by Phase I enzymes such as cytochrome P450s and alcohol dehydrogenase. Ethanol metabolism causes ROS production via both sequestering of NAD^+ and upregulation of CYP2E1 [43]. The anticonvulsant valproic acid is capable of producing ROS through an unknown mechanism [44], as is phenytoin [45]. Acetaminophen is a well-cited example of a widely-used non-prescribed drug capable of production of devastating amounts of ROS [46]. Drugs of abuse, such as cocaine [47], heroin [48], and 3,4-methylenedioxymethamphetamine (MDMA) [49] show evidence of ROS production accompanying or leading to toxicity. Some chemotherapeutic anti-cancer drugs, such as doxorubicin [50] and cisplatin [51] are shown to cause oxidative stress *in vivo*, probably due mostly to Fenton cycling via free ferrous iron (Fe^{2+}) [52], and this is one likely manner in which these drugs are able to cause apoptotic pressure on cancer cells.

Oxidative stress and lipid peroxidation: While ROS can and do affect proteins, lipids, and DNA by themselves without intermediates, the most important manner in which these molecules cause downstream chemical stress upon cells is through lipid peroxidation (LPO). LPO is an amplification process which is driven by oxidative stress and is capable of self-propagation due to the reactivity of the intermediates formed through the cascade. Membrane phospholipids and free fatty acids are attacked by hydroxyl radicals ($^.$OH) and depleted of a single electron. The lipid molecule goes through an electron-shifting stabilization which leaves a lipid radical centered at an aliphatic carbon **(figure 2)**. This lipid radical reacts with molecular oxygen (O_2) to form a lipid peroxy radical (LOO$^.$) with the unpaired electron shifting from the carbon to the terminal oxygen atom, and this peroxyl radical is quickly reduced to a lipid hydroperoxide (LOOH) molecule. While hydroperoxides are less reactive in comparison to other LPO products, they are subject to Fenton reaction cleavage in the presence of ferrous iron (Fe^{2+}), producing hydroxyl and alkoxyl radicals with much higher reactivity. As another set of $^.$OH molecules are formed, this cycle repeats indefinitely in an autocatalytic manner consuming new lipid molecules until some chain-breaking event occurs to end the process at this level. The LPO products formed at this stage are subject to a β-scission reaction which forms alkane radicals and α,β-unsaturated alkenals [53]. There are a number of such alkenals produced by spontaneous LPO β-scission such as hexenal [54], with an especially well-characterized class being 4-hydroxyalkenals. However, from a molecular toxicological standpoint, the most abundant of these 4-hydroxyalkenals is 4-hydroxy-2-*trans*-nonenal (HNE) [55].
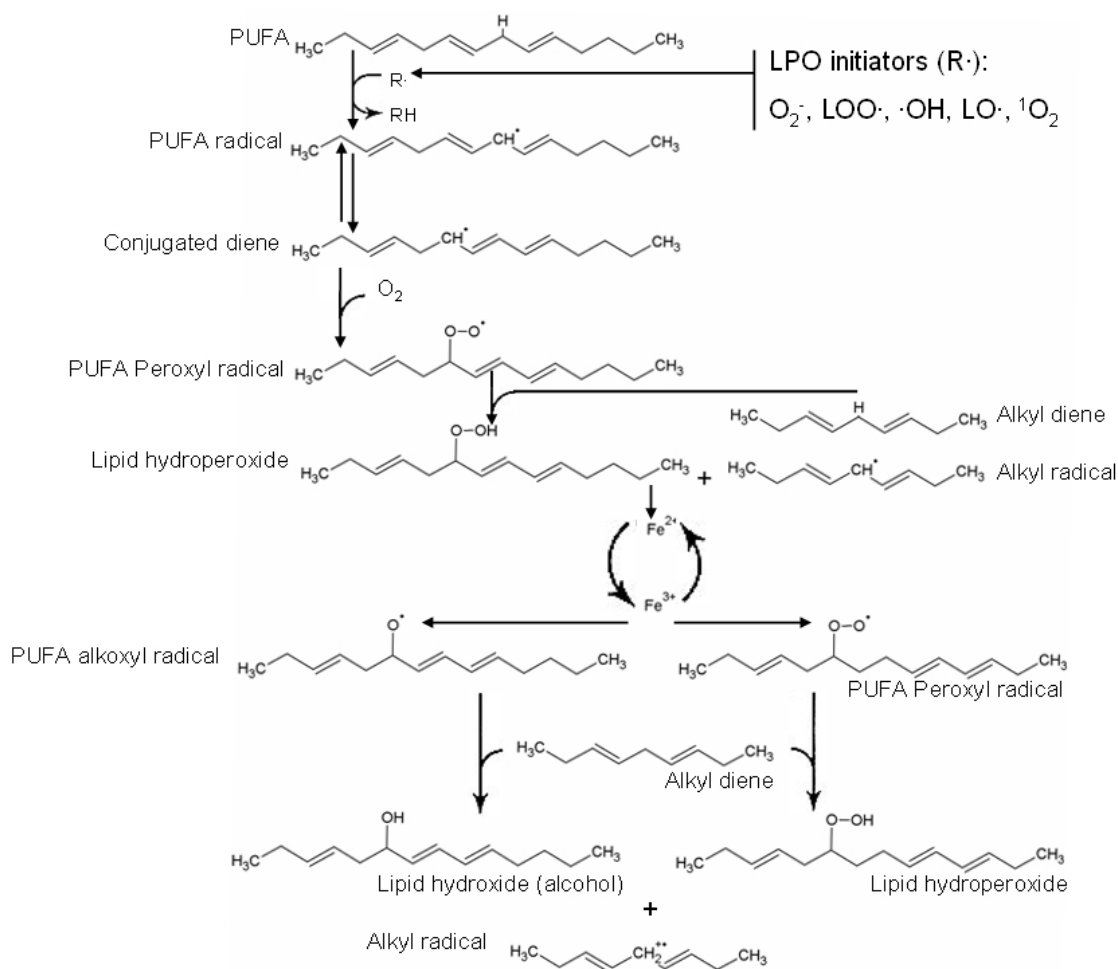
Figure 2: Propagation of lipid peroxidation. Membrane PUFA are attacked by LPO-initiating ROS which abstract an electron to leave PUFA radicals. These radicals undergo rearrangement to form conjugated dienes, which are then attacked by molecular oxygen to form peroxyl radicals. Peroxyl radicals can themselves abstract electrons from alkenes to become hydroperoxides and form alkyl radicals. Hydroperoxides are substrates of the Fenton reaction which can form either alkoxyl or peroxyl radicals, both of which electrophilically attack alkyl dienes to abstract electrons. In this last step it becomes apparent how lipid hydroperoxides act to cause continuous oxidative attack of biomolecules. For simplicity, only alkane portions of PUFA and lipids are shown.

Formation of 4-hydroxynonenal: As discussed in detail previously in this section, HNE is produced in the cell via a multi-step cascade beginning with the lipid

8

parent molecules. Membrane lipids such as phosphatidylethanolamine and phosphatidylserine exist normally at the cell surface. ROS attack at this site, either via UV light, superoxide anion, etc. and cause a carbon-centered lipid radical (L˙) to form via hydrogen abstraction (**figure 1**). If electronically rearranged to the more energetically-stable conjugated diene form, this is immediately peroxidized by molecular oxygen (O_2) to form lipid hydroperoxides (LOOH) [53, 56]. LOOH molecules are capable of serving as substrates in a Fenton reaction catalyzed by ferrous iron (Fe^{2+}), producing lipid alkoxy (alcohol) radicals (LO˙), which then undergo β-scission to form ethane and pentane radicals and unsaturated aldehydes, such as HNE and 4-hydroxhexenal [9]. HNE is formed from polyunsaturated fatty acid (PUFA) constituents of these LO˙ molecules, such as 18:2 and 20:4 [53], and mechanisms published regarding HNE formation indicate that only ω-6 PUFAs are capable of HNE formation [57]. In line with this finding, there have been published two additional pathways of HNE formation from 9-hydroxylinoleic acid and 13-hydroperoxylinoleic acid [58]. However, the final product in these pathways is 4-hydroperoxynonenal and the physiological relevance of these pathways is not clear given the finding that 15-hydroperoxylinoleic acid is not a physiologically relevant HNE-forming intermediate [59] as it is not a ω-6 PUFA. In addition to the auto-catalytic pathway, HNE can also be formed in cells via enzyme-catalyzed mechanism involving liver mixed-function oxidase system which can carve 4-hydroxyhexenal from a large tricyclic alkaloid senecionine [60], although given normal concentrations of these alkaloids it is unlikely to be physiologically relevant. There are several chemical species which induce formation of HNE and other reactive aldehydes. These include halogenated hydrocarbons [61], ferric iron [53], anticancer drugs [62], ethanol [63], among others and this induction, along with the uncontrolled natural formation due to background oxidative stress on cells, ensures that HNE formation is a constant and variable process depending on cell physiology.

Cellular defenses against LPO: Since ROS production is a continuous and largely uncontrolled processes in aerobic organisms, survival must depend on the ability of cells to decrease LPO and detoxify LPO products. Cells have two means of action at their disposal for this task: one involving enzymatic mechanisms and one involving non-enzymatic mechanisms.

Non-enzymatic mechanisms of defense: In addition to enzyme-driven defenses against ROS production and subsequent LPO, non-enzyme antioxidants are present within the cell to serve as reductants for these electrophilic molecules. In this list are included ascorbic acid, glutathione, uric acid, various polyphenols, ubiquinone, and α-tocopherol [64]. Ascorbic acid, otherwise known as vitamin C, is a highly-hydrophilic small molecule (MW 176.12) chain-breaking antioxidant which is found in cytosol. Ascorbic acid is capable of safely donating electrons to ROS due to stability of the oxidized form, dehydroascorbate [65], and therefore serves as a common antioxidant molecule. α-Tocopherol, also known as vitamin E, is a hydrophobic antioxidant likewise present in cells and is able to trap radicals due to stabilization of it benzoquinone ring [66]. Glutathione is a hydrophilic small peptide molecule (MW 307.3) which is highly abundant in cytosol, mostly in reduced form (GSH). GSH is produced constitutively by two enzymes, glutathione synthetase (GS) and the rate-limiting enzyme in the pathway, glutamate cysteine ligase (GCL) [67]. The concentrations of GSH vary from organ to organ, with primarily detoxifying organs such as liver and kidney bearing much more than other organs such as lung. Uric acid, a water-soluble antioxidant formed from guanine, has significant ability to react with and neutralize superoxide, hydroxyl radical, and peroxynitrite [68, 69]. Ubiquinone is a powerful lipophilic antioxidant in the electron transport chain capable of regenerating other antioxidants such as ascorbate and tocopherol, as well as directly reducing lipid radicals [70]. Polyphenols, a group of several classes of dietary molecules including curcumin, resveratrol, and tannins bearing multiple phenolic groups, are increasingly well-characterized quenchers of peroxyl

10

radicals and have been shown to protect against ROS-mediated LDL oxidation [71] and HNE-induced lens opacification [72], which may be via induction of GST. Glutathione is capable of measurable non-enzymatic reduction and conjugation reactions due its high abundance as the most abundant sulfhydryl-bearing molecule in the cell, between $500\mu M$-10mM [73]. However, the primary mode of the antioxidant action of GSH is through its role as a co-factor in GPx- and GST-mediated reactions.

Enzymatic mechanisms of defense: There are several enzymes whose primary function in cellular physiology is to prevent LPO and/or to detoxify those LPO products either at the level of lipid peroxidation or upstream at the level of ROS conversion. Examples of these enzymes are superoxide dismutase (SOD), catalase, glutathione peroxidase (GPx), glutathione S-transferase (GST), glutamate cysteine ligase (GCL), glutathione reductase (GR), glucose-6-phosphate dehydrogenase (G6PD), thioredoxins (Trx), peroxiredoxin (Prx), and aldose reductase (AR). Superoxide dismutases (EC 1.15.1.1) are found in both cytosol and mitochondria and act at the top of the ROS cascade, converting superoxide ($O_2.-$) to hydrogen peroxide (H_2O_2) and water through a copper/zinc- or manganese-coordinated enzymatic mechanism [74]. Catalase (EC 1.11.1.6) is an iron-centered enzyme which catalyzes the decomposition of hydrogen peroxide to water and molecular oxygen (O_2), thereby detoxifying H_2O_2 [75]. Glutathione peroxidases (EC 1.11.1.9) are a family of selenium-dependent cytosolic and membrane-associated enzymes which serve to reduce both hydrogen peroxide and organic hydroperoxides such as fatty-acid hydroperoxide (FA-OOH) and phospholipid hydroperoxide (PL-OOH) to their corresponding alcohol forms by using GSH as a cosubstrate (reducing agent). At least four members of this family are present in humans. Besides these enzymes glutathione reductase (GR) (EC 1.8.1.7) and glucose-6-phosphate dehydrogenase (G6PD) (EC 1.1.1.49) also play important roles in the detoxification of ROS. GR catalyzes NADPH-dependent reduction of oxidized glutathione (GSSG) formed from GSH during the reduction of hydroperoxides [76]. This recycling of GSSG

11

to GSH is important for maintaining pools of GSH and redox status during oxidative stress. NADPH required for the reduction of GSSG by GR is generated by G6PD in the pentose phosphate shunt [77]. The thioredoxin system (TRx) (EC 1.8.1.9) is capable of directly donating hydrogens to reduce ROS and can regenerate several other antioxidants [78]. Peroxiredoxin (Prx) (EC 1.11.1.15) is capable of reducing peroxides in the presence of Trx system [79]. Aldose reductase (AR) (EC 1.1.1.21) [80] also plays a role in defense against oxidative stress-mediated LPO, catalyzing the reduction of the aldehyde group of HNE and/or both oxygen groups of the GS-HNE hemiacetal [81], leading to its disposition. All these enzymes play an important role in the defense against ROS. In recent years the role of glutathione S-transferases (GST), which catalyze glutathione-dependent conjugation and reduction of a wide variety of LPO products, as antioxidant enzymes is being recognized as they are involved in reduction of LOOH through their selenium-independent GPx activity. This and other roles of GSTs is elaborated further in this section.

LPO and disease: Lipid peroxidation is an inevitable consequence of oxidative stress and is involved in a multitude of human diseases, such as cataractogenesis, carcinogenesis, atherosclerosis, and several neurodegenerative ailments such as Alzheimer's disease. These diseases have the commonality of increasing in occurrence and/or severity with age; with the exception of cancer, these diseases are progressive and fit a profile of exacerbation due to continual protracted exposure to ROS. The exact implications of LPO in these diseases are still not completely understood, although it has been shown to be strongly involved in these pathogeneses. Possible relevance of the etiology of LPO to these age-related disorders is briefly discussed below:

LPO and cancer: The process of carcinogenesis is a multistep pathway consisting of several factors controlling cell cycle checkpoints, control of both intrinsic and extrinsic apoptosis susceptibility, and adhesion control, among other processes [82-

84]. LPO levels in oral cancer patients increase along with progression of the disease [85] concomitant with a steady decrease in both enzymatic and non-enzymatic antioxidant mechanisms, and similar associations are seen in patients with breast cancer [86], liver carcinoma [87], and prostate cancer [88]. In fact, a rise in LPO levels is seen in many cancer cell types [89], which suggests the apparent role of this avenue of oxidative stress in the pathogenesis and malignancy of cancer in several cell types. In contrast, many cancer cell lines in culture show relatively lower levels of LPO and induction of antioxidant enzymes such as GSTs [90]. Thus correlation is not clear.

LPO and cataract: Cataracts are the leading cause of blindness throughout the world [91], and are primarily associated with the aging process. The mechanistic cause is suggested to be chronic oxidative stress, especially in the lens [92, 93]. Oxidative stress has been implicated through numerous lines of evidence with the pathology of cataracts [94-96], especially affecting the outer lens epithelial cells first and likely being an initial step in cataractogenesis [97, 98]. Superoxide anion and hydroxyl radical are generated in excess via possible nonenzymatic oxidation of glucose in diabetic hyperglycemia. In addition, LPO products have been shown to be able to directly initiate cataractogenesis in mammalian lenses [72]. For example, intra-ocular injection of phospholipids which have been previously oxidized quickly and consistently causes formation of cataracts in rat lens [99]. Additionally, in rats with dysfunctional retinal pigment epithelium (RPE), the buildup of shed oxidized phospholipid-rich outer rod segments occurs in the vitreous humor, and the detection of this buildup is coincidental with cataract formation *in vivo* [100]. Previous investigations in our laboratory have shown that rat lens cataract formation is a direct result of insult with HNE *in vitro* [101]. These findings reinforce the causal connection between exposure to superphysiological levels of LPO products and cataractogenesis.

LPO and retinopathy: PUFA are plentiful in the retina and therefore this

13

tissue makes a substrate-rich environment for LPO to occur in the presence of oxidative stress. The retinal pigment epithelium acts as a filter/feeder layer of cells between the vascular retina and the neural retina. As such, it is exquisitely situated for exposure to increased oxidative stress, and its role in phagocytosis of photoreceptor outer rod segments [102] ensures a constant influx of PUFA. It is likely because of this susceptibility of the retina to LPO damage that age-related macular degeneration (ARMD) affects approximately 5.5% of people aged over 65 years old [103], having become the most common cause of profound loss of vision in the industrialized world [104]. The deposition of lipofuscin, a phototoxic lipid-containing pigment found in several tissues, in retinal tissue is one of several LPO-mediated factors underlying the pathology of ARMD [105]. It has been proposed that buildup of lipofuscin in RPE lysosomes over time is due to inability of these cells to perform proteolysis in a normal manner, and the increased proteolytic resistance of these proteins is due to conjugation to LPO products malondialdehyde (MDA) and HNE [106, 107]. The discovery of MDA and HNE as covalently-bound protein conjugates in lipofuscin deposits strongly suggests that these compounds are involved in the pathology of lipofuscin formation and its toxicity in ARMD [108].

Diabetic retinopathy is also one of the most prevalent causes of vision loss in working-age American adults [109] with an underlying cause of LPO, caused by increased glucose levels in tissues. Concomitant with higher serum levels of LPO products in diabetics [110], increased LPO product levels in ocular tissues are found in both natural [111] and induced [112] diabetes. LPO likely contributes significantly to the overall oxidative stress burden and phenotype of this disease, which involves both accumulation and weakening of retinal vasculature [113], whose increased proliferation causes hemorrhagic occlusion of vision and disruption of retinal tissue arrangement [114].

LPO and atherosclerosis: Atherosclerosis, a progressive buildup of fatty plaques on arterial walls which causes increasing loss of elasticity and bloodflow [115], has been linked to accumulation of LPO products [116, 117] and LPO is thought to be a possible cause of initial cardiovascular events such as the direct damage of vessel endothelium and subsequent introduction of low-density lipoproteins (LDL) into the walls of arteries [118]. Oxidative modification of these LDLs has been strongly implicated as well, with suggestion that such protein modification is a necessary step in the production of foam cells from invading macrophages [119]. Oxidative modification of LDL causes several chemical changes which promote progression of the disease, including increased protein electronegativity, loss of lysine amino acids [120], and increased recognition by macrophages [121]. It is well-established that phospholipids of LDL form large amounts of HNE when oxidized, implying that concentrations necessary for these biochemical modifications are present under oxidative stress conditions [53, 122, 123]. LPO products including HNE have been shown to be agents of this oxidative modification of the LDL apolipoprotein B (ApoB) [124], producing such characteristic structural changes of LDL as described above [125]. This suggests that LPO products, particularly HNE, play a direct role in pathogenesis of atherosclerosis.

LPO and Alzheimer's disease: The link between lipid peroxidation and neurodegenerative diseases is not a new discovery. There have been implications of LPO products situated as causative agents in Alzheimer's disease (AD) [126, 127] for several years. As it has been observed that oxidation of lipids [128], DNA [129], and proteins [130] is increased in AD brain tissues, and since the precursors of LPO, the membrane PUFA, are decreased in AD brain tissues [131], the significance of the contribution of lipid peroxidation in AD is suggested and is therefore an area of strong interest for neurotoxicology and neuropathology. Direct damage of neurons involved with memory has been seen in rats after treatment with HNE [132], to the extent of impairing visual-spatial memory. In humans, LPO products are shown to accumulate in glial cells in AD

patients [133]. Such nervous tissue accumulation is significant in that in mammals increased levels are capable of affecting metal ion trafficking [134, 135], and as it occurs relatively early [136-138] in the progression of AD, even before clinical symptoms occur, a causative role in this neurodegenerative pathogenesis is suggested.

LPO and signaling: While previously it was viewed that LPO products were merely small chemical oxidizers which exist only as downstream consequences of oxidative stress events, the perspective has changed over time with understanding of the roles that ROS play in signaling cascades. Changes in levels of LPO products have long been associated with changes in cellular physiology [53, 139-141]. Therefore the relationship between fluctuations in levels of LPO and consequent modulation of signaling events has been investigated to determine its roles and importance in these biological processes. It has been known for several years [142] that LPO products are involved in signaling processes in mammals, including protein kinase C (PKC) [143, 144], Jun-N-terminal kinase (JNK) [145-147], mitogen-associated protein kinase (MAPK) [146], caspase 3 [148, 149], pathways, among many others [150, 151].

4-Hydroxynonenal:

HNE and signaling: HNE in particular has been revealed as a potent chemical second messenger of oxidative stress [150]. The evidence for involvement of HNE in signaling processes is immense [27, 90, 117, 143, 146, 152-156], including involvement in pathways of tyrosine kinase receptors [117], pRb/E2F [153], AP-1 binding [157], NF-κB [158], Jun N-terminal kinase, caspases [159, 160], protein kinase C [143], adenylate cyclase [161], transforming growth factor β1 [162], and heat shock proteins [163-165], among others. This involvement in signaling is not confined to modulation of protein function, but includes stimulation/inhibition of gene expression, affecting mRNA levels of several genes involved in regulation of cell cycle and growth [166, 167].

The influence of HNE on cell signaling mechanisms is complex and its study has been approached from two directions: 1) by investigation of physiological changes subsequent to increase of the intracellular concentrations, and 2) investigation of changes subsequent to decrease of those concentrations. In the former approach, which has been thoroughly utilized [27, 53, 141, 143, 146, 147, 155, 168-172], it has been consistently observed that while relatively 'low' levels of HNE (in the range of 0.1-1μM) are capable of inducing proliferation and growth via stimulation of their related cascades, relatively 'high' levels of HNE (in the range of 20μM and above) are sufficient for triggering a halt to cell proliferation, increase in cellular stress-response coping mechanisms, and ultimately cell death. It is not known as to what the membrane concentration of HNE. However considering that its partition coefficient into water from oil phase is less than 0.1, it is expected that its concentration within membranes would be higher than in cytosol. It is easy to envision that there would be an upper boundary for intracellular concentration of HNE, above which toxicity would occur, as this is a generally accepted tenet of toxicology. However the concept of a lower boundary for intracellular concentration, below which cellular physiology is altered towards a resistant phenotype, has only been recently explored, utilizing the alternate approaches of either overexpression or induction of HNE-metabolizing enzyme activity to decrease intracellular concentrations [27, 116, 147, 154-156, 173, 174], though the evidence thus far has been supportive of this hypothesis. The fact that 1) HNE is present in significant amounts in every cell line investigated by our laboratory and 2) HNE-metabolizing enzymes, such as hGSTA4-4, are not normally expressed at levels required to completely deplete HNE without stress induction [175] suggests that there is a constitutive level of this LPO product which may be essential to cell physiology.

Interactions of 4-hydroxynonenal with biomolecules: HNE is capable of interacting chemically with various types of biological molecules, such as nucleic acids, phospholipids, and proteins [53]. The chemical structure of HNE includes three reactive groups, which allow a large pool of substrate with which it may react to form conjugates **(figure 3)**.
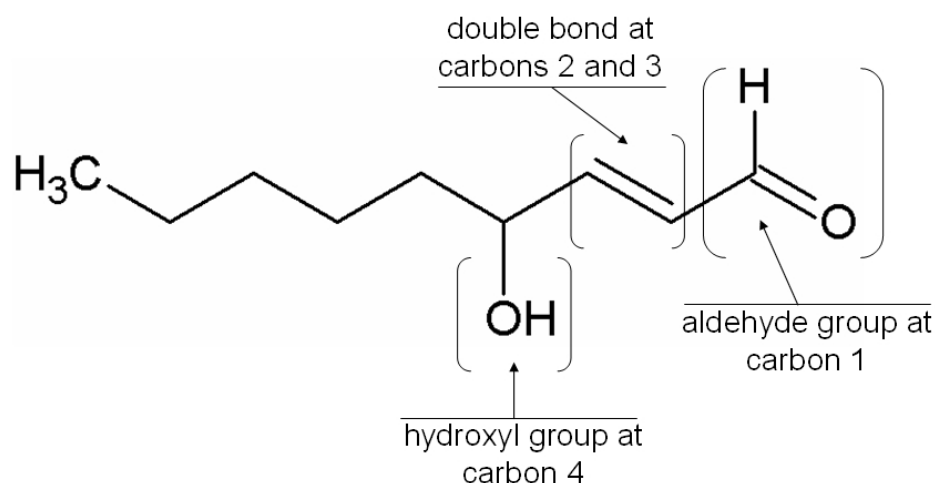
Figure 3: Structure of HNE and identification of chemically reactive groups.

These groups include the aldehyde group (carbon 1), the double bond between carbons 2-3 (α-β), and the hydroxyl group at carbon 4 [53]. Interaction between HNE and other molecules, as it is understood as yet, depends on these reactive groups. One possible reaction of HNE with DNA is the Michael addition of nucleic acid primary amines (such as those found in guanine) with the 3(β)-carbon, which then allows secondary binding of the HNE aldehyde carbon to the nearby amino acid secondary amine **(figure 4a)**. Another possible reaction involves an epoxide metabolite of HNE (formed by interactions with organic hydroperoxides) bonding to an amino acid primary amine via its aldehyde group, followed by cleavage to yield a tricyclic etheno adduct [176].

18

Interactions with membrane phospholipids, such as phosphatidylethanolamine and phosphatidylserine, which bear primary amines, are via both Schiff base formation with those terminal amino groups and subsequent formation of a cyclic HNE pyrrole **(figure 4b)**, and Michael addition with primary amines at the 3 (β)-carbon. These interactions are much more likely to occur with phosphatidylethanolamine (PE) than with phosphatidylserine (PS), possibly due to interference by the extra carboxyl group present on PS [176]. Interaction with primary amines such as lysine occurs at the aldehyde group on carbon 1, which causes the formation of Schiff base intermediates **(figure 4c)**. Interaction between the hydroxyl group at carbon 4 and O_2 can form ketones. The unsaturated bond is capable of reacting with thiol groups found in GSH cysteine moieties of proteins. It can also react with LOOH via an epoxidation reaction. The 2,3-double bond acts as a Michael acceptor group, which enables it to alkylate nucleophilic alkenes with higher selectivity over other HNE carbons.

Metabolism and detoxification of 4-hydroxynonenal: Because HNE is produced in a continuous manner in cells, the ability of cells to survive depends on an ability to detoxify it and/or remove it from the cellular milieu. HNE is detoxified in cells via a number of different mechanisms involving several enzymes **(Figure 5)**. The most important and efficient method of detoxification is its conjugation to glutathione by glutathione S-transferases (GST). GSTs catalyze the linking of HNE to the substrate GSH, which bears its higher-affinity cysteine sulfhydryl group (due to catalytic lowering of –SH pKa and thereby acidification of this hydrogen and activation for nucleophilic attack) in the place of lower-affinity protein sulfydryl groups and reduces the α,β-unsaturated bond to form glutathionyl-HNE (GS-HNE). Conjugation of HNE with GSH is accelerated by more than 600 fold via GST over a non-enzymatic reaction [177]. Besides GST, several other enzymes are known to metabolize HNE. Aldehyde dehydrogenase (ALDH) and aldo-ketoreductase (AKR) catalyze NAD(P)H-dependent addition of 2 hydrogens to the aldehyde group to form 1,4-dihydroxynonenone (DHN),

and ALDH converts HNE to 4-hydroxynonenoic acid (HNA) with NAD+. Likewise γ-glutamyltransferase (γ-GT), acetyl transferase (AT), and endopeptidase (EP) cleave the GS-HNE ring to allow formation of HNE-mercapturic acid adducts. Since GST conjugation to HNE is most
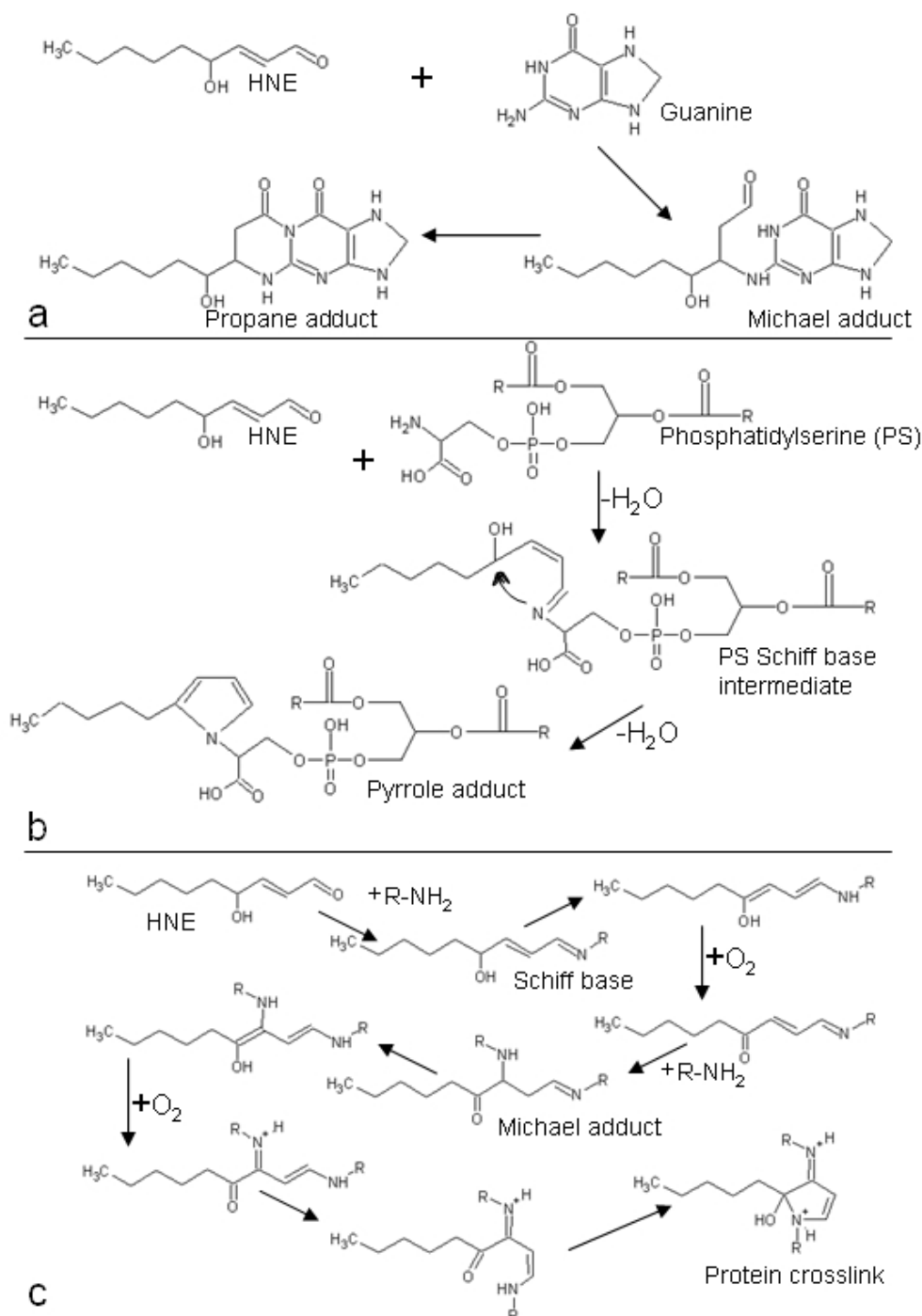
Figure 4: Reactions of HNE and biological molecules. A, HNE forms Michael adducts with guanine residues (DNA). **B,** HNE forms Schiff base intermediates with phosphatidylserine (phospholipid). **C,** HNE forms intermediate Schiff base conjugates with primary amine residues of proteins (as 'R') followed by Michael addition to a second protein primary amine. Adapted from [176].

21

relevant physiologically, the adduct GS-HNE is a common target of these same oxidizing/reducing enzymes. As 1,4-dihydroxynonenone (in the form of 1,4-dihydroxynonane-mercapturic acid), a product of the mercapturic acid pathway, is the major HNE metabolite present in urine (in human and rat) [178], AKR is likely necessary in GS-HNE metabolism via mercapturic acid pathway [179]. ALDH oxidizes the cyclic GS-HNE adduct into HNA-lactone-GSH, which can be cleaved of its GSH moiety for a separate CYP450-mediated pathway or be broken open via reduction to GSH-HNA, which then can enter mercapturic acid pathway.

Glutathionylated HNE is efficiently shuttled out of the cytoplasm through the phase III biotransformation machinery **(figure 6)**. This transport is performed mostly via Ral-interacting protein 76 (RLIP76), and to a lesser degree by ATP-binding cassette (ABC) family transporters such as multi-drug resistant protein 1 (MRP1) [180]. RLIP76 is the most important of the phase III biotransformation enzymes involved in HNE disposition from cells, comprising the majority of such activity at approximately 70% as shown by transport studies [181].

Glutathione S-transferases (GSTs)

Overview of GSTs: The glutathione S-transferase (EC 2.5.1.18) superfamily comprises a large, multi-class group of biotransformation enzymes capable of catalyzing glutathionylation reactions and reductions on a wide variety of xenobiotics and endogenous substrates [182-184]. GSTs are primarily cytosolic proteins, but membrane-bound GSTs including the microsomal GSTs and those belonging to the MAPEG family are also present in mammals and in lower organisms. The vast majority of GSTs are found in the cytosol [185], and most of those are found in the cytoplasm, with some
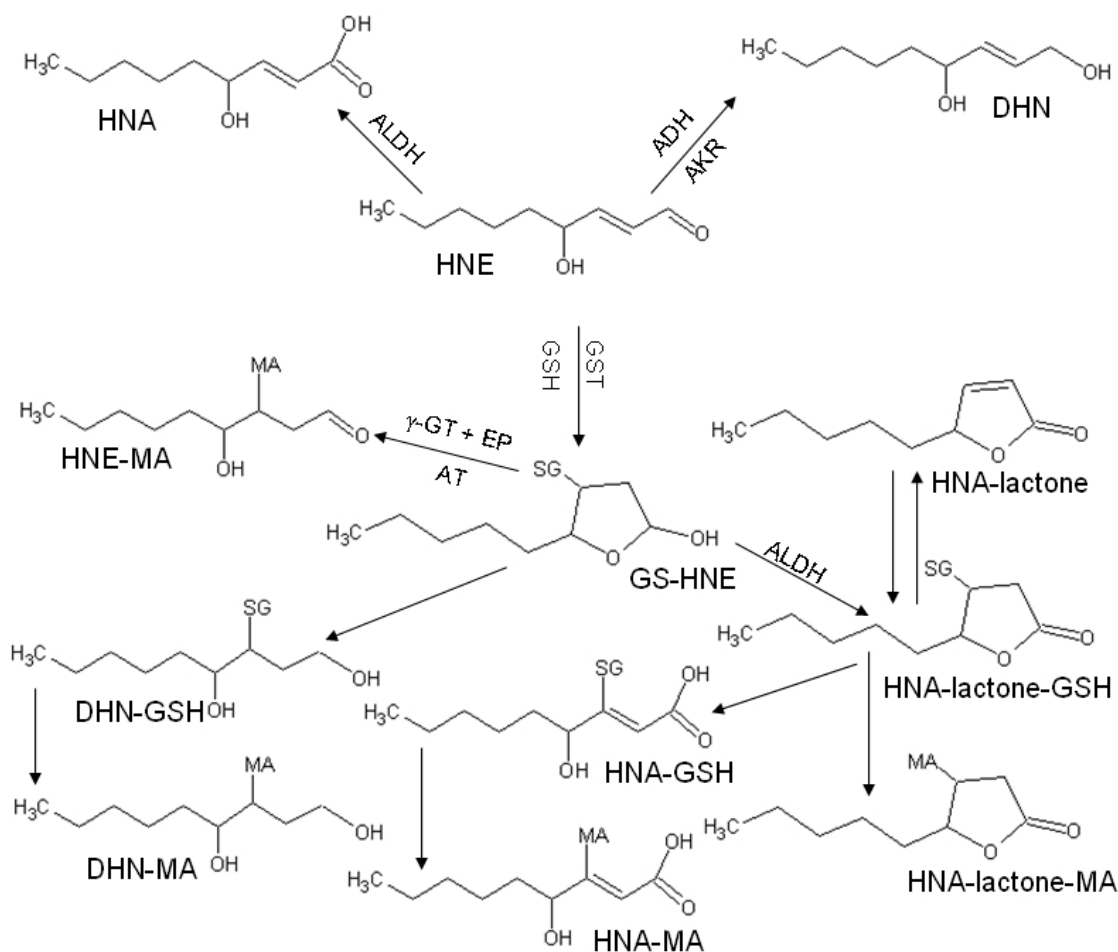
Figure 5: Enzymatic pathways of HNE metabolism. HNE is oxidized via ALDH to HNA, with ADH/AKR to form DHN, or with GST to form GS-HNE. GS-HNE is acted on by mercapturic acid pathway enzymes (γ-GT/EP/AT) to form HNE-MA. GS-HNE can also form DHN-MA through a combined pathway. GS-HNE is metabolized by ALDH to form HNA-lactone-GSH, which can lose GSH to become free lactone, progress directly through the MA pathway, or hydrolyze first to HNA-GSH and then through the MA pathway.

found in nucleus [186], mitochondria [187-190], and microsomes [182, 191]. However, some isozymes (such as mGSTA4-4) are known to be found at higher concentrations near cell membranes [192], likely due to weak charged interactions.

23
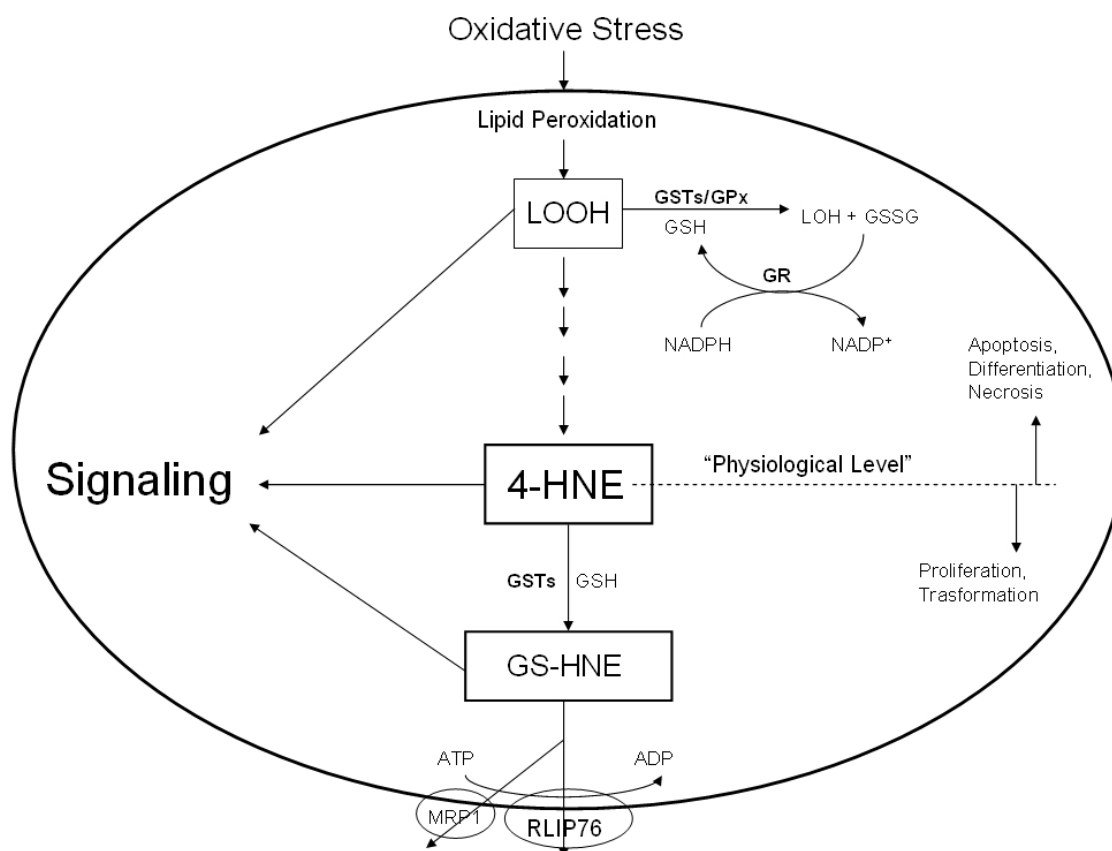
Figure 6: Metabolism and export of LPO products by GSTs and RLIP76 in the cell.

Along with cytosolic GSTs, there are families of GST which are expressed in microsomes and mitochondria. Microsomal GSTs are also known as membrane-associated proteins associated with eicosanoid and glutathione metabolism (MAPEG). As their name suggests, the majority of the enzymes comprising this family possess strong activity towards synthesis of eicosanoids, as well as production of prostaglandin E2 and leukotriene C4 [193].

Mitochondrial GSTs in mammals assayed (mouse, rat, and human) are GSTA4-4, which while characterized as cytosolic has been shown as partly present in mitochondria,

and Kappa class GSTs with one known member [194]. Kappa GST has a tertiary structure unlike other family members and similar to bacterial oxidoreductases [195, 196]. While structurally dissimilar to cytosolic GSTs, mitochondrial GST is known to possess activities against characteristic GST substrates such as aryl halides and some hydroperoxides [194].

Families and chromosomal location of GSTs: Currently cytosolic GSTs in mammals are organized into seven families: alpha, mu, pi, sigma, zeta, theta, and omega. These families share highly conserved sequence [197], although sequence similarity with mitochondrial and MAPEG GSTs is considerably less as non-cytosolic GSTs tend to be identified by protein function alone. The organization of GST genes into respective classes is based on their members sharing at least 50% sequence homology [198], and because of this the genes in each class are found near each other on the same chromosome. This phenomenon, along with each class of cytosolic GST being found on a different chromosome, tends to reinforce the current method of classification. The chromosomal location of soluble GSTs are presented in **table 1**.

Table 1: Human GST classes and chromosomal locations.

Alpha	6p12
Mu	1p13
Pi	11q13
Theta	22q11
Sigma	4q22.3
Zeta	14q24
Omega	10q24

25

Nomenclature and Structure of GSTs: Over the years several nomenclatures based on Greek numerals, PI of these isozymes, and chronology of their discovery have all been used. In currently used nomenclature, cytosolic GSTs are named in a manner similar to the cytochromes P450, with family name listed along with isozyme number, although without further division. In addition, however, the species is included in lowercase at the beginning of the enzyme name. For instance, with human GSTs labeled 'h', murine GSTs as 'm', bovine as 'b', and so forth [199]. The class of GST is listed in uppercase in the name with Alpha-class as 'A', Mu-class as 'M', Pi as 'P', etc. Finally, the subunit numeral (generally, the isozymes are ordered numerically according to the system devised by *Mannervik et al.*[199]) is listed last. This gives rise to names of specific enzymes such as hGSTA4-4 for human GST A4-4, the homodimer of the fourth isozyme in the human alpha class. Cytosolic GSTs are found in homodimers and possibly heterodimers and the proteins are referred to by their dimers, as evidenced in the nomenclature with names such as hGSTM2-2, mGSTP1-1, etc. for the protein. When referencing the gene, the form is italicized and the dimer reference is dropped, leading to gene names referencing the subunit alone, such as *hGSTA4, mGSTP1*, etc. This holds true for the mitochondrial GSTs as well, but not so for the microsomal MAPEG GSTs, which are trimeric in structure and exhibit different physiological functions [182].

Regulation and Expression of GSTs in human tissues: The gene encoding hGSTA4-4, *hGSTA4*, is under control of the antioxidant response element (ARE) (**TGAC**nnn**GC**)**,** which is activated by nuclear factor-erythroid 2 p45-related factor 2 (Nrf2) [200], as well as several antioxidants including Michael acceptors, quinines, and polyphenols [201]. This is a commonality in many GSTs [202] (although not microsomal GSTs and apparently mitochondrial GST, which do not appear to contain an ARE [184]), as they belong to the 'ARE gene battery' [182] of antioxidant enzymes along with

superoxide dismutase, catalase, glutathione peroxidase, cytochrome P450, and aryl hydrolase, among others.

Expression of GSTs in tissues is relatively high, and while GSTs are expressed in some form in every human tissue type measured, the specific isoforms are not evenly expressed throughout the body [203]. Since the Alpha-, Mu-, and Pi-classes form more than 90% of expressed GSTs in humans, these three classes contribute the vast majority of GST activity as well. In the liver, alpha-class GSTs are the predominant isoforms expressed, while in extra-hepatic tissues, mu and especially pi-class isoforms are much more abundant, often with alpha-class GSTs expressing at below the detection limit for Western blots. *hGSTA1* and *A2* are the most abundantly expressed α-class GSTs in human tissues, with *A3* and *A4* less commonly so and *hGSTA5* expression not observed in any assayed tissues. In individuals with a double *GSTM1* deletion (approximately half of the Caucasian population), and therefore no expression of that isoform, the Pi-class is the only major GST class expressed outside the liver.

Induction and inhibition of GSTs: The GST superfamily contains several isozymes which are capable of upregulation in response to injurious stimuli, both endogenous and exogenous. The number of known inducers of GSTs is well over one hundred [204], and many if not most of these are (or produce metabolites which are) also substrates for either transferase or reductase activity catalyzed by one or more GST isoforms. There are many possible mechanisms for induction of GST expression, including interaction with a 5' *cis*-acting regulatory motif termed the antioxidant response element (ARE) [205], which has been found to play a role in regulation of other antioxidant enzymes. Activation of GSTs via the ARE appears to be regulated in large part by the translocation and binding of transcription factor Nrf2 along with interaction with Keap1 [206] It has been shown that HNE adduct GS-HNE is a potent inhibitor of GST activity [207], possibly through competitive inhibition, and its removal from the cell is a requisite to continued conjugation activity of GSTs against HNE. Ebselen [208], (1)-

Taxifolin [209], and sodium taurocholate [210] are also potent inhibitors of GSTs, through various mechanisms including antioxidant prevention of ROS production, direct chemical interaction, and buildup of inhibitory glutathione conjugates.

Functions of GSTs: There are a number of known functions of the GST superfamily of enzymes **(figure 7)**: GSTs are multifunctional and several activities are assigned to members of this supergene family of enzymes, which are described below:
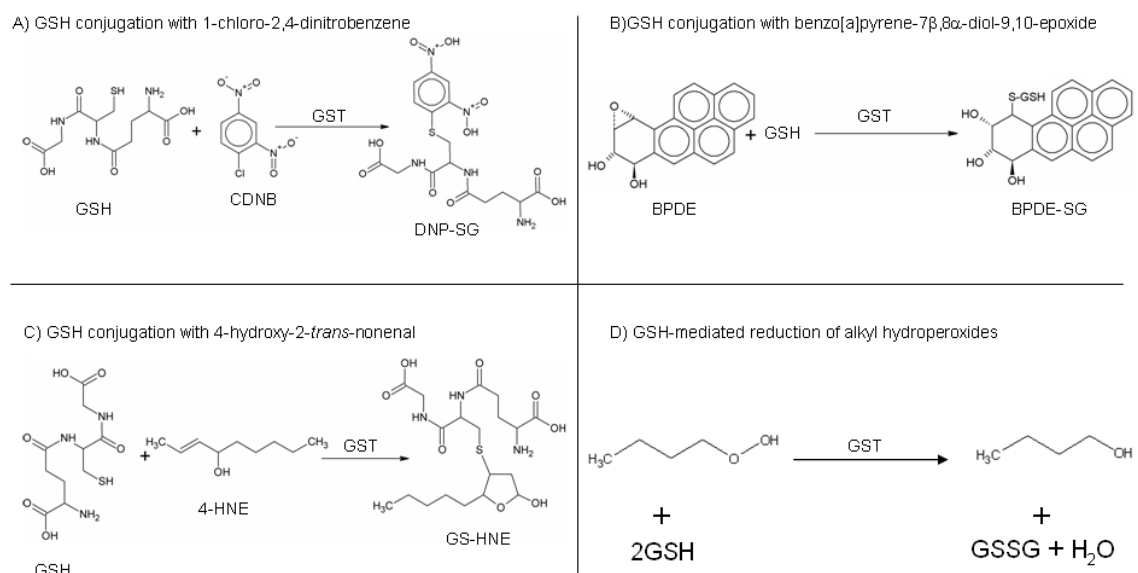
Figure 7: Biochemical reactions catalyzed by GSTs.

GST and the mercapturic acid pathway: The first pathway to which GSTs were found to contribute physiologically was the mercapturic acid system of metabolism and disposition, in 1879 [211, 212], a system that has been thoroughly characterized and is a major pathway contributing to the biotransformation of both endobiotics and xenobiotics in animals [213]. Conjugation of xenobiotic compounds to GSH by glutathione transferases (several transferase activities that were later revealed to

be due to overlapping specificities of GST isoforms) was actually reported much later [214-216]. This widely recognized activity of GSTs towards exogenous and endogenous electrophiles is the first step in the formation of mercapturic acids. GSTs catalyze the first step in the mercapturic acid pathway [213, 217], a four-step conversion of precursor molecules for detoxification which allows the recovery of glycine and glutamatic acid. In the first step, the drug is conjugated to GSH via GST, producing a hydrophilic metabolite. Second, γ-glutamate is removed from the glutathione group via γ-glutamyltranspeptidase, revealing a cationic amino group. Third, glycine is removed from the group via cysteinyl glycinase to reveal an anionic carbonyl group, thereby leaving only a zwitterionic cysteine amino acid conjugate. Lastly, the cysteine is converted by N-acetyltransferase to N-acetylcysteine, thereby recycling two of the three amino acids necessary for GSH synthesis. In fact the mercapuric acid pathway has been shown to be involved in HNE metabolism as the major metabolites found in urine of HNE-treated rats contain metabolites of this pathway, such as HNE-mercapturic acid, 1,4-dihydroxynonenone mercapturic acid, and 4-hydroxynonenoic mercapturic acid [218]. Furthermore, 1,4-dihydroxynonenone mercapturic acid has been found in the urine of untreated rats and humans [178], suggesting that this is a common GST-mediated pathway in mammals for the disposition of physiological levels of LPO products.

GST and noncovalent binding of ligands: Another characterized activity of this enzyme family includes ability to modulate the uptake of several different aromatic molecules with different functional groups. Ability of "ligandin" to non-enzymatically bind various ligands was discovered in 1971 [219] which was shown to be identical with rGSTA1-1 (then called "GST B") [220, 221] through immunological identification of seemingly disparate proteins characterized by separate laboratories. Intracellular binding of ligands by GSTs is usually associated with anionic planar aromatic compounds, including anionic dyes, steroids, and porphyrins, non-substrate compounds which often act as inhibitors to conjugation activity of GSTs [222]. In

addition the expression of ligandin in rat liver was correlated to organic anion uptake, in studies which led to elucidation of the role of GSTs as ligandins in the solubilization of xenobiotics within the metabolizing environment of liver where they are detoxified [223].

GST and xenobiotics substrates: Along with other transferases such as methyltransferases, sulfotransferases, and acetyltransferases, GSTs are involved in the phase II biotransformation of xenobiotics. GSTs are able to detoxify many carcinogenic xenobiotics such as industrial products and pesticides, including benzo[a]pyrene derivatives [224-226] as well as several anti-cancer chemotherapeutic drugs such as doxorubicin [227], vinca alkaloids [228], and cyclophosphamide [229], and have been increasingly viewed as a system of detoxification against these chemotherapeutic agent in concert with members of membrane-bound ATP binding cassette (ABC) and non-ABC drug transporter protein groups including multidrug resistance associated protein (MRP) and P-glycoprotein (Pgp) as well as RLIP76 [230-232]. Overexpression of GST isozymes have been implicated in carcinogenesis [233]. Pi-class GST GSTP1 was found to be very strongly upregulated in liver tissues after subjecting rats to carcinogenic stimuli [234].

GST and endogenous substrates: GSTs are involved in the metabolism of endogenous compounds: amino acids, arachidonic acid products, and oxidative stress metabolites **(table 2)**. Fatty acid, phospholipids [235], and cholesterol hydroperoxides [236] can be reduced by GSTs via Se-independent peroxidase activities, which serve to stop these upstream LPO precursors before they are converted to downstream LPO products. This process, while efficient, is not perfect and (especially after high stress events) must be supplemented with detoxifying activity against downstream endogenous LPO products. hGSTA4-4 is capable of conjugating a variety of these LPO products, including MDA and acrolein [5, 184] and 9-15 carbon aliphatic 4-hydroxyalkenals [237]. The most physiologically relevant of these is 4-hydroxy-2-*trans*-nonenal, with which the

enzyme has high efficiency of conjugation **(table 3)**. Ability to effectively conjugate these variegated substrates along with many others (cholesterol-5,6-oxide, epoxyeicosatrienoic acid, 9,10-epoxystearic acid, crotonaldehyde, 1-palmitoyl-2-(13-hydroperoxy-*cis*-9, *trans* octadecadienoyl)-L-3-phosphatidylcholine, epoxyaldehydes, ketoaldehydes, etc.) [182, 184] is a hallmark of the wide control GSTs exert on the concentrations of cytotoxic endogenous compounds.

Table 2: Physiological substrates of GSTs, products, and isozymes involved in reactions.

Substrate	Related Isozyme(s)	Product
Acrolein	Pi class	GSH conjugate
Androst-5-ene-3,17-dione	Alpha class	Androst-4-ene-3,17-dione
Cholesterol alpha epoxide	Alpha class	GSH conjugate
HNE	Alpha class	GSH conjugate
5-HPETE	hGSTA1/A2, microsomal GSTs	5-HETE
9-Hydroperoxylinoleic acid	Alpha class	9-Hydroxylinoleic acid
Maleyl acetoacetate	Zeta class	Fumarylacetoacetate
Malondialdehyde	Alpha class	GSH conjugate
Phenyl propenal	GSTA1, M1, P1	GSH conjugate
PC-OOH	Alpha class	Phosphatidylcholine hydroxide
PE-OOH	Alpha class	Phosphatidylethanolamine hydroxide
Pregn-5-ene-3,20-dione	GSTA3	Pregn-4-ene-3,20-dione
Prostaglandin H2	GSTM2/M3	Prostaglandin E2
Prostaglandin A2/J2	Alpha, Mu, Pi class	GSH conjugate
Thymine propenal	Pi class	GSH conjugate
Uracil propenal	Pi class	GSH conjugate

Table 3: Preferred substrates of alpha-class GSTs involved in detoxification of LPO products.

Enzyme	Species	Class	Preferred Substrate
hGSTA1-1	*H. sapiens*	Alpha	LOOH
hGSTA2-2	*H. sapiens*	Alpha	LOOH
hGSTA4-4	*H. sapiens*	Alpha	HNE
hGST5.8	*H. sapiens*	Alpha	HNE
mGSTA4-4	*M. musculus*	Alpha	HNE
rGSTA4-4	*R. norvegicus*	Alpha	HNE

hGSTA4-4 and HNE: HNE, as a 4-hydroxyalkenal, is an endogenous substrate of GSTs [238]. hGSTA4-4 has high catalytic efficiency against HNE (above 10^6 $M^{-1} \cdot s^{-1}$) and is among the primary biological catalysts for metabolism of HNE in humans [239-241] **(figure 8)**. While not normally expressed at high levels in extra-hepatic tissues, hGSTA4-4 is highly inducible upon oxidative stress events, and is known to be upregulated by HNE via the ARE [242].

(2E)-4-hydroxynon-2-enal

GSH | hGSTA4

GS-hydroxynonenal
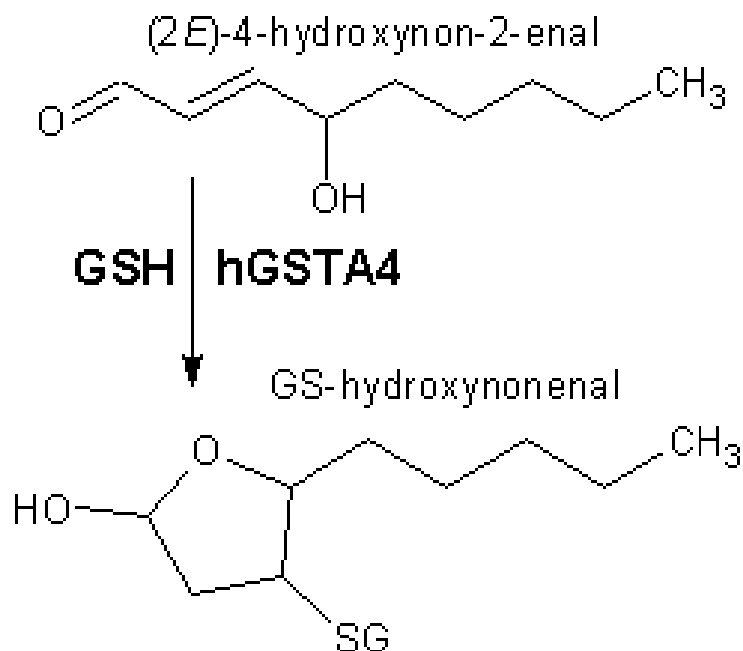
Figure 8: Conjugation of HNE to GSH catalyzed by hGSTA4-4.

The chemistry of hGSTA4-4-HNE conjugation is mediated partially by the reactive nature of HNE. The 3 carbon of HNE, which is on the distal end of the 2-3 double bond, carries a partial positive charge and therefore is electrophilic. This electrophilicity is augmented by the interaction of the partial-negative aldehyde oxygen of HNE with tyrosine 212 (accepting a hydrogen bond from Tyr-212 hydroxyl group), which stabilizes the aldehyde oxygen, thereby polarizing the 2-3 double bond. The polarization of the HNE double bond facilitates the GSH nucleophilic attack, which is a characteristic of GST-catalyzed conjugation reactions [243]. This nucleophilic attack is somewhat different, however, in that GSH is not ionized to thiolate before attack, instead being assisted by a water molecule positioned between GSH and Tyr-9 (adjacent to Tyr-212 in the active site) which has been suggested to act as both a proton acceptor (from GSH) and a proton donor (to carbon 2 of the HNE double bond), thereby obviating the need for GSH ionization to complete the conjugation reaction with HNE. After this

33

conjugation, GS-HNE, a potent inhibitor of GST activity, is quickly shuttled out of the cell by membrane-bound RLIP76 via an ATP-dependent transport mechanism **(figure 9).**
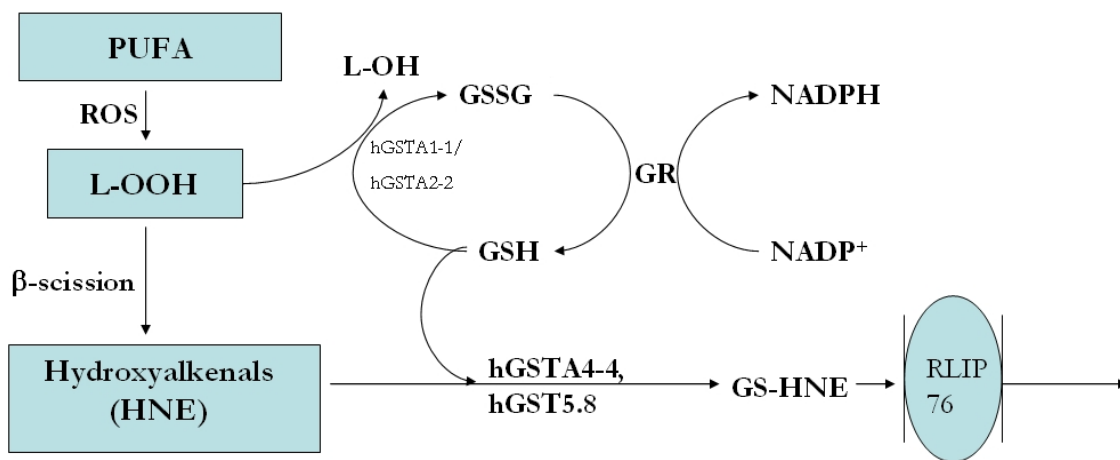
Figure 9: HNE is conjugated and excluded via actions of hGSTA4-4 and RLIP76. Polyunsaturated fatty acids are peroxidized to lipid hydroperoxides, some of which are reduced to alcohols by enzymatic activity of hGSTA1-1/A2-2 via GSH cosubstrate, which is replenished by NADP+-dependent glutathione reductase. Lipid hydroperoxides which escape reduction can undergo b-scission to form hydroxyalkenals such as HNE, which are conjugated to GSH by enzymatic activity of hGSTA4-4 (and hGST5.8) to form GS-HNE, which is transported out of the cell by enzymatic activity of RLIP76.

Glutathione peroxidase activity of GSTs: Alpha-class GST members possess significant activity to reduce organic hydroperoxides including those of lipids, phospholipids, cumene, cholesterol, etc. [244], while Mu and Pi class cytosolic and microsomal GSTs bear little peroxidase activity [245]. Selenium-independent peroxidase activity of GSTs was discovered in 1976 [246]. Such activity (called GPxII, in contrast to the Se-dependent glutathione peroxidase activity of the GPx enzyme family) does not include activity against hydrogen peroxide, which is limited to selenium-dependent glutathione peroxidases (GPx) and catalase.

In addition to their activities against free fatty acid hydroperoxides in cytosol, GST activity against the hydroperoxides of membrane phospholipids has been confirmed

[154, 247, 248] at a physiologically relevant rate, which suggests that these enzymes, while cytosolic, can exert their effects against membrane-bound hydroperoxide substrates. It was the observation of this activity against intact phospholipids hydroperoxides that began research into the role of GSTs as key antioxidant enzymes in defense against toxicity of the LPO cascade.

GST peroxidase activity is physiologically significant. More than 50% of GPx activity in human liver is contributed by GST [154], which is consistent with higher observed expression of Alpha class GSTs in this tissue, while in extra-hepatic tissues with much lower Alpha class GST expression, Se-dependent GPx would be expected to be the major contributor. The ability of GSTs to reduce lipid hydroperoxides along with their conjugating activity against reactive aldehydes serves both to prevent the LPO cascade at the source level and to neutralize the LPO cascade at the product level. It has been observed that overexpression of hGSTA1-1, hGSTA2-2, and hGSTA4-4, three isozymes possessing reducing activity against LOOH, in cells leads to protection against inducers of LPO-mediated toxicity [147, 154, 249]. Since LPO has been suggested to be responsible for numerous disease states such as Alzheimer's disease [130, 136, 172], cancer [85, 86, 89], and cataract [34, 94, 250], prevention of the formation of toxic LPO products is a key step in protection against their downstream effects.

Polymorphisms of GSTs and disease states: Polymorphisms in Alpha-class GSTs are well-correlated with carcinogenesis in humans. The GSTA1*B allele of *hGSTA1* has significantly lower expression levels in liver, with concomitantly lower activity for detoxification of the DNA-adductive, electrophilic heterocyclic amine 2-amino-1-methyl-6-phenylimidazo[4,5-*b*]pyridine (PhIP) and its genotype has been correlated with higher risk of colorectal cancer [251].

Need for present studies:

It can be noted that in the process of carcinogenesis there are three types of genes whose members are modulated to some degree to allow the transformation from healthy cells to full, metastatic cancer cells. To break free of normal cell division constraints, they must change expression of cell cycle regulation genes. To protect themselves from their own suicide mechanisms and the organism's anti-cancer checks, they must affect the expression of apoptotic control genes. To achieve metastasis, they must alter their interaction with the extracellular matrix by modulating cell adhesion genes. Overexpression of GSTs has been observed in a number of human cancers and cancer cell lines , as well as rat liver carcinoma and preneoplastic nodules [184]. In fact Pi class GST overexpression is used as a biomarker for carcinogenesis in rat liver [252, 253] as its induction is an early event, occurring within 2-3 days after chemical administration [254]. The importance of GSTs in carcinogenesis is established and its relevance to genes involved in processes which control the transition of cells from normal to cancerous are discussed below. In addition, we discuss the rationale for the present studies which are necessary to correlate GST overexpression leading to depletion of steady-state HNE levels with global changes in gene expression including emphasis on several key genes involved in cell cycle regulation, apoptotic control, and cell adhesion.

Cell cycle regulation: GSTs have been observed to be involved in regulation of cell cycle through both direct and indirect interaction with JNK. Direct interaction of GSTP1 with JNK has been shown to inhibit kinase activity towards c-Jun[255] and thereby prevent formation of the AP-1 transcription factor complex, decreasing cell proliferation. Conversely the decrease of GSTP1 increases JNK activity and leads to increase of cell proliferation [256]. Likewise the action of GSTs to indirectly modulate proliferation in cells via controlling intracellular LPO levels has been investigated [150]

and along with decrease in LPO product concentrations, increased proliferation has been observed [171].

Regulation of mammalian cell cycle is very complex and is briefly summarized below: Cells begin the cell cycle at G_0 phase, which is common for mammalian non-dividing cells; Normal cellular physiology occurs in this phase, as it is the phase in which normal cells spend most of their lifetime. Cells which are prepared to divide pass into G_1 phase via the upregulation of cyclin D and its partner protein cyclin-dependent kinase 4 (Cdk4). During this time the G_1/S checkpoint is in place: retinoblastoma protein (Rb) is active and coupled to E2F, preventing E2F-mediated induction of transcription factor DP-1, cyclin E and thereby transition to S phase; this checkpoint is closed by p53 via p21 and p16 [257]. However, ubiquitination and degradation of p53 allows phosphorylation of Rb, releasing E2F and allowing the degradation of the cyclin D-Cdk4 complex and the upregulation of cyclin E and its partner Cdk2, allows the cell to cross the G_1/S phase checkpoint and enter S phase [258-260]. During S phase synthesis of replicate DNA occurs; at the end of DNA replication, the progression into G_2 phase occurs, where Cyclin A (associated with Cdk2) and its partner protein Cdk1 are upregulated, allowing for a rapid expression of mitosis-related proteins. Once the G_2/M phase checkpoint is passed, cyclin A is degraded and cyclin B then couples with Cdk1, triggering entry into M phase where cell division actually occurs. After cell division, the cell passes across the M/G_1 checkpoint automatically and resides again in G_1 with the upregulation of cyclin D and its partner CDK4.

Apoptotic control: GSTs have been known for several years to be involved in protection from apoptosis through their activities in conjugation of toxic electrophiles. Their role in phase II biotransformation protects cells from damage caused by reactive intermediates formed by metabolism of xenobiotics. We have shown previously in

37

studies involving HL-60 [147, 227], HLE B-3 [248], and K562 cells [27, 154], that overexpression of alpha-class GSTs protects these cells against apoptosis mediated by a variety of inducing factors.

Normal cells have a highly-organized ability to commit suicide during organism development [261, 262] and also in times of extreme stress, when there has been significant damage to increase the threat to the organism (i.e., carcinogenesis), due to genomic damage [263], and has been studied in several tissues including ocular tissues [264, 265]. Paths toward apoptosis, the pre-planned and strictly-controlled form of cell death, include the caspase-mediated intrinsic pathways and the extrinsic pathway [266], with some mediators acting in more than one pathway [267]. The influence of lipid peroxidation products on both pathways has been shown recently [27, 268-270], which illustrates the relevance of LPO-mediated signaling to the various cell survival pathways necessary for carcinogenesis.

Cell adhesion/mobility: Adherent cell types are so called because of their non-suspended morphology and arrangement into organized, polarized layers, due to expression of intracellular and extracellular proteins which are capable of forming and interacting with the extracellular matrix (ECM). There are a number of protein families involved in the ECM, including fibronectins [271], Integrins [272], laminins [273], connexins [274], collagens [275], and elastins [276], and along with various proteoglycans these proteins form a structurally intricate network capable of supporting the surrounding cell layers and forming the basis of tissue organization. ECM-mediated intracellular signaling is common and affects a large variety of pathways [277] through specialized focal adhesions [278] made up of clustered integrin proteins which transduce the received signals intracellularly to a number of protein kinases [279]. The loss of anchorage-dependence is a common occurrence in carcinogenesis, and it is a prerequisite

38

of metastasis [280, 281], where cancerous cells leave the original tumor site and travel through the circulation to nucleate other, distant tumors in other areas of the body. Loss of interaction is also a characteristic of apoptotic cells, which, along with observation of protective functions of the ECM [282-286], further connects the mechanisms of cell adhesion and cell survival. This connection suggests that those cells which have surpassed the reliance on the ECM have expressed adaptive mechanisms which allow them to thrive in the absence of regulation afforded by physiological tissue organization.

Rationale for the studies presented in this dissertation: The overexpression of hGSTA4-4 in HLE B-3 cells leads to a large decrease in LPO levels, specifically in the intracellular levels of HNE. These cells repeatedly underwent transformation from attached cells to cells growing in suspension, multiply at a faster rate, and acquire immortality. In order to examine the mechanism of transformation we have studied the effect on expression of genes involved in cellular adhesion, mobility, survival and apoptosis, and cell cycle regulation in transformed cells. After establishing that depletion of HNE is necessary for transformation of the cells (via transfection and microinjection studies with several GST isozymes either active or inactive against HNE), we have studied the effect of HNE depletion on genes by microarray studies. We then confirmed the microarray results and narrowed the scope of our studies with quantitative RT-PCR and Western blot techniques to focus on a subset of genes most relevant to processes involved in procarcinogenic transformation. Focusing studies on the effect of HNE on expression of Fas, we have also addressed the question of whether or not the changes in gene expression in transformed cells precede the transformation or are a consequence of transformation. Studies described in this dissertation confirm previous observations that HLE B-3 cells undergo transformation when HNE is depleted in these cells through stable transfection of *hGSTA4*. Using gene microarray, quantitative PCR and Western blot techniques we demonstrate that depletion of HNE results in a global change in

expression of genes, particularly involved in cell adhesion, survival, and cell cycle regulation. This is further evidence that directed decrease of LPO levels within cells to sub-physiological levels can and does bring about a vast and global series of changes in the expression of proteins in those cells.

CHAPTER II – Materials and Methods

Reagents used in these studies were high-quality and were either prepared in our laboratory or were purchased through well-established reputable distributors. Most protocols used in these studies were standardized in our laboratory. Experimental techniques used in these studies were performed essentially as were performed in previous publications [27, 72, 147, 149, 152, 155], with changes made only as necessary to fit new experimental aims and any changes are noted below in text.

Materials

Reagents: Epoxy-activated Sepharose 6B resin, GSH, glutathione reductase, 1-chloro-2,4- dintrobenzene (CDNB), β-NADPH, cumene hydroperoxide (CU-OOH), 3-(4,5-dimethylthiazol-2-yl)-2,5-diphenyltetrazolium bromide (MTT), were obtained from Sigma Chemical Co. (St Louis, MO). HNE was purchased from Cayman Chemical (Ann Arbor, MI) and was stored at -80°C under nitrogen atmosphere. H_2O_2 was purchased from Fisher Chemicals (Fair lawn, NJ). All reagents for SDS-polyacrylamide gel electrophoresis (SDS-PAGE) and Western transfer were purchased from Bio-Rad (Hercules, CA) or Invitrogen (Carlsbad, CA). Sources for specific reagents and kits for cell and molecular biology studies are identified at appropriate places. DmGSTD1-1 protein (Drosophila melanogaster) was obtained with gratitude from Dr. Piotr Zimniak.

Antibodies: The polyclonal antibodies raised in rabbits against the Alpha, Mu, and Pi class GSTs were identical to those used in the previous publications from our laboratory [249]. The polyclonal antibodies raised in chicken against the A4 isoform of human GST were identical to those characterized previously and used in our laboratory

[149]. The human GPx-1 antibodies were raised as described later in this publication. Other antibodies used in this publication were purchased from Santa Cruz Biotechnologies (Santa Cruz, CA), Alpha Diagnostics, Inc (San Antonio, TX), and Cell Signaling Technology (Danvers, MA).

Animal tissues: Mouse tissues were obtained from mice bred by and housed in the UTMB Animal Resource Center. Mice were C57 black 6 strain and were genotyped as either WT, *mGSTA4* knockout (-/-), or *mGSTA4* heterozygous (+/-) and were identified by ear marking. Mice between 6-8 weeks of age were housed in plastic cages with 12h light/dark cycles at 25°C and given free access to food and water. All interactions with mice occurred on premises of the ARC. Tissues were harvested from mice after euthanasia via CO_2 suffocation and placed into microfuge tubes on ice and were stored in liquid nitrogen until use. Protocols relating to animal studies were approved by Institutional Animal Care and Use Committee.

Methods

Microbiology Techniques:

Growth of bacterial cultures: *Escherichia coli* bacteria (XL1-Blue , JM109, and DH5α strains) were grown in Luria-Bertani (LB) broth (Sigma) composed of 10g tryptone, 10g yeast extract, and 5g NaCl per liter. 5mL cultures were grown from frozen glycerol stock (derived from single colony) overnight and larger cultures were grown from these starter cultures at a 1:1000 dilution. Large cultures were grown either overnight (for plasmid yield) or over 4-8 h (for protein yield). Bacteria were grown in the presence of appropriate antibiotics (100μg/ml ampicillin or 30μg/ml kanamycin) to

ensure selection of plasmid-bearing cells. Cultures were shaken at ~150rpm at 37°C in sterilized vessels.

Transformation of bacteria with plasmid DNA: Introduction of plasmid DNA into bacterial stock was achieved by a heat-shock induction. Cells were obtained from UTMB Sealy center for Molecular Medicine Recombinant DNA Laboratory and thawed on ice for 30 minutes. Tubes were lightly agitated to resuspend bacteria and 100mL of this stock was pipetted into another microfuge tube, and remaining stock was refrozen at -80C. 1-10ng of plasmid DNA was added to bacteria and solution was gently mixed. Bacteria was incubated on ice for 30 minutes, and then heat-shocked at 42°C for 45 seconds, followed by a 1 minute rest on ice. 900mL of recovery medium (1.2% tryptone, 2.4% yeast extract, 0.4% glycerol, 10mM NaCl, 20mM $MgSO_4$) was added to bacteria and tubes were incubated at 37°C for 60 mins while shaking at 150-200 rpm. Aliquots of 50, 100, 200, and 650 μL were plated onto LB-agar plates containing appropriate antibiotics with Isopropyl β-D-1-thiogalactopyranoside (IPTG) and 5-bromo-4-chloro-3-indolyl-beta-D-galactopyranoside (X-Gal) for selection.

Purification of plasmid DNA from bacteria: Bacterial cultures were centrifuged at 5000g for 5-15 minutes after overnight agitation and pellets were used in purification according to Birnboim et al [287]. Commercial kits used were either Qiaprep Spin Mini (Qiagen) for small (<5mL cultures) or PureYield (Promega) for medium-sized (50-150mL) cultures. Briefly, pellets were reconstituted in a Tris/EDTA reconstitution solution and then lysed in a NaOH/SDS lysis buffer. Lysis proceeded for 5 minutes at room temperature and was halted by an guanidine HCl/acetate neutralization solution. Unprecipitated material from this lysis was separated either by centrifugation or vacuum filtering and loaded onto a silicate filter column where it passed through, allowing plasmid DNA to selectively bind (precipitate) to the filter. Filters were washed several times with alcohol/high-salt solutions to remove non-DNA material (such as endotoxin)

and plasmids were eluted into tubes using a low-salt (normally nuclease-free water) elution solution in either one or two steps. In addition, plasmid purification services from UTMB Sealy Center for Molecular Medicine Recombinant DNA Laboratory were employed for large-scale purification. In all cases, plasmid DNA of only high quality ($OD_{260/280}$ >1.8) was used for later experiments.

Purification of protein from bacteria: As large cultures were grown, samples were measured for optical density at 600nm in a UV/Vis spectrophotometer to approximate cell growth. When OD_{600} reached approximately 0.6 (against a LB medium blank), cultures were induced to express protein coded in plasmid genes by addition of 0.5 mM IPTG, a lacZ operon inducer, for 4-6 h. After this the cells were taken from the incubator and centrifuged at 5000 rpm for 5-10 minutes to pellet cells. Pellets were lysed via sonication in 10 mM $NaPO_4$ buffer, pH 7.4 and centrifuged at ~28,000g for 15 minutes to pellet insoluble material. Supernatant was assayed for GST activity against CDNB and loaded onto a GST affinity column to separate soluble GST protein. Columns were washed free of non-specifically bound protein until OD_{280} ~ 0 and then GST was eluted with high-salt buffer containing GSH. Fractions were assayed for concentration and GST activity. If necessary, eluent was concentrated using Centricon filter cartridges.

Molecular Biology and Cell Biology Techniques:

Determination of DNA/RNA concentration: Concentrations of DNA and RNA were determined on a Pharmacia Biotech UV/Visual spectrophotometer., which calculates a ratio of A_{260}/A_{280}. Only purified DNA samples with a (OD_{260}/OD_{280}) ratio between 1.8 – 2.0 were used in experiments, with 1 OD_{260} unit equal to 50μg/ml dsDNA and 1 OD_{260} equal to 40μg/ml ssRNA.

Reverse transcriptase PCR and quantitative RT-PCR: Cellular RNA was collected and purified using RNAqueous-4PCR kit (Ambion) according to manufacturer instructions and RT-PCR was performed using Enhanced Avian RT-PCR kit (Sigma) according to manufacturer instructions. Briefly, 5μL 10x PCR buffer (100mM Tris-HCl, pH 8.3, 500mM KCl), 3μL 25mM MgCl$_2$, 1μL deoxynucleotide mix (200μM each nucleotide), 1μL (20 units) RNAse inhibitor, 1μL (10 ng) RNA template, 1μL specific primers (forward and backward primers for *hGSTA4*, 100-1000ng/μL), 1μL (5 units) enhanced avian reverse transcriptase, 1μL (2.5 units) JumpStart LA AccuTaq DNA polymerase, and sufficient water to reach 50μL final volume were all added to thin-wall 200μL PCR tubes. Tubes were mixed, loaded into a PCR cycler, and run according to the following cycle: first-strand synthesis – 45°C – 50mins; denaturation/activation – 94°C – 2mins; (denaturation – 94°C – 15sec; annealing – 55°C – 30sec; extension – 68°C – 60sec) x 35 cycles; final extension – 68°C – 5mins; hold – 4°C – indefinitely. Samples of RT-PCR product of equal volume were observed on RNA agarose gel electrophoresis.

Quantitative RT-PCR was performed at the UTMB Sealy Center for Cancer Cell Biology under direction of Dr. Huiping Guo. Assays-On-Demand 20x assay mix of primers and FAM (5'-carboxyfluorescein) dye-labeled TaqMan MGB probes (Applied Biosystems, Foster City, CA) were employed with the selected genes and pre-developed 18S rRNA (VIC-dye-labeled probe) TaqMan assay reagent for endogenous control. Separate tube (singleplex) RT-PCR was performed with 80 ng RNA. The cycling parameters for one-step RT-PCR using TaqMan one-step master mix reagent kit (Applied Biosystems, Alameda, CA) were: reverse transcription at 48 °C for 30 min, AmpliTaq activation at 95 °C for 10 min, denaturation at 95 °C for 15 s, and annealing/extension at 60 °C for 1 min (repeated 40 cycles in total). Fluorescence excitation of FAM was at 494nm and fluorescence emission was at 520nm. Duplicate C_T values were analyzed in Microsoft Excel using the comparative C_T ($\Delta\Delta C_T$) method as described by the manufacturer. The amount of target ($2^{-\Delta\Delta C_T}$) was calculated and normalized to

endogenous reference (18S rRNA) and relative to a calibrator (one of the experimental samples).

Protein Determination: Protein concentration in samples was determined by the Bradford method [288]. Briefly, 100mg Coumassie Brilliant Blue G was mixed with 50 mL 95% methanol and 100 mL phosphoric acid (85%) and 850 mL dH_20 overnight, and then filtered through a Whatman #1 paper and stored at room temperature in a dark bottle. The assay factor was calculated via a bovine serum albumin standard curve.

SDS-PAGE: Slab-gel electrophoresis was performed essentially consistent with the method of Laemmli [289]. Basically, tris-glycine polyacrylamide gels were either prepared in-laboratory or were purchased (Invitrogen and Bio-Rad). All gels were of 12% polyacrylamide unless otherwise specified. Protein samples were prepared by boiling with SDS-PAGE sample buffer (1.25 mL Tris-HCl, 0.5M, pH 6.8, 0.15 mL 2-ME, 0.2 g SDS, 0.2 mL bromophenol blue, 0.1%, and 1.5 mL glycerol) for 3-5 minutes and then run at 125 V constant (Invitrogen Sure-Lock) or 100 V constant (Bio-Rad Mini-Protean) with all lanes holding equal volume to promote even dye front movement. Bio-Rad Broad-range Kaleidoscope protein marker was used unless otherwise specified.

Western blotting: SDS-PAGE gels were transferred to poly(vinylidene difluoride) (PVDF) or nitrocellulose membranes in Transfer Buffer (20% methanol, 25 mM Tris-HCl, pH 8.3, 190 mM glycine) at either 380 mA constant at 4ºC for 1.5 hours (Bio-Rad) or 35 V constant for 2.5 hours (Invitrogen X-Cell). After transfer the membrane was set to shake for 30 minutes in 5% (w/v) non-fat dry milk (NFDM) in 10 mM Tris, pH 7.4, 150 mM NaCl (TBS) at room temperature to block non-specific binding of antibodies to the membrane.

46

Immunodetection: Blocked membranes were placed in Tris-buffered saline (TBS) with 5% nonfat dry milk (NFDM) including primary antibodies overnight at 4°C or for 1-2h at room temperature, with mild shaking. The primary antibodies were then removed and the membrane washed thrice for 10 minutes each in TBS with 5% NFDM, and then treated with horseradish peroxidase (HRP)-conjugated secondary antibodies (Southern Biotech) diluted in TBS with 5% NFDM for 1 to 4 hours at room temperature. The secondary antibodies were removed and the membrane was again washed thrice for 10 minutes each in TBS with 5% NFDM. The bands were detected using SuperSignal (Pierce) chemiluminescent substrate and exposed on Hyperfilm ECL film (Amersham), as per manufacturer instructions.

Culture of HLE B-3 and RPE28 SV4 cells: Human lens epithelial cells (HLE B-3) and fetal male retinal pigment epithelial cells (RPE28 SV4) were cultured in complete growth medium (for RPE: DMEM supplemented with 10% fetal bovine serum, 1% penicillin/streptomycin, 5 mL 100x MEM non-essential amino acids (Sigma), 10 mM HEPES; for HLE B-3: MEM supplemented with 20% FBS and 0.1% gentamycin) at 5% CO_2, 95% humidified air at 37 °C. In these cell lines, medium was changed 2-3x weekly and cells were passaged as they approached confluence, according to protocols previously published by this laboratory [248, 290].

Preparation of eukaryotic expression vector: For overexpression of hGSTA4-4 protein in HLE B-3 and RPE28 cells, the open reading frame of *hGSTA4* was ligated into pTarget-T expression plasmid (Promega, Madison, WI) and verified using restriction enzyme digest. To improve expression of *hGSTA4* in RPE28 cells, the Kozak sequence [291] (-5 ACCATGG -3) was altered by site-directed mutagenesis at the Sealy Center Recombinant DNA Laboratory (UTMB) according to template sequence provided by our laboratory to return the correct sequence after ligation. hGSTA4-4 expression vector was transformed into XL 1-Blue strain of *E. coli* (Stratagene) and glycerol stocks were

prepared. For overexpression of mutant hGSTA4-4 lacking enzyme activity towards HNE (*hGSTA4* Y212F), site-directed mutagenesis was performed to change amino acid 212 tyrosine (Y) to phenylalanine (F).

Transient and stable transfection of RPE cells: 2×10^6 RPE cells were seeded into 10cm cell culture dishes in 10mL full medium and allowed to attach and grow overnight to between 60-80% confluence. Cells were then transfected with 10 μg of either empty pTarget-T plasmid, pTarget plasmid ligated with the ORF of *hGSTA4* with a restored Kozak sequence, or the Y212F mutant *hGSTA4* plasmid, using Lipofectamine PLUS reagents (Invitrogen, Carlsbad, CA) designed for transfection of adherent cell cultures and used as per manufacturer instructions (30 μL Lipofectamine, 60 μL PLUS reagent per 10cm dish) in serum-free medium. After 3 hours incubation, an equal amount of full medium containing 2X FBS without antibiotics was added to each dish to return FBS concentration to 1X. The medium was changed every 48h as necessary. Cells were rinsed 3x with cold PBS to remove medium and harvested on ice with cell scrapers (Fisher) when harvesting was required. For stable transfection, cells were selected after 48h in 600 μg/ml G418 antibiotic (Gibco) with medium replaced 2-3 times weekly until control (untransfected) RPE cells were completely dead, with G418 concentration confirmed via toxicity curve.

Gene microarray: Stably-transfected HLE B-3 cells were assayed for changes in gene expression using Affymetrix gene microarray. Briefly, empty vector- and *hGSTA4*-transfected cells (~2×10^6 in 10cm dishes) were harvested on ice using RNAqueous-4PCR kit (Ambion) as per manufacturers instruction, and RNA was quantified and measured for purity, then kept at -80°C until use. Samples of RNA were given to UTMB Molecular Genomics Core Facility to perform microarray analysis on samples. One microarray chip (Affymetrix Human Genome U133 Plus 2.0) was used per sample and four eukaryotic genes (*bioB*, *bioC*, *bioD*) from *Escherichia coli* biosynthetic pathway and *Cre*

48

recombinase gene from Bacteriophage P1 were added to the hybridization cocktail as internal controls. Chips were then scanned using a GeneChip scanner 3000 built with GeneChip operating software (Affymetrix). The array control and treated groups were scaled using the trimmed mean (excluding the highest and lowest 2%). Probe sets showing an absolute fold-change of at least 2.0 were selected and placed in functional groups. Twelve genes were selected from this group for further confirmation based on involvement in pathways relevant to procarcinogenic transformation and relative fold-change detected in microarray data.

Cytochemistry and immunocytochemistry: Transfected cells were visualized for both localization of protein expression and activation of caspase using fluorescence microscopy techniques. Briefly, approximately $5x10^4$ cells were grown on 4-chamber slides (Falcon) overnight and cultures were treated experimentally as described in later chapters. For cytochemistry: after treatment, cells were treated with 5 mM CaspACE-FITC-VAD-FMK caspase inhibitor (Promega) per chamber for 1h and then washed from cells. Chambers were removed from slides and slides were washed with PBS for 30 minutes. Cells were fixed with 4% paraformaldehyde in PBS for 30 minutes, and then washed for 30 minutes. Slides were covered with coverslips using Vectashield DAPI-containing mounting medium (Vector Labs) and sealed with clear nailpolish and kept at 4°C away from light. For Immunocytochemistry: after treatment, cells were fixed in 4% paraformaldehyde for 30 minutes and washed for 30 minutes, then incubated with 5 µg/mL Fas primary antibody for 2h at room temperature in 1% BSA blocking solution. After washing off primary antibody, 3µg/mL secondary FITC-conjugated antibody was incubated for 1h at room temperature with cells and subsequently washed off. Slides were covered with coverslips in Vectashield and sealed with clear nailpolish. Slides were viewed under fluorescence microscopes at the UTMB Infectious Disease and Toxicology Optical Imaging Core.

Enzyme assays: Protein concentration was determined for samples prior to conducting assays to calculate specific activity for all enzyme assays in these studies.

Determination of GST activity towards CDNB: Activity of GSTs to conjugate 1-chloro-2,4-dinitrobenzene (CDNB) was measured essentially according to Habig et al. [292]. Briefly, 20-50 μg of cell lysate was mixed with 50 μL 20mM CDNB, 100 μL 10mM glutathione, in a 100 mM phosphate buffer pH 7.4, and the conjugation of CDNB to GSH leading to the formation of yellow-colored *S*-(2,4-dinitrophenyl)-glutathione which absorbs light at 340nm.

Determination of GST activity towards 4-hydroxynonenal: Activity of GST to conjugate HNE was measured essentially according to Alin et al. [238]. Briefly, 20-50 μg cell lysate/tissue homogenate was mixed with 100 μL of 5mM glutathione, pH 6.5, and 780 μL of 100 mM phosphate buffer, pH 7.4, and the reaction was started by the addition of 100 μL of 10mM HNE solution suspended in PBS to give a final volume of 1mL. The conjugation of HNE to GSH was measured against a blank without sample at 224 nm to monitor consumption of HNE.

Determination of catalase activity: Catalase activity was determined essentially according to Beers and Sizer [293]. Briefly, cells were lysed in 50mM phosphate buffer, pH 7.0. A reaction mixture containing 30-90 μg of cell lysate and 633 μL of phosphate buffer was allowed to incubate at 25 degrees for 5 minutes. The reaction was initiated with the addition of 333 μL of 59 mM H_2O_2 in phosphate buffer, and the absorbance at 240nm was followed for 45 seconds against a blank without cell lysate. One unit of

activity is defined as the amount of enzyme which decomposes 1 μmol of H_2O_2 per minute at 25 degrees.

Determination of superoxide dismutase (SOD) activity: SOD activity was determined essentially according to the method of Paoletti and Mocali [294]. Briefly, cells were rinsed once with 10mM phosphate buffer and harvested in the same buffer on ice, sonicated, and centrifuged 22,000g for 30 minutes. From 10-200 μL of the supernatant was added to 0.8 mL triethanolamine-diethanolamine-HCl buffer, 40 μL 7.5mM NADPH, 25 μL 100mM EDTA, and 50 mM $MnCl_2$ in a semimicro cuvette. A blank was employed which contains phosphate buffer in place of cell homogenate. The reaction mixture was equilibrated to 25°C for 5 minutes and the reaction was started with the addition of 0.1 mL of 2-mercaptoethanol. The absorbance at 340nm was measured for 20 minutes and one unit of SOD activity was calculated as the amount of enzyme required to inhibit the rate of NADPH oxidation by 50% as compared to control.

Determination of glutathione peroxidase (GPx) activity: GPx activity was determined essentially according to the method of Paglia and Valentine [295], with slight modification [296]. Briefly, 980 μL of a reaction mixture containing 0.1 M potassium phosphate buffer, pH 7.0, 4mM EDTA, 0.2 mM NADPH, 1 unit glutathione reductase, 4 mM GSH, and 10-30 μg of cell homogenate was incubated at 37°C in a cuvette for 5 minutes, and the reaction was initiated with the addition of substrate, either 10 μL of 10mM H_2O_2 or 10 μL of 10 mM organic hydroperoxide (*t*-butyl or cumene). The absorbance at 340nm was measured for 4 minutes against a blank without enzyme and a blank without substrate, to account for all non-specific reduction of NADPH. One unit of GPx activity is defined as the amount which catalyzes the oxidation of 1 μmol of GSH to GSSG per minute at 37°C.

Nonenzymatic assays:

Determination of HNE concentration via spectophotometric analysis:
Intracellular HNE levels were determined using LPO-586 spectrophotometric kit (Oxis International, Foster City, CA) according to manufacturer instructions. Briefly, $1\text{-}2\text{x}10^7$ cells were rinsed and harvested in PBS at $\sim 5 \text{ x}10^7$ cells/mL via sonication for 15-30s. Cell lysates were centrifuged at 3000g for 10 minutes to pellet insoluble material, and divided into 200μL aliquots in microcentrifuge tubes. Standards for MDA and HNE were prepared and measured for absorbance at 586nm to construct a standard curve against which to compare absorbances for samples. 650μL of R1 reagent was added to each aliquot and mixed. Next 150μL of R2 reagent was added to each aliquot and mixed, then incubated at 45°C for 60 minutes. Then tubes were centrifuged at 14000g for 10 minutes to clear the precipitate, and each supernatant was pipetted to a cuvette. Absorbance was measured at 586nm to determine [MDA+HNE]. To measure [MDA] the assay was repeated with the 150μL R2 reagent step replaced with addition of 150μL 12N HCl.

Determination of cellular GSH concentration: Concentration of GSH in cell extracts was determined according to the method of Beutler [297]. Briefly, $\sim 10^7$ cells were lysed in 10mM phosphate buffer without 2-mercaptoethanol. Extracts were prepared and 200 μL of cell extracts were added to 300 μL precipitating solution (0.2 M glacial metaphosphoric acid, 5.1 M NaCl, 5mM EDTA) and incubated 5 minutes at 25°C. This reaction mixture was centrifuged at 22,000 g for 5 minutes to pellet precipitated proteins and the supernatant was removed. 200 μL of this supernatant was added to 800 μL of 0.3 N Na_2HPO_4 and the absorbance at 412 nm was measured. 100 μL of 5,5'-dithio-bis (2-nitrobenzoic acid) (DTNB) (0.02% in 1% sodium citrate) was then mixed

into the sample and the absorbance at 412 nm was once again measured. The concentration of GSH was calculated as follows: *[(absorbance with DTNB) – (absorbance without DTNB)] x (13.75 empirical factor) x (1000) / (13.6 molar extinction coefficient) = concentration of GSH in μM*; GSH (*μM*) ÷ *protein concentration (mg/mL) = nmol GSH/mg protein.*

Quantification of HNE levels by high performance liquid chromatography: $\sim10^7$ cells were assayed for intracellular HNE concentrations after being suspended in PBS (1 mL) and sonicated (3x10s, 30 W) on ice. Cell lysates were incubated with 2mL ice-cold 70% perchloric acid to precipitate proteins and centrifuged at 10000*g* for 10 min. The supernatants were extracted with 2 mL of dichloromethane (HPLC-grade) by gentle vortexing and subsequently centrifuged at 1500 rpm for 10 min. The organic layer was collected and dried under flow of nitrogen, resuspended in 100 μL of ethanol, and filtered through nylon 66 filters (Micron Separations Inc.). Filtrate was analyzed on Beckman Coulter System Gold HPLC equipment with visualization on a Beckman 168 photodiode array (PDA) detector, using a Beckman Ultrasphere (5 μm, 4.6 cm × 25 cm) C_{18} column using 70% sodium phosphate buffer (pH 2.6) and 30% acetonitrile as the mobile phase. HNE in the column eluate was monitored at 202 and 224 nm with the PDA detector and areas under peaks were recorded.

CHAPTER III – Morphological transformation of human lens epithelial cells upon 4-hydroxynonenal depletion by hGSTA4-4 overexpression and protective effects against oxidative stress

Introduction:

In recent years GSTs have acquired the status as important antioxidant enzymes. Mammalian Alpha-class GSTs have been shown to attenuate ROS-induced LPO and to protect cells from oxidative stress. GSTs, specifically GSTs A1-1 and A2-2, have been shown to protect against LOOH, while hGSTA4-4 protects cells from the toxicity of HNE by conjugating it to GSH. Earlier studies in our laboratory have shown that induction of GSTA4-4 protects lens against oxidative stress-induced cataract. Likewise it has been shown that hGSTA4-4-like activity is induced in RPE cells subjected to oxidative stress, suggesting its role in protection of retinal tissue against ROS toxicity. In previous studies in our laboratory, involving overexpression of GSTs which are capable of preventing the formation of LPO products, have shown effects on intracellular signaling and protection from apoptosis. In recent studies our investigation of *mGSTA4* overexpression in HL-60 cells showed changes in the response to HNE-induced apoptotic signaling, with significant protection from JNK activation, phosphorylation of c-Jun, binding of AP-1, caspase activation, and PARP cleavage [147]. These studies suggest that by modulating LPO, GSTs can regulate various signaling processes. We therefore hypothesized similar effects might be observed in HLE B-3 and RPE cells overexpressing the HNE-conjugating activity of hGSTA4-4 and used these cell lines to investigate effects of overexpression of *hGSTA4* and subsequent depletion of HNE on such signaling.

54

HLE B-3 and RPE cells: Human lens epithelial cells have been used previously in other laboratories as a model for oxidative stress research because their anatomical location puts them at a prime location for ROS production secondary to UV exposure, low vascularization, and maintaining homeostasis for the inner lens. The HLE B-3 cell line was characterized in 1994 by Usha Andley of University of Missouri St. Louis [298]. These cells were transformed with a SV-40/adenovirus hybrid, and their lifespan is approximately 75 population doublings. This cell line has been shown to be functionally and morphologically similar to native lens epithelium and has been utilized in numerous studies [299-303] as a model for oxidative stress research, including in studies by our laboratory [248, 304]. This cell line is applicable to such studies for these reasons and because of high relevance of oxidative stress-induced LPO to physiology and pathophysiology of ocular tissues.

Similar to lens epithelium, retinal pigmented epithelium is a tissue critical for proper visual function found in the eye. RPE is situated between the vascular and neural retinal layers where it acts as a filter/feeder layer protecting cells involved in the visual cycle, and as such is subjected to high levels of oxidative stress [305]. SV-40 virus-transformed retinal pigment epithelial line RPE28 SV4 was derived by the Coriell Cell Repositories (Camden, NJ) from fetal tissue. When sub-confluent the cells have epithelioid morphology similar to HLE B-3 and maintain the characteristic ability to phagocytize retinal outer rod segments, and do not become pigmented. These cells have no known set lifespan although have not been cultured past passage 60 by us. We have previously utilized this cell line twice as a model for research into LPO [290, 306] because it has been well characterized and RPE cells are a popular and obvious model for research involving oxidative stress and signaling [307-311] due to the physiologically UV-prone localization within mammals. These cells are applicable to these studies because they suitably approximate primary RPE cell physiology and are similar in morphology and physiology to HLE B-3, allowing a second model for comparative

analysis of the effects of modulation of HNE levels on cell signaling and possible phenotypic transformation.

Present studies:

Activities of antioxidant enzymes and GSH and HNE concentrations: Cells were characterized for their antioxidant enzyme environment to obtain a better understanding of their capabilities against oxidative stress and to verify their suitability as a model for these studies. Cells were assayed for antioxidant enzymes glutathione S-transferase activity (against HNE and CDNB), glutathione peroxidase, glutathione reductase, superoxide dismutase, catalase, gamma-glutamyl synthetase, and glucose-6-phosphate dehydrogenase, as well as for physiological concentrations of reduced glutathione and HNE **(table 4)**. The results of these studies indicate that both RPE28 SV4 and HLE B-3 have considerable physiological antioxidant capacities and therefore are suitable models for proposed studies in the area of oxidative stress-mediated LPO.

Table 4: Activities of antioxidant enzymes and GSH and HNE concentrations in HLE B-3 and RPE28 SV4 cell lines.

Parameter	HLE B-3	RPE28 SV-4
SOD	8.13 U ± 0.747	7.16 U ± 0.948
CAT	0.490 U ± 0.020	0.614 U ± 0.064
GPx: H_2O_2	0.027 U ± 0.011	0.022 U ± 0.007
GST: CDNB	0.119 U ± 0.005	0.088 U ± 0.007
GST: HNE	0.056 U ± 0.015	0.076 U ± 0.018
GSH	81.64 ± 5.11 (nmol/mg protein)	58.74 ± 2.04 (nmol/mg protein)

HNE	38.0 (pmol/mg protein)	48.5 ± 6.95 (pmol/mg protein)

U=units (μmol/min·mg protein).

Transfection of HLE B-3 cells with *hGSTA4*

Construction of hGSTA4 expression vector: To achieve overexpression of *hGSTA4* in HLE B-3 it was necessary to construct an expression vector which could be transfected into the cells. We have previously employed other expression vectors in our research for the purpose of overexpression of GSTs in mammalian cell lines, although recently we have found pTarget-T (Promega) to have high transfection efficiency in both suspended and adherent cell lines. pTarget contains an ampicillin resistance gene for effective prokaryotic selection after transformation, as well as a neomycin resistance gene for effective eukaryotic selection after transfection. In addition, this plasmid contains a SV40 enhancer/promoter and a cytomegalovirus (CMV) enhancer/promoter to facilitate sequencing and to maximize transcription, and therefore both copy number and protein yield. The polylinker site has sequence targets for 11 restriction enzymes and there are thymidine overhangs on the 3' and 5' ends to facilitate ligation of inserts, and in addition 2 lacZ operons for color selection via IPTG/X-GAL.

Confirmation of stable overexpression of hGSTA4 and depletion of HNE: As previously described in the Methods section, conditions for stable transfection were optimized using the Profection kit (Promega), which utilized a calcium phosphate system for introduction of plasmid DNA into adherent cells. As is often the case with transfection, previous attempts using different kits such as Lipofectamine PLUS (Invitrogen), which utilized lipid vesicle systems, were unsuccessful. Briefly, $\sim 8 \times 10^5$ cells were plated to achieve 30-60% confluency in 10cm culture dishes. Three hours

prior to transfection the medium was replaced with fresh serum-free medium, and reagents were thawed to room temperature and DNA was thawed on ice. 10μg plasmid DNA was added to 62μL 2M CaCl$_2$ in a microfuge tube along with H$_2$O to a volume of 500μL and allowed to mix, and then 500μL HEPES-buffered saline was added dropwise to the DNA to precipitate the calcium phosphate-DNA product. This was resuspended in solution and added dropwise to the cells and allowed to incubate for 4h, when a 10% dimethylsulfoxide (DMSO) shock was performed for 45-60s. Afterwards cells were allowed to rest until harvested or until stable selection occurred 24-48h later. However once conditions were optimized using 10μg double-stranded plasmid DNA, transfected HLE B-3 reliably and reproducibly expressed hGSTA4-4 protein as confirmed by Western blot. Transfected cells were harvested 48h post-transfection in 10cm dishes, and 50μg samples were loaded onto SDS-PAGE gels and immunoblotted for hGSTA4-4 expression. For appropriate control, we used an inactive mutant of hGSTA4-4 for these studies. This *hGSTA4* mutant with a single amino acid mutation, in which switching tyrosine 212 to phenylalanine results in almost complete loss of activity against HNE but not towards other GST substrates such as CDNB, was reasoned to be the best possible control [312] for these studies because of its structural and immunological similarities to WT recombinant hGSTA4-4. As is seen in **(figure 10)**, expression of both active hGSTA4-4 and inactive mutant hGSTA4-4 protein is evident in HLE B-3 after transfection, far higher than is normally expressed in this cell line, confirming overexpression. It is important to note that in extrahepatic tissues, alpha-class GST isozymes are normally not detected by Western blot as their expression is very low; RT-PCR analysis, a more sensitive assay technique, is sufficient to detect expression.
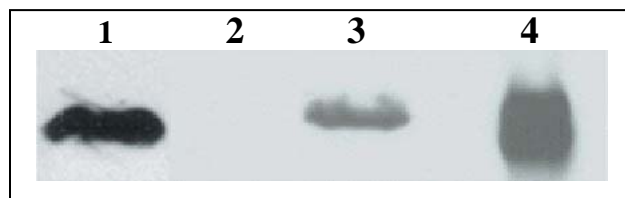
Figure 10: Expression of hGSTA4-4 in HLE B-3 cell lines. *lane 1*, Y212F inactive mutant *hGSTA4*-transfected line. *lane 2*, WT cell line. *lane 3*, *hGSTA4*-transfected line. *lane 4*, hGSTA4-4 positive control. Adapted from [173] with permission.

After determining overexpression of *hGSTA4* in HLE B-3 it was necessary to determine whether HNE-conjugating activity of hGSTA4-4 had affected intracellular levels of HNE. Steady-state levels of HNE were measured via spectrophotometric analysis to determine whether HNE depletion was achieved in HLE B-3 cells, which would indicate an increase of HNE-conjugating hGSTA4-4 activity. Each population was grown to at least $2x10^7$ cells, harvested on ice, and HNE was extracted according to LPO-586 kit (Oxis) manufacturer's protocol. Using this spectrophotometrically-based method to measure intracellular HNE concentrations it was observed that steady-state HNE levels in *hGSTA4*-transformed HLE B-3 had decreased by roughly 50% as compared to WT or vector-transfected cells **(figure 11),** while inactive mutant *hGSTA4*-transfected cells elicited only a very minor decrease in HNE. This showed that overexpression of *hGSTA4* was sufficient to dramatically deplete intracellular HNE levels in HLE B-3 cells relative to WT, while stable transfection with empty vector or inactive *hGSTA4* mutant did not cause such depletion.
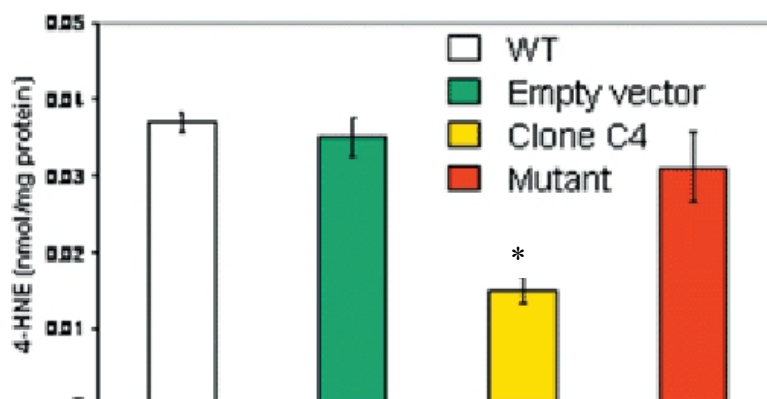
Figure 11: Decrease of HNE concentration in hGSTA4-transfected HLE B-3 cells. Depletion of HNE occurs in *hGSTA4*-transformed cells but not WT, VT, or inactive mutant *hGSTA4*-transformed cells. Concentration of HNE in HLE B-3 cells measured spectrophotometrically via LPO-586 (Oxis). Mean +- standard deviation, n=3. Adapted from [173] with permission. *significantly lower than WT, $P < 0.05$.

Effects of stable hGSTA4 transfection: During the first several days post-transfection we did not observe any significant morphological changes in HLE B-3 **(figure 12Aa and b)** However, approximately 2 weeks after stable transfection, with transfected cells being selected via G418 at a dose toxic to WT HLE B-3, cells began exhibiting an unusual morphological phenotype compared to normal physiological HLE B-3 morphology **(figure 12Aa)**, spreading outwards on the cell culture dish substrate and becoming slightly less spindle-shaped **(figure 12Ab)**. This spreading continued until at 4 weeks cells became very wide and flattened, and unlike their WT epithelioid, fibroblast-like counterparts **(figure 12Ac)**. During this time the cells stopped dividing and were senescent, although did not give an outward appearance of cell death. By 8 weeks post-transfection the attached cells were budding off 'ghost' cells as blebs of their outer membrane **(figure 12Ad)**, which were recoverable in media but not viable.   This continued for some time afterwards until these 'ghost' cells budding off of the main blast-like attached parent cells became viable and were collected in medium and cultured on their own. These budded cells were not attached to the substrate as their WT or vector-transfected counterparts were, and were smaller and rounded shape **(figure 12Ae)** in

60

contrast to the spindle-shaped untransformed cell lines **(figure 12Aa)**. In order to confirm expression of hGSTA4-4 protein in transfected cells *in situ* we employed fluorescence microscopy techniques. Cells transfected with both active and inactive *hGSTA4* were plated on cover slips and fixed with 4% paraformaldehyde. Cells were then incubated with anti-hGSTA4-4 antibodies for 1h and rinsed, then incubated with fluorescent fluorescein isothiocyanate (FITC)-conjugated secondary antibodies, rinsed, and visualized under fluorescence microscopy. Both the active hGSTA4-4-expressing transformed **(figure 12Ba-p and a-f)** and inactive mutant hGSTA4-4-expressing non-transformed **(figure 12Bm-p and m-f)** HLE B-3 cells expressed recognizable protein, indicating that lack of transformation by inactive mutant *hGSTA4*-transfected cells was not due to lack of protein expression. In addition it was observed that these *hGSTA4*-transfected HNE-decreased cells grew at an accelerated rate, with doubling time decreasing by more than 50% from approximately 50h to approximately 20h, and acquired immortality in contrast to the WT HLE B-3 which continued to grow as attached cells with limited lifespan.

Figure 12: Morphological transformation in HLE B-3 cells after stable transfection with active hGSTA4. A, Transformation of hGSTA4-transfected cells. (a) Control cells; (b) cells 2 weeks after hGSTA4 transfection; (c) growth arrest and enlargement of cells 4 weeks after transfection; (d) budding of small rounded cells from giant cells 8 weeks after transfection; (e) anchorage-independent growth of transformed rounded cells. **B**, Transfection with WT-hGSTA4 and Y212F mutant hGSTA4 with no activity towards HNE. (a-p) phase contrast micrograph of transformed cells after transfection with WT-hGSTA4; (a-f) fluorescence micrograph showing expression of WT-hGSTA4-4 in transformed cells detected using hGSTA4-4 antibodies; (m-p) phase contrast micrograph of cells 8 weeks after transfection with mut-GSTA4; (m-f) fluorescence micrograph showing expression of mut-hGSTA4-4 in transfected, nontransformed cells. Adapted from [173] with permission.

62
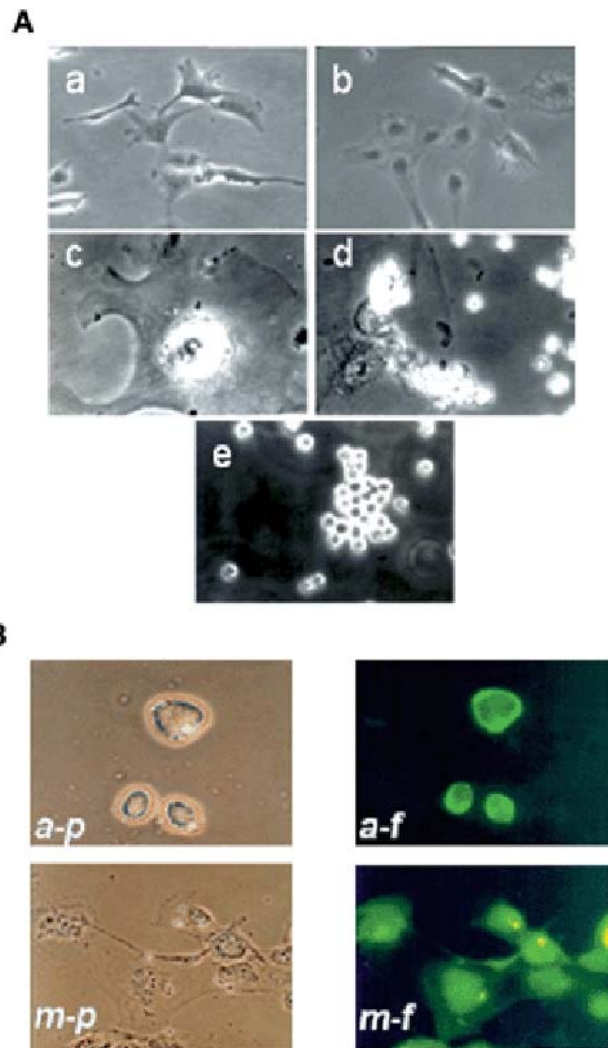
Microinjection studies: The possibility that the method of overexpression of *hGSTA4* in the cells contributed to the physiological changes was examined by using direct microinjection of recombinant hGSTA4-4 into WT cells in both nuclear and cytoplasmic localization. For these studies the collaborative help of Dr. David Brown, an expert in microinjection techniques was acquired. Cells were plated in 35mm dishes and recombinant proteins (WT and mutant hGSTA4-4, mGSTA4-4, hGSTA1-1, and hGSTP1-1) were amplified in *E. coli* bacteria, purified via affinity chromatography, dialyzed against an isotonic buffer, and mixed with an inert fluorescent dextran marker to facilitate visualization of microinjection. Needles pulled to an outer diameter of ~2.5-3 μM were used to manually inject cells with a volume of ~5 fL of either protein/dextran or plasmid DNA/GFP for cytoplasmic or nuclear injections, respectively, with 75 cells injected per dish for each separate set, with each set repeated at least twice. Controls for nuclear injection were green fluorescent protein (GFP) plasmid (eGFP, Stragatene) and empty pTarget vector, and controls for cytosolic injection were inactive mutant hGSTA4-4, hGSTA1-1 and hGSTP1-1 (isozymes possessing only minor HNE-metabolizing activity). Injected cells were monitored after injection under phase microscopy to determine morphological changes and/or apoptosis. The same morphological alterations occurred in HLE B-3 after the microinjection as were seen after transfection. Cells microinjected with active hGSTA4-4 were observed to round up and assume a smaller diameter than untransfected HLE B-3 (**figure 13Aa-p and a-f**), while cells microinjected with inactive hGSTA4-4 showed no such change (**figure 13Am-p and m-p&f**). This implies that the effects were due to the presence of the protein and not any side-effects of the gene uptake.

Furthermore, it was investigated whether it was the increased activity in these cells against HNE which contributed to the transformation or rather some other effect of overexpression of *hGSTA4*. Cell nuclei were microinjected with plasmid DNA which was used for previous transfection studies, along with coinjection of plasmid containing GFP to confirm uptake and expression of DNA. Similar to protein microinjection, DNA microinjection with active *hGSTA4*-bearing plasmid elicited a phenotypic transformation in cells **(figure 13Ba-p&f and a-f)** while microinjection with inactive *hGSTA4*-bearing plasmid showed no change in morphology **(figure 13Bm-p and m-f).** Fluorescence of GFP visualized by fluorescence microscopy indicated that genes encoded on coinjected marker eGFP plasmids (and therefore those on *hGSTA4* plasmids) were transcribed and translated in the cells. It is noteworthy that not all of the injected HLE B-3 responded to introduction of active hGSTA4-4 by transformation. A proportion of these cells underwent apoptosis after microinjection **(figure 13C)**, possibly due to variations in susceptibility due to cell cycle or unseen problem with technique. However, this proportion was small and the vast majority of cells microinjected with hGSTA4-4 underwent morphological transformation **(figure 13D)**, with small number either remaining untransformed or undergoing cell death afterwards. This is compared with almost all cells microinjected with inactive mutant hGSTA4-4 remaining untransformed or undergoing apoptosis. The phenomenon of transformation in microinjected cells occuring much more rapidly than in cells following normal transfection (which occurred over a period of weeks) is as yet unexplained. This may be due to some ability of HLE B-3 cells to resist the effects of *hGSTA4* overexpression via this mechanism as opposed to the bypass of cellular integrity via injection, and its exploration may in the future yield insight regarding the mechanistic basis of this transformation.
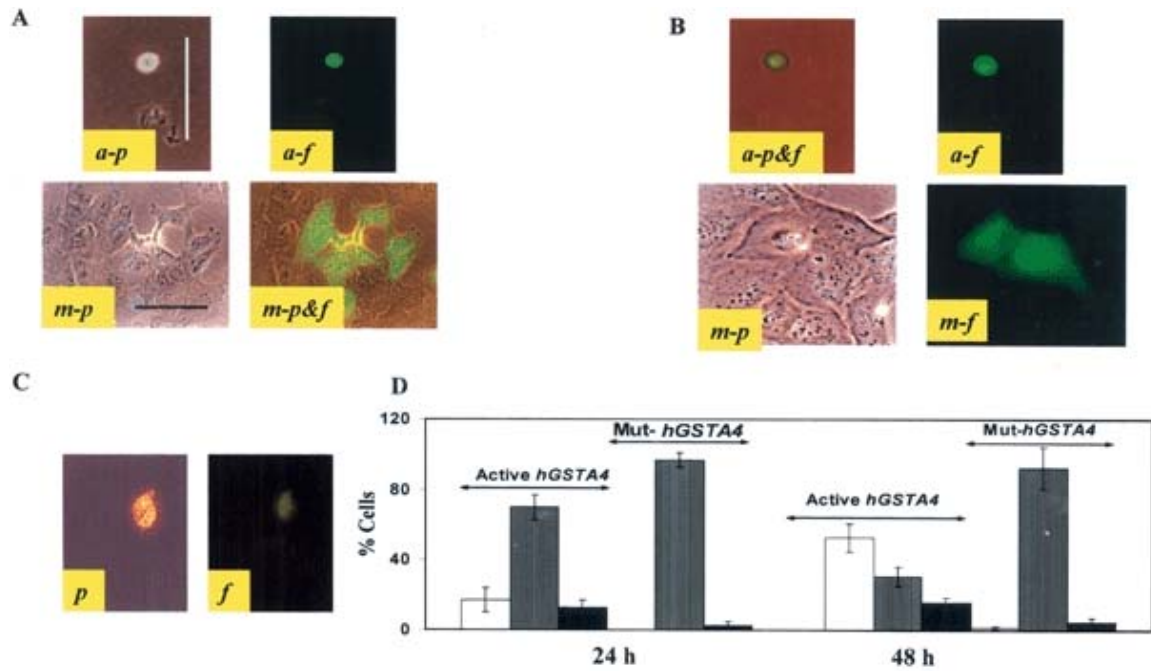
Figure 13: Morphological transformation in HLE B-3 cells after microinjection with active hGSTA4-4 recombinant protein. **A**, (*a-p*) Phase contrast micrograph of transformed cell 24 h after cytosolic microinjection with WT hGSTA4-4; (*a-f*) fluorescence micrograph of same cell showing coinjection of OG-dex fluorescent marker; (*m-p*) phase contrast micrograph of cell after microinjection with inactive mut-hGSTA4-4 protein; (*m-p&f*) combined phase contrast micrograph and fluorescence micrograph. Bar denotes 30 μm. **B,** (*a-p&f*) Combined phase contrast micrograph and fluorescence micrograph of transformed cell 24 h after nuclear microinjection with WT-*hGSTA4* and the marker eGFP cDNAs; (*a-f*) fluorescence micrograph of same cell; (*m-p*) phase contrast micrograph of cells 24 h after microinjection with inactive mut-*hGSTA4* and eGFP cDNAs; (*m-f*) fluorescent micrograph of same cells. **C,** A small percentage of hGSTA4-4 microinjected cells undergo apoptosis. (*p*) phase contrast micrograph of apoptotic cell; (*f*) fluorescence micrograph of same cell. **D,** Quantitation of transformed (unfilled bars), nontransformed (grey bars) and apoptotic cells (black bars) after microinjection with WT-*hGSTA4* or mut-*hGSTA4* expression vectors. Adapted from [173] with permission.

Studies with CCL-75 cells: To investigate whether hGSTA4-4-induced transformation was a cell type-specific phenomenon or was capable of occurring in similar attached lines, we switched models to human lung fibroblast line CCL-75 and performed microinjection of hGSTA4-4 recombinant protein as was done in HLE B-3. CCL-75 (also listed as WI-38) is a normal lung fibroblast line of limited lifespan taken from fetal tissue, similar in morphology to HLE B-3, and used in numerous studies involved in oxidative stress [313-316]. It was used as an experimental model primarily to

determine if such phenotypic effects were dependent on previous viral transformation of the cell model.

CCL-75 cells were plated onto culture dishes and microinjected using methods identical to those with HLE B-3, using both active and inactive hGSTA4-4. Similar to the results obtained with HLE B-3, it was observed that CCL-75 cells also became rounded and detached from the substrate surface within 72h of microinjection. This transformation occurred after both cytosolic microinjection with protein **(figure 14Aa-p and a-f)** and nuclear microinjection with plasmid DNA **(figure 14Ab-p and b-f)**. In CCL-75 transformation was observed approximately 72h post-microinjection, as opposed to HLE B-3 cells which transformed within 24h post-microinjection. The reason for the relative delay in transformation is not known. It can be speculated that it could be due to cell type-specific differences in physiological intracellular levels of HNE or regulatory pathways involving cell anchorage. This delay also may be related to the relative resistance of this cell line to transformation after microinjection. Relatively fewer CCL-75 cells were observed to become rounded and detached after microinjection with active hGSTA4-4 **(figure 14B)** although as time passed this proportion increased, which was not the case with cells microinjected with inactive mutant hGSTA4-4 **(figure 14C)**, which remained untransformed. Nuclear microinjection proved the most efficient for transformation, resulting in proportions similar to those seen in HLE B-3 cells, with slightly less transformation after 48h due to previously-mentioned delay **(figure 14D)**. Results of these studies suggest that transformation of cells due to introduction of superphysiological levels of hGSTA4-4 is not restricted to HLE B-3 and therefore may be a general phenomenon of HNE depleted cells.
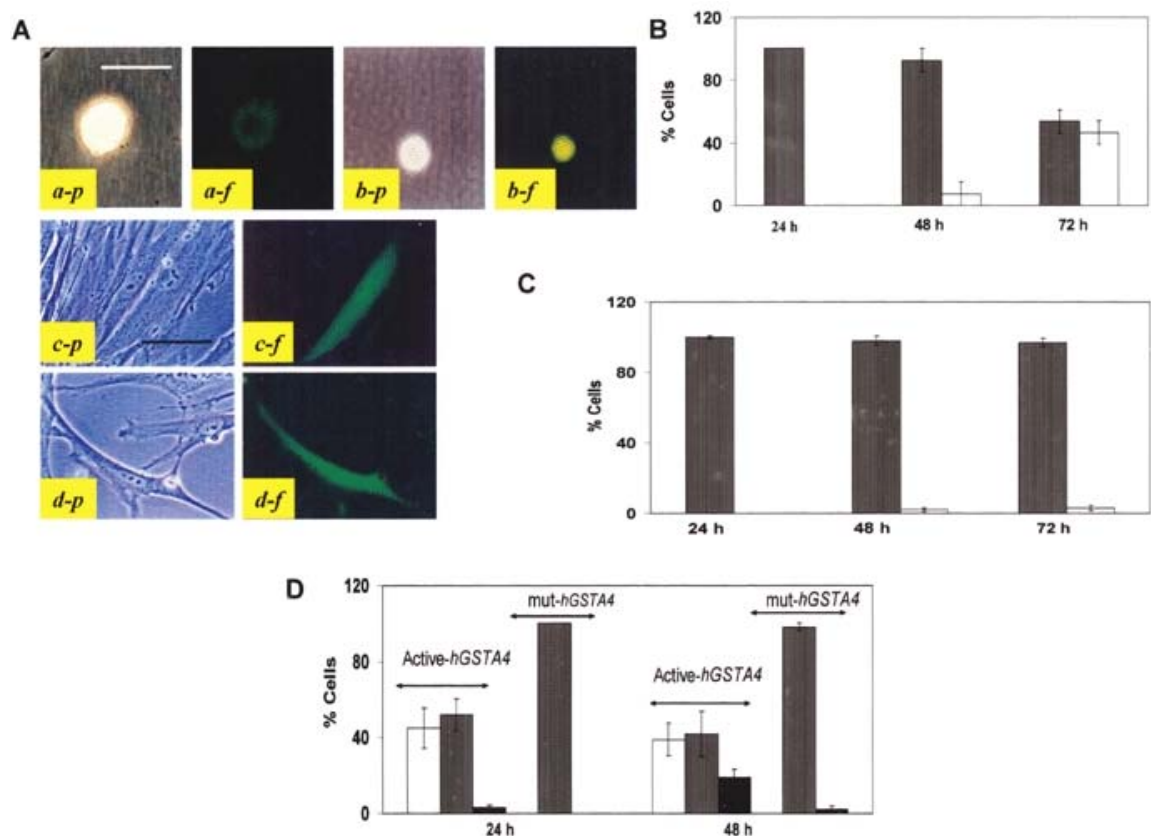
Figure 14: **Morphological transformation in CCL75 fibroblasts after microinjection of active hGSTA4-4 recombinant protein.** **A,** *a-p* is phase-contrast of cytoplasmic microinjection. *a-f* is fluorescence of OG-dextran from cytoplasmic microinjection. *b-p* is phase-contrast of nuclear microinjection. *b-f* is fluorescence of OG-dextran from nuclear microinjection. *c-p* is phase contrast of mut-hGSTA4-4 cytoplasmic microinjection. *c-f* is fluorescence of mut-hGSTA4-4 microinjection OG-dextran. *d-p* is phase contrast of mut-hGSTA4-4 nuclear microinjection. *d-f* is fluorescence of mut-hGSTA4-4 nuclear co-microinjection w/eGFP. **B-D,** percentage of transformed (empty bars), untransformed (gray bars), and apoptotic (black bars) cells after microinjection. **B,** microinjection of active *hGSTA4*. **C,** microinjection of mutant *hGSTA4*. **D,** nuclear microinjection. Adapted from [173] with permission.

Effect of microinjection of other GST isozymes: The cause of the previously-observed phenomenon of transformation due to expression of higher-than-physiological levels of GST in cells was still unclear. Therefore we investigated whether or not other isoforms of GST which are actually expressed in tissues could elicit transformation and whether the transforming effect of these physiologically-relevant GSTs were correlated

with their ability to deplete HNE. Cells were subjected to cytoplasmic microinjection (using the same protocols as previous HLE B-3 microinjection studies) of two human GSTs, hGSTA1-1 (from the same Alpha class of GST as hGSTA4-4*)* and hGSTP1-1 (a highly-expressed Pi-class isoform), both with relatively low catalytic efficiencies for HNE conjugation. Observation of microinjected cells showed that overexpression of neither hGSTA1-1 **(figure 15A)** or hGSTP1-1 **(figure 15B)** caused measurable changes in HLE B-3 morphology, with proportions of transformed cells almost zero **(figure 15C)**. This strengthened the suggestion that the presence of superphysiological HNE-conjugating activity was most likely the factor responsible for the transformation of HLE B-3 or CCL-75 cells.

Conversely, microinjection with other GSTs having high catalytic efficiency against HNE yielded results similar to those observed with hGSTA4-4. Two enzymes from non-human organisms, mGSTA4-4 (a *Mus musculus* Alpha-class GST) and DmGSTD1-1 (a *Drosophila melanogaster* Delta-class GST), have been previously characterized to utilize HNE as a preferred substrate [317, 318]. We microinjected these proteins into HLE B-3 using the same protocol as before, and results of these studies showed that overexpression of both mGSTA4-4 **(figure 16A)** and DmGSTD1-1 **(figure 16B)** were sufficient to elicit a transformation from adherent to rounded, floating cells, with proportions of transformed cells becoming the majority by 48h **(figure 16C)**, similar to results after microinjection with HNE-specific hGSTA4-4. These results further implied that irrespective of species origin, the GST isozymes having high activity towards catalyzing HNE conjugation to GSH (and thereby ability to deplete HNE) can cause transformation of these cells.

68
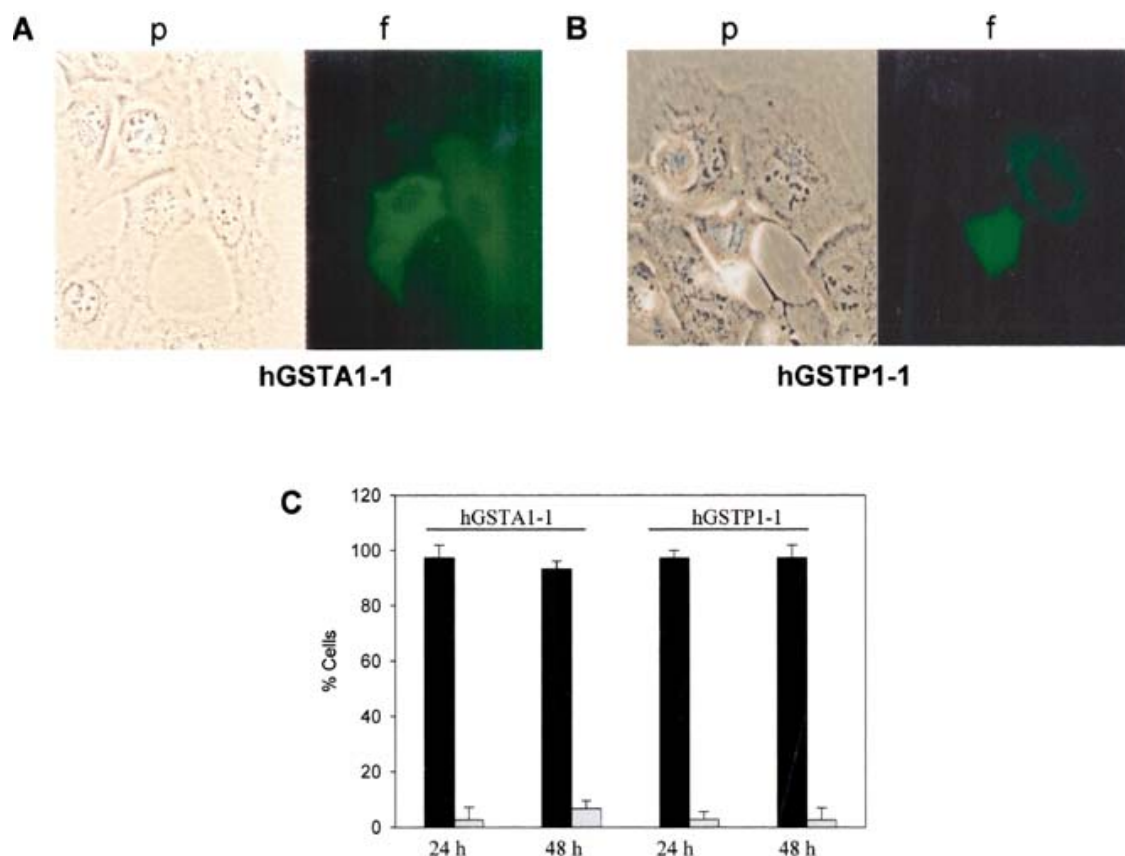
Figure 15: Absence of morphological transformation in HLE B-3 cells after microinjection of active hGSTA1-1 or hGSTP1-1 recombinant protein, with low activity against HNE. **A,** hGSTA1-1-microinjected cells 48h post-microinjection: *(p)* phase-contrast micrograph of cells, *(f)* fluorescence micrograph of same field. **B,** hGSTP1-1-microinjected cells 48h post-microinjection: *(p)* phase-contrast micrograph, *(f)* fluorescence micrograph of same field. **C,** count of hGSTA1-1- and hGSGTP1-1-microinjected cells 24h and 48h post-microinjection. Black bar=nontransfected cells, White bar=transformed cells. Adapted from [173] with permission.
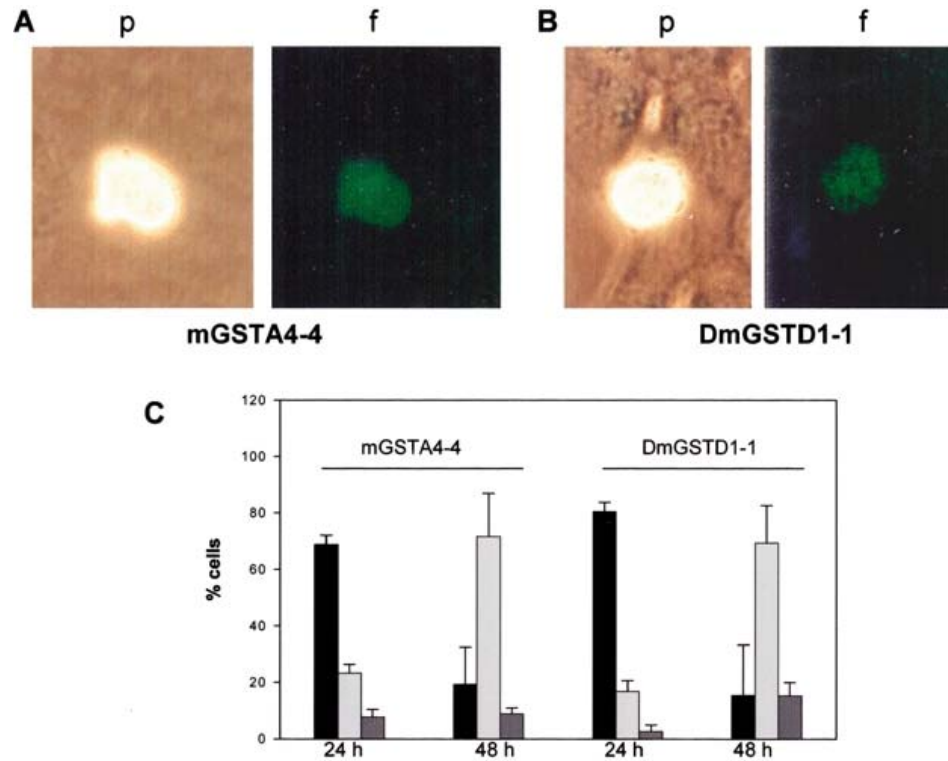
Figure 16: Morphological transformation in HLE B-3 after microinjection of mGSTA4-4 and DmGSTD1-1, GST enzymes active against HNE. A, Typical mGSTA4-4-microinjected cell: *(p)* phase-contrast microscopy, *(f)* is fluorescence microscopy of GFP/GST coinjection. **B,** Typical DmGSTD1-1-microinjected cell: *(p)* phase-contrast microscopy, *(f)* is fluorescence microscopy of GFP/GST coinjection. **C,** Percentage of microinjected cells undergoing transformation: Black bars=untransformed cells, light gray bars=transformed cells, dark gray bars=apoptotic cells. Adapted from [173] with permission.

Studies with RPE cells: Our investigations involving CCL-75 allowed us to determine whether transformation due to HNE depletion was a phenomenon capable of occurring in a non-virally-transformed cell line. However the functional differences between that line and HLE B-3 led to investigation of this phenomenon in a more similar cell line. In an attempt to determine whether overexpression of *hGSTA4* could cause transformation of cells with similar physiological function and location, we utilized retinal pigment epithelial line RPE28 SV4 as a model. Using similar conditions we

70

transfected this line both stably and transiently with empty pTarget vector and pTarget/*hGSTA4* and observed these cells for morphological transformation.

RPE cells were stably transfected using Lipofectamine PLUS (Invitrogen) liposome-based kit with 10 μg plasmid DNA per $2x10^6$ cells in 10cm cell culture dishes, after standardizing the transfection technique. Initially the same methods were attempted to overexpress *hGSTA4* in this cell line as was successfully used in HLE B-3, however this proved unsuccessful at any parameter. Additionally, RPE appear to be more susceptible to transfection-induced toxicity than HLE B-3 as there was more cell death observed (for both vector- and *hGSTA4*-transfected cells) after overexpression. To verify *hGSTA4* overexpression at both transcriptional and translational levels, RT-PCR and Western blot analyses were performed on transfected cells. RPE transfected in 10cm dishes were harvested 24-48h post-transfection in RNAqueous resuspension buffer (for RT-PCR) or radioimmunoprecipitation (RIPA) buffer (for Western blot) and processed accordingly. Briefly for RT-PCR analysis, ~10ng high-quality RNA was placed in a PCR tube along with reverse transcriptase, deoxynucleotides, Taq DNA polymerase, RNase inhibitor, $MgCl_2$, and PCR buffer according to manufacturer instructions for Enhanced Avian HS one-step RT-PCR (Sigma) and run according to protocols published in Methods section with 1 cycle of reverse transcription followed by 35 cycles of PCR and 1 final extension using primers specific for the open reading frame of *hGSTA4*. Aliquots of DNA were run on agarose gel electrophoresis to confirm expression of *hGSTA4* transcripts. Western blots were performed identically to studies with HLE B-3. Results confirmed that RPE was capable of overexpression of *hGSTA4* relative to WT at the parameters utilized for these studies at the level of transcription and translation after transfection with *hGSTA4* **(figure 17)**. For stable transfection, RPE cells were selected for *hGSTA4* overexpression via constant incubation with 600 μg/mL G418 antibiotic, after determining necessary concentration via toxicity curve, for approximately 10-14 days until all untransfected control cells treated with selection agent had died. Selection of RPE was essentially the same as selection of stably-transfected HLE B-3. For

71

transient transfection, this selection was not performed as cells were harvested within days. Cells existed as a mixture of populations due to insufficient clonal proliferation and therefore transfection efficiency was not quantifiable (although via microscopy studies efficiency was estimated to be similar to that achieved in HLE B-3). Unfortunately, there were not enough stably-transfected RPE remaining in cultures to harvest sufficient quantities of RNA or protein to measure overexpression of *hGSTA4* over longer periods after transfection, although continued survival in selection medium containing normally toxic concentrations of antibiotic suggests that cells expressed antibiotic resistance protein coded on plasmid vector and therefore it is likely that they continued to express *hGSTA4*.
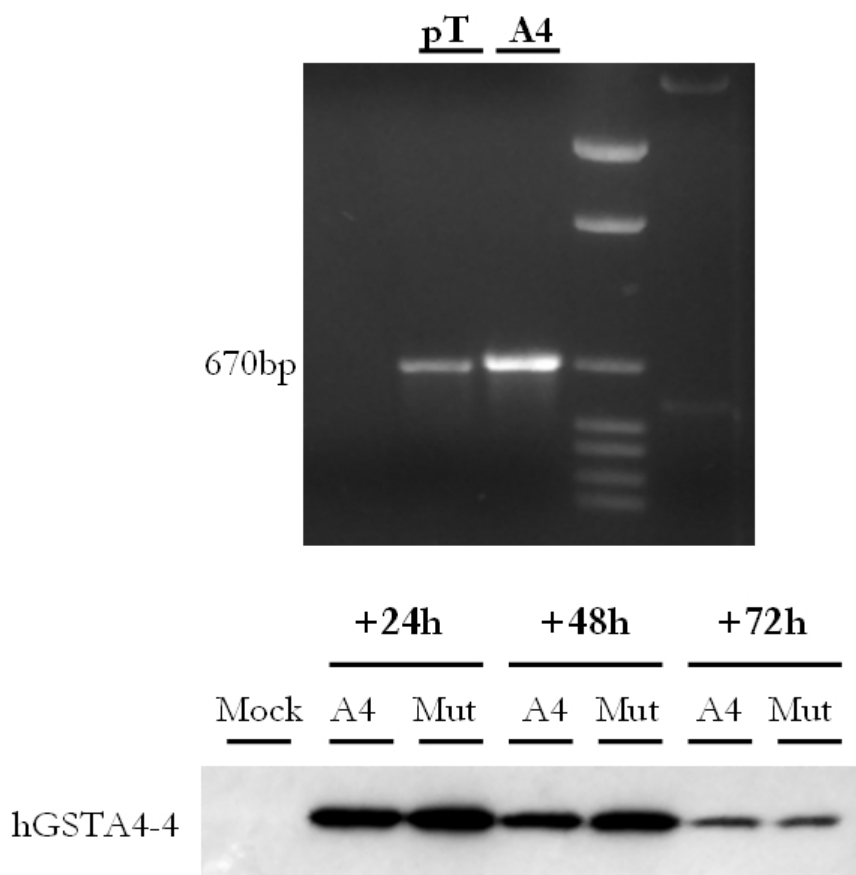
Figure 17: Confirmation of hGSTA4 overexpression in RPE via RT-PCR. Above, DNA was run on 1.5% agarose gel at 10V/cm. *Lane 1,* vector-transfected cells. *Lane 2, hGSTA4*-transfected cells. *Lane 3,* pGEM ladder (Promega). *hGSTA4* open reading frame is ~670bp in length. **Below**, 12% polyacrylamide gel electrophoresis of 30μg protein sample of WT *hGSTA4*- and mutant *hGSTA4*-transfected RPE 24-72h after transient transfection.

After determining overexpression of *hGSTA4* in transfected RPE, cells were assayed to determine if intracellular HNE levels had been affected. Transiently-transfected cells (transfected using exact protocol as for stable transfection without selection) were harvested in hypotonic phosphate buffer 24, 48, and 72h post-transfection, assayed for protein concentration, and twice extracted with dichloromethane to separate organic HNE from lysate. 20 μL samples containing HNE were quantified by high performance liquid chromatography (HPLC) using a C_{18} column connected to a photodiode array detector. For this assay, approximately 1.0-2.0 x10^6 cells were used as this was the number remaining after transient transfection; this number is sufficient to achieve a strong signal for HNE identification. The HNE peak came at approximately 14.25 minutes (correlated to an HNE standard run for each assay) and was usually well-separated from other peaks as it was taller and usually surrounded only by low peaks. Results of these studies showed that HNE was strongly depleted with respect to mock-transfected as well as inactive mutant *hGSTA4*-transfected controls in *hGSTA4*-transfected RPE cells up to 72h post-transfection **(figure 18)**. These results suggest that the underlying physiological change which caused transformation in HLE B-3 (depletion of intracellular HNE) does occur in RPE consequent to overexpression of HNE-metabolizing activity.
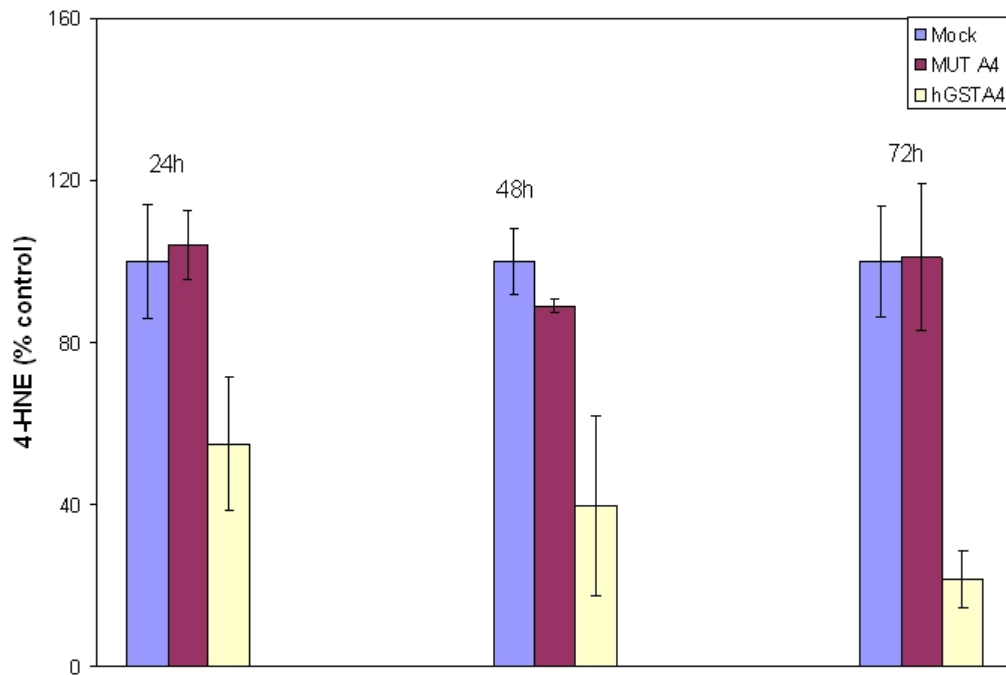
Figure 18: Depletion of HNE in RPE cells after transient overexpression of *hGSTA4*. RPE cells were transiently transfected with either *hGSTA4* or mutant *hGSTA4* and harvested 24-72h later. HNE was twice extracted with dichloromethane and measured via HPLC. Values were normalized to both protein concentration and mock-transfected (transfection without DNA) control values. n=3.

After stable transfection, RPE cells were observed to go through similar long-term senescence as was observed in HLE B-3. Cells were viewed under inverted light microscope every few hours after transfection for 3 days and at least once per day thereafter for several weeks until it became apparent that no further physiological changes were likely to occur in cultures. Numerous attempts were made at colony selection using both serial dilution and selection cylinder techniques, although in all cases no cells survived the procedures. In neomycin (Geneticin/G418, 600μg/mL, Gibco) resistance-selected transfected RPE cells it was observed that flattening and spreading consistently occurred in between 40-50% of the population over the same period post-transfection as was noted in HLE B-3 cells **(figure 19A-C)**. Also similar to HLE B-3

was the shedding of nonviable 'ghost' cells into medium for a period of weeks, in numbers that exceeded cell populations. However, after several weeks of culture, during which medium was changed 3 times per week and cells were observed daily, these transfected cells did not become proliferative, and eventually underwent apoptosis. Transient *hGSTA4* transfection did elicit very minor, although probably physiologically insignificant, morphological changes in cells relative to WT or empty vector-tranfected cells **(figure 19D-F).** However, this lack of striking changes is not surprising since the timecourse of experiments involving transient transfection were at most 240 h, while earliest morphological events visible via phase-contrast microscopy for phenotypic transformation occurred after ~4 weeks in HLE B-3.
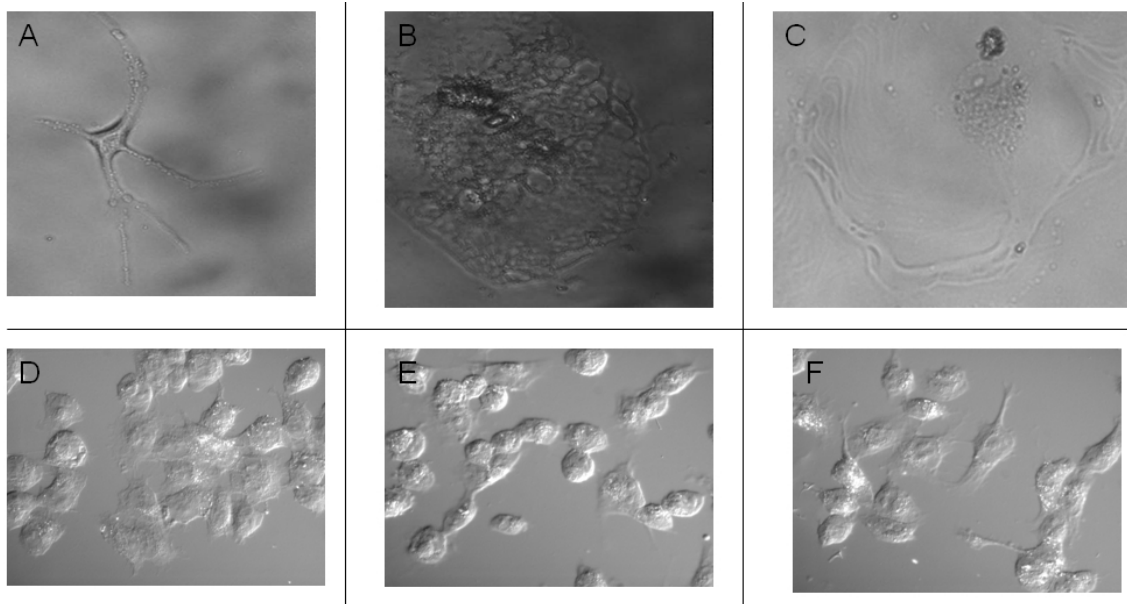
Figure 19: Initial morphological aberrations after stable transfection of RPE cells with *hGSTA4*. A-C, stably transfected cells undergo membrane blebbing and spreading over several days, similar to HLE B-3. **D,** WT RPE. **E,** transient VT. **F,** transient *hGSTA4*-transfected cells show only minor changes in morphology at 24h. No further morphological changes occurred after **A-C** in stably-transfected RPE during 16+ week culture**.** Pictures taken at 100x magnification.

There may be a secondary effect of transfection that is ultimately too toxic to overcome in this line, or the depletion of HNE may cause unexplained changes to physiology in RPE. However, morphological changes secondary to *hGSTA4* transfection and HNE depletion did occur in this cell line, suggesting that maintenance of steady-state HNE homeostasis is required for normal cell function. The apparent inability of this cell line to undergo transformation as observed in HLE B-3 and CCL-75 cells is not understood, and suggests that this phenomenon may not be universal, although there may still be the potential for many cell types to undergo procarcinogenic transformation in this manner. Such difference in susceptibility to transformation may partially explain the observed disparity in growth rates, likelihoods of metastasis, and resistance to chemotherapeutic agents seen in cancers derived from various cell types.

Although morphological transformation was not observed in RPE after stable transfection with *hGSTA4*, it was clear that HNE depletion had some effect on cell morphology and proliferation. Therefore we investigated whether there was any consequent effect on resistance to apoptosis as well. Cells (5×10^4) were plated into chamber slides and transiently transfected with 0.25μg of either empty vector or active *hGSTA4*, and after 24h were subjected to a toxic dose (20μM) of HNE for 2h, and then afterwards rinsed, incubated with 5mM CaspACE-FITC-VAD-FMK (Promega) caspase inhibitor for 30 mins, fixed, and assayed for caspase activation via fluorescence microscopy. This caspase inhibitor is designed to irreversibly and specifically bind to activated caspases and thereby indicate by FITC fluorescence the abundance and localization of overall caspase activity. Caspases are cytosolic cystein-aspartate proteases which are activated by a number of upstream stress-signaling cascades and act as messengers of death-related pathways through cleavage of several targets such as poly(ADP ribose) polymerase (PARP), inhibitor of caspase-activated DNase (CAD), and nuclear lamins [266, 319, 320]. Caspase activation is a common biomarker of apoptotic

signaling in mammalian cells. Results showed that while vector-transfected cells were susceptible to HNE-induced apoptosis as measured by the activation of caspase, *hGSTA4*-transfected cells were relatively resistant to HNE-induced apoptosis **(figure 20)**. These results are consistent with a protective role of hGSTA4-4 against toxicity of LPO product HNE. Furthermore these results are consistent with previous studies which have suggested that HNE is involved in stress-induced apoptosis and that cells with the capacity to metabolize HNE at a faster rate are relatively more resistant to apoptosis, a finding further examined in HLE B-3 in later studies.
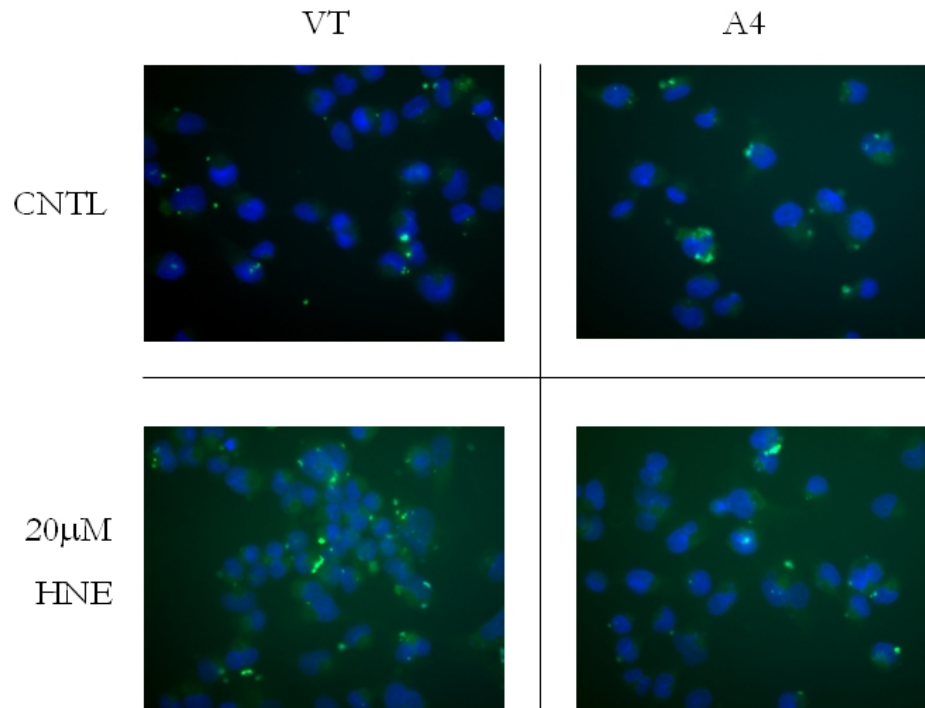
Figure 20: Protection against HNE-induced caspase activation in RPE after transient *hGSTA4* transfection. 5×10^4 cells were transiently transfected in chamber slides with either empty vector or *hGSTA4*. After 24h cells were subjected to 20μM HNE treatment for 2h and visualized for caspase activation with CaspACE-FITC-VAD-FMK marker. Visible are nuclei (DAPI, blue) and activated caspase (FITC, green). 100x magnification.

Protection of hGSTA4-transfected HLE B-3 cells from HNE- and H$_2$O$_2$-induced apoptosis: Previously we have observed increased resistance to oxidative stress and apoptosis caused by UVA irradiation in anchorage-independent erythroleukemia line K562 [27] after a mild preconditioning event which increased enzymatic conjugating activity against HNE and thereby depleted HNE levels in those cells. Therefore we investigated whether along with increase in cell proliferation and loss of anchorage dependence, *hGSTA4*-transformed cells had acquired a resistance to oxidative stress and apoptosis, from both HNE-mediated H$_2$O$_2$-mediated caspase activation. For studies involving HNE-induced apoptosis, 5×10^4 WT, vector-transfected, and *hGSTA4*-transfected HLE B-3 cells were seeded in chamber slides and incubated with 20μM HNE for 2h, and afterwards rinsed, incubated with CaspACE-FITC-VAD-FMK caspase inhibitor for 30 mins, fixed, and assayed for caspase activation via fluorescence microscopy as performed previously with RPE. Results showed that these HNE-decreased transformed HLE B-3 are protected against activation of caspase from exogenous HNE **(figure 21)**.

For studies involving H$_2$O$_2$-induced apoptosis, WT, empty vector-transfected, and *hGSTA4*-transfected HLE B-3 (5×10^4) were plated into chamber slides overnight and then subjected to oxidative stress via a toxic concentration (100μM) of hydrogen peroxide. After 6h of incubation, activation of caspase was measured via fluorescence microscopy exactly as before. Similar to results from studies involving K562, HNE-decreased *hGSTA4*-transfected HLE B-3 cells were observed to possess less susceptibility to H$_2$O$_2$-induced caspase activation relative to WT and vector-transfected cells which displayed moderate activation, suggesting that these cells acquired a resistant phenotype along with previously-mentioned morphological characteristics **(figure 22)**. This finding is interesting when viewed in context of numerous studies showing the common characteristic of increased resistance of cancer cell lines against oxidative stress and apoptosis [321-324] and may suggest a mechanism by which such resistance is acquired.

78
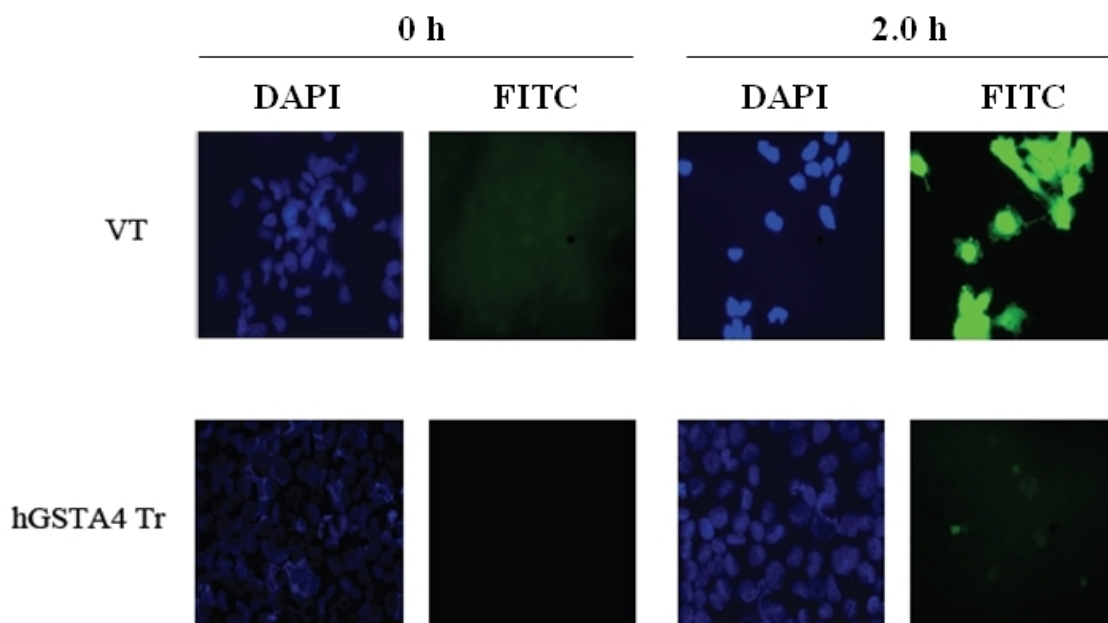
Figure 21: Protection of transformed HLE B-3 against HNE-induced caspase activation. Vector- and *hGSTA4*-transfected cells (5×10^4) were treated with 20μM HNE in serum-free medium for 0 and 2 h at 37°C and incubated with 10uM CaspACE-FITC-VAD-FMK fluorescent caspase marker for 30 minutes. Cells were then washed and fixed, then mounted with Vectashield DAPI-containing medium and visualized under fluorescence microscopy for nuclei (DAPI, blue) and activated caspase (FITC, green). Adapted from [156]with permission.
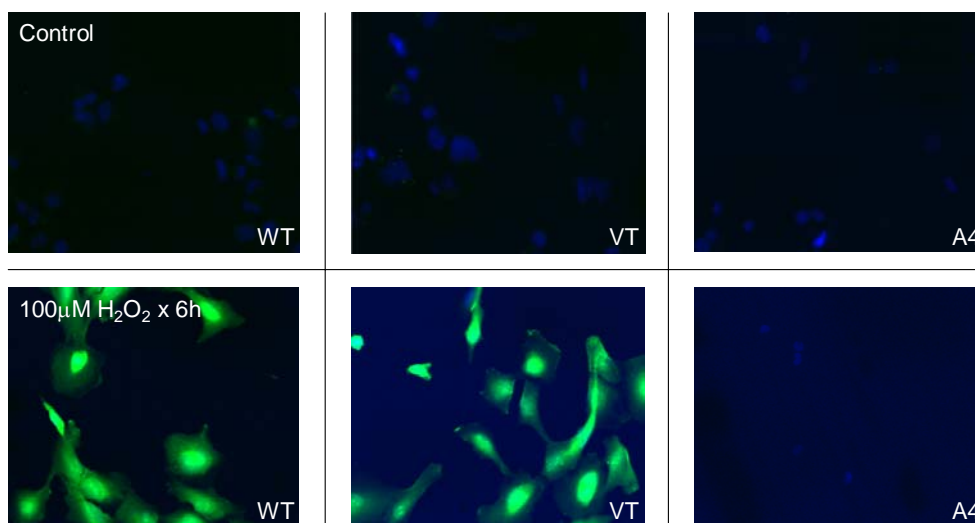
Figure 22: H₂O₂-induced caspase activation in HLE B-3 cells after stable transfection with *hGSTA4*. 5×10^4 WT, vector-transfected, and *hGSTA4*-transfected cells were seeded into chamber slides and treated with 100μM H₂O₂ for 6h, then assayed for caspase activation with CaspACE-FITC-VAD-FMK marker. Visible are nuclei (DAPI, blue) and activated caspase (FITC, green). 100x magnification.

Preliminary studies on effect of HNE depletion on gene expression in HLE B-3: Since it has been shown previously in our laboratory that overexpression of GSTs in mammalian cells was correlated to changes in expression of important genes relevant to signal transduction, survival and apoptosis, we investigated the possibility that such changes in gene expression may be present in this model as well concomitant with obvious changes in phenotype. *hGSTA4*-transformed HLE B-3 were investigated to determine if any changes in gene expression were concomitant with phenotypic changes. WT, stably vector-transfected, and stably *hGSTA4*-transfected HLE B-3 cells ($\sim 2 \times 10^6$ in 10cm dishes) were harvested (approximately 18 months post-transfection) and lysates were sonicated on ice and centrifuged at 22,000g for 30 minutes to clear insoluble material. Samples of supernatants containing between 20-60μg protein (depending on relative abundance of protein investigated) were loaded onto SDS-PAGE gels and run at 100V for ~1h, then immunoblotted onto PVDF membrane for ~3h at 35V. This was done

to visualize expression of p53, transforming growth factor beta 1 (TGFβ1), cyclin-dependent kinase 2 (CDK2), and extracellular signal-regulated kinase 1 and 2 (ERK 1/2), which have all been previously correlated with carcinogenesis [325-329] and therefore make obvious targets of investigation for elucidation of a molecular basis of this apparently pro-carcinogenic phenomenon, the rationale behind which is discussed in later chapters. We observed that p53 expression sharply decreased in *hGSTA4*-transfected cells **(figure 23A)**, which might help explain the sharp increase in cell proliferation observed. Furthermore, large increases in TGFβ1 (whose role in proliferative as opposed to anti-proliferative signaling is admittedly not completely elucidated at present), and CDK2 are consistent with these same increases in cell growth and division. Total ERK 1 and 2 expression, while undetected in WT and vector-transfected lines, is expressed in transformed HLE B-3 after 10% serum stimulation following 24h starvation **(figure 23B)**, indicating that signaling through this pathway may be involved in processes governing the observed morphological changes in this cell line.
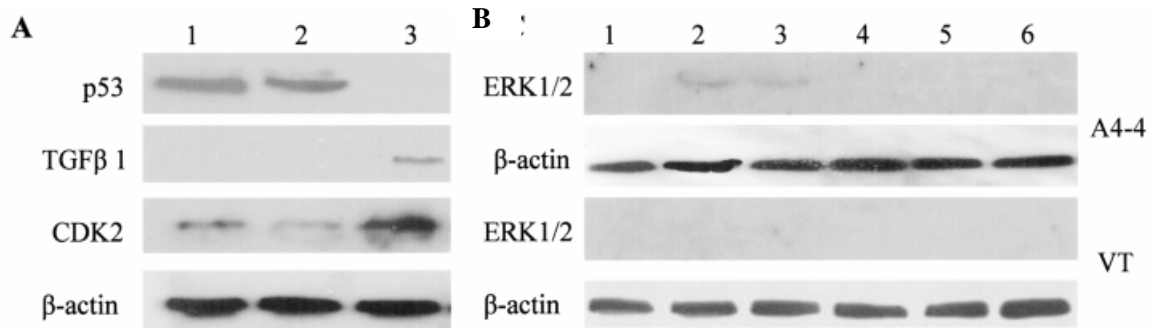
Figure 23: Modulation of p53, TGFβ1, CDK2, and ERK1/2 genes after stable transfection of HLE B-3 with *hGSTA4*. A, *lane 1,* WT. *lane 2*, VT. *Lane 3,* transformed cells. **B,** *lane 1,* before serum stimulation. *lanes 2-6*, after 10% serum stimulation for 2, 5, 10, 15, and 30 minutes, respectively. Adapted from [173] with permission.

Depletion of HNE appears to be an essential initial step in progression of HLE B-3 and CCL-75 from attached cells with a limited lifespan and modest resistance to oxidative stress to an anchorage-independent cell line with unlimited lifespan and resistance to otherwise lethal levels of chemical and oxidative stress. Some similarities in response to HNE depletion are apparent in both CCL-75 and RPE. However, the mechanism by which HNE depletion effects these changes is unknown. Therefore in the next chapter we describe studies which investigated possible modulations in gene expression using an array of genes relevant to the phenotypic alterations seen here in HLE B-3 to determine whether targets can be found which may better explain the manner in which HNE causes these alterations.

Significance: This data is consistent with the hypothesis that HNE plays a central role in mediating cellular signaling processes which are essential for regulation of cell cycle progression, cellular adhesion (anchorage dependence), and susceptibility to apoptosis. In RPE cells no observed phenotypic transformation occurred following overexpression of *hGSTA4* and subsequent depletion of intracellular HNE levels. However, there were observable changes in RPE morphology similar to those observed in HLE B-3 during the same time period following stable transfection, and this suggests (along with morphological changes observed in CCL-75 fibroblasts after microinjection) that overexpression of HNE-metabolizing active hGSTA4-4 protein in these cells causes morphological changes of varying severity to occur resulting (in two of the three cell lines investigated) loss of anchorage dependence as observed by phase-contrast microscopy.

Along with observations of morphological changes we demonstrate that *hGSTA4*-transfected cells are protected against apoptotic signaling via both H_2O_2 and HNE. Activation of caspase is a common consequence of H_2O_2- and HNE-mediated toxicity and is usually seen within hours of insult, however cells transfected with active *hGSTA4*

did not show such activation which suggests that concomitant with morphological changes to these cells there is an abrogation of caspase-mediated apoptosis signaling following HNE depletion.   This further identifies HNE as a mediator of apoptotic susceptibility in mammalian cells.

CHAPTER IV – The effect of depletion of 4-hydroxynonenal levels on the expression of procarcinogenic regulatory genes in human lens epithelial cells

Introduction

HNE is an important signaling molecule and its effects on cells seem to be concentration-dependent. As described in previous chapter, after a set of morphological changes were observed in HLE B-3 cells, resulting in a transformed and immortalized cell line capable of resisting ROS-induced toxic insult, it became clear that further investigation of possible genomic changes to these cells was needed in order to explain the phenotypic changes observed after HNE depletion. It was reasoned that profound changes in gene expression could account for such transformation. In order to investigate possible global changes in gene expression, gene microarray technology was employed to detect any significant changes in mRNA levels in relevant genes between transformed and non-transformed cell lines. This was followed up by quantitation of changes in mRNA of selected genes which could be relevant to the processes involved in phenotypic transformation of *hGSTA4*-transfected HLE B-3. Thus from this large list of significantly-modulated transcripts indicated by gene microarray results we chose 12 of the most affected genes from various signaling pathways known to be involved in the processes affecting the phenotypic changes seen by us. We subjected samples of RNA from transformed and non-transformed lines to quantitative real-time polymerase chain reaction (RT-PCR) analysis for purposes of verification of microarray data, and further verified these changes in expression using Western blot assays. In the following sections details of these studies are described and possible relevance of the alterations in these genes to the mechanisms leading to transformation of *hGSTA4*-transfected, HNE-decreased HLE B-3 cells is discussed.

Present Studies:

Gene microarray studies: Because it is well-established that HNE exerts control over a variegated set of signaling cascades and pathways extending into several major physiological processes, attempting to investigate a phenomenon which appears to be mediated by a global set of gene changes would be difficult and inefficient to undertake using more traditional methodology. In recent years the technology of gene microarray has been established as a reliable tool capable of assaying a large pool of characterized gene transcripts and determining the extent and magnitude of changes in expression of those genes due to the modulation of a single parameter of cell physiology. We utilized this technology for the first time in these studies to determine what changes in global gene expression occur following the depletion of HNE in HLE B-3 cells.

Total RNA from empty vector-transfected (used as control) and *hGSTA4*-transfected HLE B-3 cultures was purified, their concentrations and purities were verified for quality. High-quality samples were assayed using Human Genome U133 Plus 2.0 GeneChip (Affymetrix) array chips, which held the widest range of available targets. These chips contain more than 54,000 probe sets, which includes more than 47,000 gene transcripts and their variants, which contain approximately 38,500 characterized genes. Microarray analyses were conducted at the UTMB Molecular Genomics Core laboratory and results were statistically analyzed by the UTMB Bioinformatics Program facility.

Results of these studies showed a significant change in gene expression (translating to a more than two-fold modulation upwards or downwards with respect to vector-transfected controls) in 6944 genes in *hGSTA4*-transformed cells. The magnitude of this data prohibits presentation in this dissertation for space considerations; the data was submitted to the National Center for Biotechnology Information Gene Expression Omnibus (GEO) database (http://www.ncbi.nlm.nih.gov/projects/geo/) under the series accession   number   GSE2298

85

(http://www.ncbi.nlm.nih.gov/geo/query/acc.cgi?acc=GSE2298).   Sample submissions are listed as sample accession number GSM42834 for vector-transfected cell data (http://www.ncbi.nlm.nih.gov/geo/query/acc.cgi?acc=GSM42834&token=) and sample accession   number   GSM42833   for   *hGSTA4*-transformed   cell   data (http://www.ncbi.nlm.nih.gov/geo/query/acc.cgi?acc=GSM42833&token=).

Among the list of genes presented in table 5 which were modulated as measured by gene microarray were several known to play roles in diseases whose pathology is modulated by LPO levels, including levels of HNE. Amyloid β precursor protein (APP) is involved in the pathogenesis of Alzheimer's disease. APP cleavage by secretases forms amyloid β proteins, which aggregate within neurons to cause progressive disruption of cellular physiology and eventual cell death [330] Cytochrome P450 1B1 is known to play a causative role in carcinogenesis, especially hormone-influenced [331] and polyaromatic hydrocarbon (PAH)-influenced cancers, and is a target of anti-cancer therapy [332].   Nitric oxide synthase 3/endothelial nitric oxide synthase is involved in production of the potent signaling molecule and vasodilator nitric oxide, and modulation of expression of this enzyme has been shown to play a role in vascular signaling processes mediated by both phosphatidylinositol 3 kinase and AKT [333], and plays a preventative role in atherosclerosis [334-336] via control of antiatherosclerotic NO production. The modulation of these genes away from levels which would promote their roles in disease in HNE-decreased HLE B-3 is an interesting finding as it correlates with what is already known about the roles of increased HNE levels in those diseases.

There were a large number of well-characterized genes in the list of results, and it was a difficult task refining these myriad key signaling targets to a more manageable subset most relevant to the scope of our investigation. Initially the list was eventually narrowed down to a few dozen genes including amyloid precursor protein, p15, fibroblast growth factor, insulin-like growth factor 1 receptor, and so forth, however the scope was narrowed to a list of 12 genes which were chosen on their perceived relevance to processes governing the phenotypic transformation, and the magnitude of their fold-

change relative to controls. While there were many hundreds of genes identified by microarray assay as modulated after stable transfection of *hGSTA4* and subsequent HNE depletion, we chose to narrow the scope of our investigation to genes more relevant to the pathophysiological processes which underlie the target of our overall investigation. While this may seem an arbitrary or biased selection process, it should be noted that there were many dozens of genes which have obvious implications into these same processes which were not chosen for further investigation, simply on the basis of keeping the scope of these studies sufficiently narrow. Furthermore, many if not most of the most obviously relevant genes to these processes were found to be among the most heavily modulated subsequent to HNE depletion. This opens up avenues of further studies into the global effects of HNE depletion on gene expression which may be pursued in the future. Magnitudes of fold-changes of targets of microarray studies ranged from the baseline of 2.00 to more than 4800 with dozens achieving a more than 100-fold change and hundreds achieving a more than 10-fold change, which correlated well with what we hypothesized as necessarily profound modulations to achieve such long-lived effects in cell physiology as observed in HLE B-3. As there were such a large number of highly-modulated genes identified in the gene microarray results and since presenting that data in its entirety would be onerous and space-expansive, a table comprising 50 of the more well-known genes, with obvious relevance to previously-characterized morphological changes in HLE B-3 after transformation is presented **(table 5)** to give a picture of the variegated nature of the global changes in gene expression observed in the results of the microarray. Using these criteria a list was generated **(table 6)** comprising important genes involved in three processes observed to be involved in transformation: cell cycle control, survival/apoptotic control, and cell adhesion/ECM interaction.

Table 5: Prominent genes whose expression was modulated more than 5-fold after stable transfection with *hGSTA4* and depletion of HNE.

Gene Name	Affymetrix ID	Description	Fold change
APP	200602_at	Amyloid β precursor protein	-4803.93
TIMP2	231579_s_at	Tissue inhibitor of metalloproteinase 2	-2936.74
CYP1B1	202437_s_at	Cytochrome P450 1B1	-1833.01
SNK	201939_at	Serum-inducible kinase	-1618.00
CTGF	209101_at	Connective tissue growth factor	-1370.04
PLS3	201215_at	Plastin 3	-910.17
ALCAM	201951_at	Activated leukocyte cell adhesion molecule	-765.36
MYO1B	212364_at	Myosin 1B	-744.43
CKAP4	200999_s_at	Cytoskeleton-associated protein 4	-694.58
COL1A1	202310_s_at	Collagen type Iα1	-634.73
GJA7	228776_at	Gap junction protein α7	-508.46
RIN2	209684_at	Ras and Rab interactor 2	-494.56
IGFBP7	201163_s_at	Insulin-like growth factor binding protein 7	-451.94
COL5A2	221730_at	Collagen type Vα2	-415.87
AHR	202820_at	Aryl hydrocarbon receptor	-374.81
CDH2	203440_at	Cadherin 2 type 1	-319.57
NGFRAP1	217963_s_at	Nerve growth factor receptor-associated protein 1	-254.23
MGP	202291_s_at	Matrix Gla protein	-250.73
PTPRM	1555579_s_ata	Protein tyrosine phosphatase receptor type M	-233.94
PAWR	226231_at	Protein kinase C regulator	-232.32
PRSS11	201185_at	Protease, serine, 11	-216.77
CALD1	212077_at	Caldesmon 1	-147.03
PSMB8	209040_s_at	Proteasome subunit β-type 8	-98.36
RDC1	212977_at	G protein-coupled receptor	-94.35
AXL	202685_s_at	AXL receptor tyrosine kinase	-46.85
VEGF	210512_s_at	Vascular endothelial growth factor	+8.63
STAT5A	203010_at	Signal transducer and activator of transcription 5A	+9.06
TIF1	213301_x_at	Transcriptional intermediary factor 1	+9.92
PIP5K1B	205632_s_at	Phosphatidylinositol-4-phosphate 5-kinase type Iβ	+10.20
RAB27A	210951_x_at	RAB27A, member of Ras oncogene family	+11.47
TNFSF13B	223501_at	B-cell activating factor	+11.71
PIM2	204269_at	PIM1 oncogene	+12.04
HIRA	217427_s_at	HIR cell cycle regulation defective homolog A	+12.82
CBS	212816_s_at	Cystathionine-β-synthase	+13.36
CTH	217127_at	Cystathionase	+13.64
SCAP2	225639_at	Src family associated phosphoprotein 2	+14.12
DAPP1	222859_s_at	Dual adaptor of phosphotyrosine and 3-phosphoinositides	+18.13
PRKCQ	210038_at	Protein kinase C θ	+19.16
ITPKA	205874_at	Inositol 1,4,5-triphosphate 3 kinase A	+20.11
ANGPT1	205609_at	Angiopoietin 1	+22.63

IL23R	1561853_a_at	Interleukin-23 receptor	+24.08
HIST1H1C	209398_at	Histone 1C	+24.76
MAPK1	1552263_at	Mitogen-activated protein kinase 1	+31.78
MYB	204798_at	Myeloblastosis viral oncogene homolog	+35.02
GPR54	242517_at	G protein-coupled receptor 54	+38.05
TMOD1	203662_s_at	Tropomodulin 1	+40.22
BMX	206464_at	BMX non-receptor tyrosine kinase	+45.89
NOS3	205581_s_at	Nitric oxide synthase 3	+47.84
SYK	207540_s_at	Spleen tyrosine kinase	+48.84

Fold change is relative to vector-transfected control. Values are according to gene microarray results.

As described in the previous section the most remarkable changes in HNE-decreased transformed HLE B-3 cells were: 1) suspended vs. attached morphology, 2) increased growth rate by more than 100%, and 3) acquisition of immortality, all characteristics of cancer cells. Therefore a final list of the following genes was generated for further studies: Connexin 43, Fas (CD95), Fibronectin 1, Integrin α6, Laminin γ1, c-Myc, p16, p21, p53, and Transforming growth factor alpha (TGFα). Known functions of these genes and their possible relevance to mechanisms of transformation is summarized below (**table 6).**

Table 6: Expression fold-changes and relevant functions of genes of interest.

Gene Name	Genbank ID	Fold Change (Microarray)	Fold Change (RT-PCR)	Suggested Functions
p16	**NM_000077**	-894.5	$-\infty$ (ND)	Inhibitor of CDK4 kinase; stability of p53; Regulation of G_1 progression [337]
Laminin γ1	**NM_002293**	-598.0	$-\infty$ (ND)	Differentiation; Cell adhesion; Development; Epithelial polarity; Wound healing and regeneration; structural support; Stability; Stimulation of DNA synthesis; Tumor growth and metastasis [273]

Connexin 43	**NM_000165**	-185.6	-6.0	Gap junctions; Connexan channel activity; Cell cycle progression; Cell growth; Differentiation; Cell signaling; Suppression of carcinogenesis [274]
Integrin α6	**AV733308**	-70.1	-∞ (ND)	Cell adhesion; Growth and initiation of differentiation; Actin polymerization; Suppression of apoptosis; Cell invasion and migration; Gene expression; Cell surface-mediated signaling [272]
Fibronectin 1	**AJ733308**	-6.5	-∞ (ND)	Cell adhesion; Structural integrity; Migration processes; Cell condensation; Oncogenesis; Wound healing; Metastasis [271]
p53	**NM_000546**	-52.9	-36.0	Tumor suppression; Cell cycle control; DNA repair; Apoptosis; DNA damage response, Induction of Apoptosis; Negative regulation of cell cycle [338]
Fas	**AA164751**	-31.4	-∞ (ND)	Regulation of programmed cell death; Activation of MAPK3/ERK1 and MAPK8/JNK [339]
TGFα	**NM_003236**	-8.8	-∞ (ND)	40% sequence homology with epidermal growth factor (EGF); Receptor phosphorylation; Mitosis [340]
p21	**NM_00389**	-7.5	-72.0	p53-dependent G_1 phase progression; Arrest in response to stress [341]
c-Jun	**NM_002228**	-4.6	-2.8	Proliferation; Colony survival; Apoptosis; Chemotaxis [342]
Bad	**U66879**	-3.6	-4.1	Mitochondrial release of cytochrome c; Apoptosis [343]
c-Myc	**NM_002467**	+3.8	+2.3	Replication; Apoptosis; Cell cycle progression; Transformation [344]

Fold-change is relative to VT cells for microarray values and WT for RT-PCR values. ND = level below detection limit. Adapted from [1] with permission.

Verification of microarray results via quantitative RT-PCR analysis: While gene microarray analysis is a well-established technique for investigation of gene expression changes, the prohibitive costs involved necessitate a small sample size. The number of samples for our microarray studies was 2 (one for vector-transfected cells and one for *hGSTA4*-transformed cells), and because of this limitation there was a

90

requirement for follow-up experiments to verify these results, especially since the magnitude of the fold-changes was high for several targets. Target genes as well as the justifications for their selection in these studies are described below.

Cell cycle progression genes: The genes p53, p21, p16, and TGFα are involved in control of cell cycle progression. p53 is one of the archetypical tumor suppressors, having been cloned in 1982 [345] and since then been implicated in a number of cancers. Deletion or mutation of p53 can cause the type of uncontrolled cell proliferation seen in the cells transformed after *hGSTA4* transfection. p21, a downstream mediator of p53 signaling, is an inhibitor of cyclin-dependent kinase 2 and its downregulation is found in cancer cells as well [341]. p16, an inhibitor of cyclin-dependent kinase 4, prevents progression through G_1 phase and its downregulation could be a necessary step in carcinogenesis [257]. As it was observed that transformed HLE B-3 have a population doubling time of less than half of WT cells (20h as opposed to 50h) and that these cells do not appear to have a limited lifespan as WT cells are restricted by (approximately 75 doublings), investigation of the possible roles of these cell cycle regulatory genes in this phenomenon appeared to be a prudent choice. The results of the quantitative RT-PCR showed that p53 levels were approximately 36-fold decreased and p21 approximately 72-fold decreased with respect to WT, and p16, and TGFα were both downregulated to the point of being below detection limits, which were referenced as ∞-fold decreases (mRNA levels not detected in transformed cells) in table 6.

Cell survival/apoptosis genes: The genes Bad, Fas, and c-Jun are involved in cell survival and apoptosis. Bad is a member of the Bcl-2 protein family of among at least 13 known mitochondrial pro-apoptotic regulators of apoptosis. Both pro- and anti-apoptotic members of the Bcl-2 family are modulated in several cancers [346-349]. Fas, also known as CD95, is a member of the TNF receptor family of transmembrane proteins. Fas is activated by binding of Fas ligand (FasL) and forms the death-associated signaling

complex (DISC) along with Fas-associated death domain (FADD), TNFR1-associated death domain (TRADD), and procaspase 8/10 to mediate the extrinsic programmed cell death pathway [350]. Fas expression is often down-regulated in cancer lines which are often more resistant to apoptosis [351, 352] . c-Jun is a cytosolic protein which forms (with c-Fos) the AP-1 transcription factor upon activation from stress and after localizing at the nucleus initiates the transcription of several stress-response and pro-apoptotic genes [342]. Since it has been observed by us that HNE-decreased, transformed HLE B-3 are resistant to apoptosis caused by lethal doses of H_2O_2 **(figure 21)**, we reasoned that investigation of genes known to play a role in regulation of apoptosis may yield more understanding of how that protection arises. The results of the quantitative RT-PCR showed that Bad RNA levels were approximately 4.1-fold decreased and c-Jun approximately 2.8-fold decreased with respect to WT, while Fas RNA level was downregulated to the point of being below detection limits, which were referenced as ∞-fold decreases (not detected) on table 6.

Cell adhesion/mobility genes: The genes Integrin α6, Fibronectin 1, Laminin γ1, and Connexin 43 are involved in cell adhesion. Integrin α6 serves as one part of the heterodimeric Integrin α6β1 which is found characteristically spanning the outer membrane surface of epithelial cells [353]. Laminin γ1 is a member of the Laminin family of extracellular matrix proteins which bind Integrins to hold cell layers together [273], while Fibronectin 1 binds Integrins from completely within the ECM [281]. The justification for the choice of these genes involved in ECM function is obvious when viewed in the context of the loss of anchorage dependence of transformed HLE B-3 and their transition from attached to suspension cells **(figure 24)**. Cells in the below figure were photographed in $75cm^2$ culture flasks in normal conditions. The results of the quantitative RT-PCR showed that Connexin 43 RNA levels were approximately 6-fold decreased relative to WT, while Laminin γ1, Integrin α6, and Fibronectin 1 RNA levels

all downregulated to the point of being below detection limits, which were referenced as ∞-fold decreases (not detected) on table 6.

Wild-Type	pTarget-transfected	*hGSTA4*-transfected
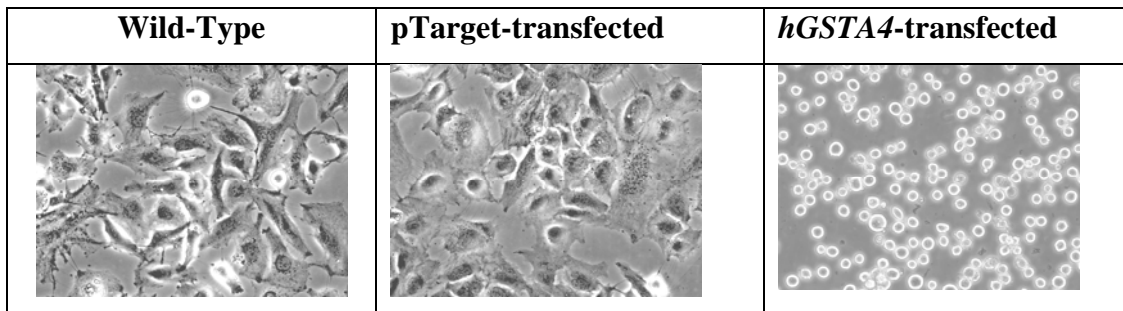
Figure 24: Phase-contrast microscopy view of sub-confluent HLE B-3 cells in culture. Cells (3-5 x10^6) were cultured in 150cm^2 vented-cap cell culture flasks in full media until between 70-90% confluent and viewed on phase-contrast microscope at 100x. Adapted from [1] with permission.

Determination of DNA primers for quantitative RT-PCR analysis: Observed changes in the expression of genes referred above were further validated by quantitative RT-PCR. A key step in the determination of modulation of these genes of interest was choosing correct primers for quantitative RT-PCR, because the accuracy of this highly-sensitive and specific technology depends a great deal on the ability of the primers to target the genes of interest. There were TaqMan primers available for several transcripts for many of the genes, as many of these genes are present in multiple splice variants and via polymorphisms. We determined the appropriate primer (out of the pool of several for each gene) for each of the genes based on the relative commonality of the splice variants/polymorphisms as determined by literature, the commonality of the primer use by other investigating laboratories for the same genes of interest, and the similarity of each available primer gene sequence to the sequence matched in the Affymetrix gene microarray chips. After careful determination we decided on commonly-used primers

approximately 25 nucleotides in length **(table 7)** for the twelve genes which were probed by quantitative RT-PCR. These fluorescent FAM dye-labeled TaqMan MGB (Applied Biosystems) primers listed below were used to probe the genes of interest using the protocol described below.

Table 7: Fluorescent DNA probe information for used in quantitative RT-PCR.

Target gene	Affymetrix ID	Genbank ID	PCR Probe ID	Probe Sequence	T_M (°C)
Integrin α6	215177_s_at	AV733308	Hs00173952_m1	AGCGGCTGTTGCTCGTGGGGGCCCC	85.7
Laminin γ1	200771_at	NM_002293	Hs00173952_ml	AGCCCTGTGCTGCAGGAATGGGTAA	77.5
Bad	1861_at	U66879	Hs00188930_ml	GCCATCATGGAGGCGCTGGGGCTGT	82.4
p16	207039_at	NM_000077	Hs00233365_m	GTCCCTCAGACATCCCCGATTGAAA	75.8
Fas	204780_s_at	AA164751	Hs00163653_m	TGTCCTCCAGGTGAAAGGAAAGCTA	74.2
p21	202284_at	NM_00389	Hs00355782_m1	GACCAGCATGACAGATTTCTACCAC	74.2
Connexin 43	201667_at	NM_000165	Hs00748445_s	TGGTGCGCTGAGCCCTGCCAAAGAC	80.7
c-Jun	201466_s_at	NM_002228	Hs00277190_s	CTTAGGCTTCTCCACGGCGGTAAAG	77.5
TGFα	205016_at	NM_003236	Hs00177401_m	GCCAGCATGTGTCTGCCATTCTGGG	79.1
c-Myc	202431_s_at	NM_002467	Hs00153408_m	GCAGCGACTCTGAGGAGGAACAAGA	77.5
p53	201746_at	NM_00546	Hs00153349_m	TTCACCCTTCAGATCCGTGGGCGTG	79.1
Fibronectin 1	214701_s_at	AJ733308	Hs00277509_m	CACCACTCTGGAGAATGTCAGCCCA	77.5

PCR probe ID is used by Applied Biosystems. Probe sequences are 5' to 3'. Adapted from [1] with permission.

Quantitative RT-PCR analysis of genes of interest from microarray: After the correct primers were chosen and ordered, wild-type cells, cells which were stably transfected with empty vector or *hGSTA4* were harvested and total RNA was purified. Concentrations and purities were determined spectrophotometrically and high-purity samples were analyzed at the Sealy Center for Cancer Cell Biology Real-time PCR Core Facility at UTMB under the direction of Dr. Huiping Guo using the following cycle **(figure 25)**:
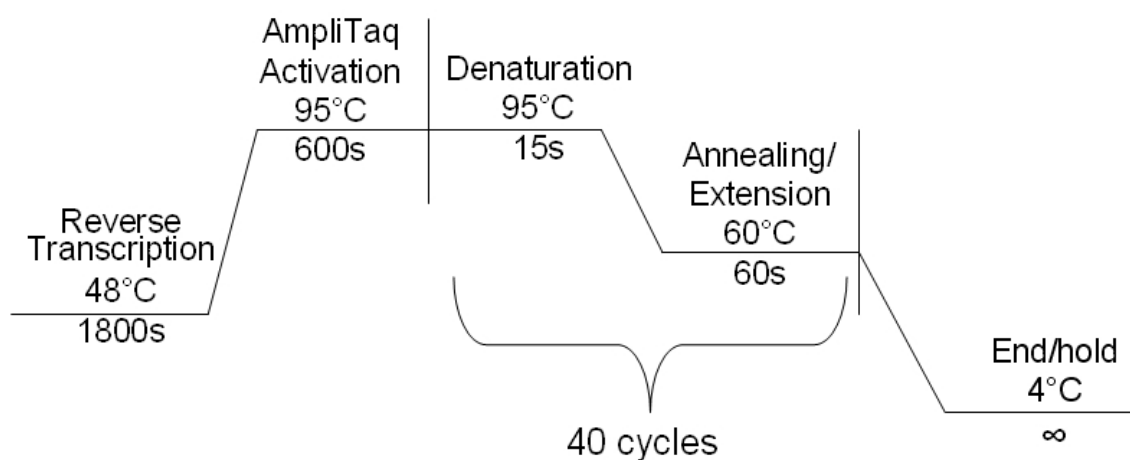
Figure 25: Quantitative RT-PCR cycle parameters. Reactions were performed and visualized by ABI PRISM 7000 using PrimerExpress software.

Excitation occurred at 494nm and emission was recorded at 520nm during the reaction as the purified RNA samples were used as templates to produce cDNA. 18S ribosomal RNA was used as a control, and the levels were normalized to those observed in the WT cells. As was described in results above, we observed that in 11 of the 12 genes that were assayed, the *hGSTA4*-transfected transformed cells showed considerably lower expression levels, and in the 1 other gene the transformed cells showed a considerably higher expression level **(figure 26)**. The 11 down-regulated genes are well-known and can be grouped into three functional categories – cell cycle regulation, cell adhesion, and survival/apoptosis. The upregulated gene, c-Myc, is a well-characterized oncogene involved in carcinogenesis [354, 355].
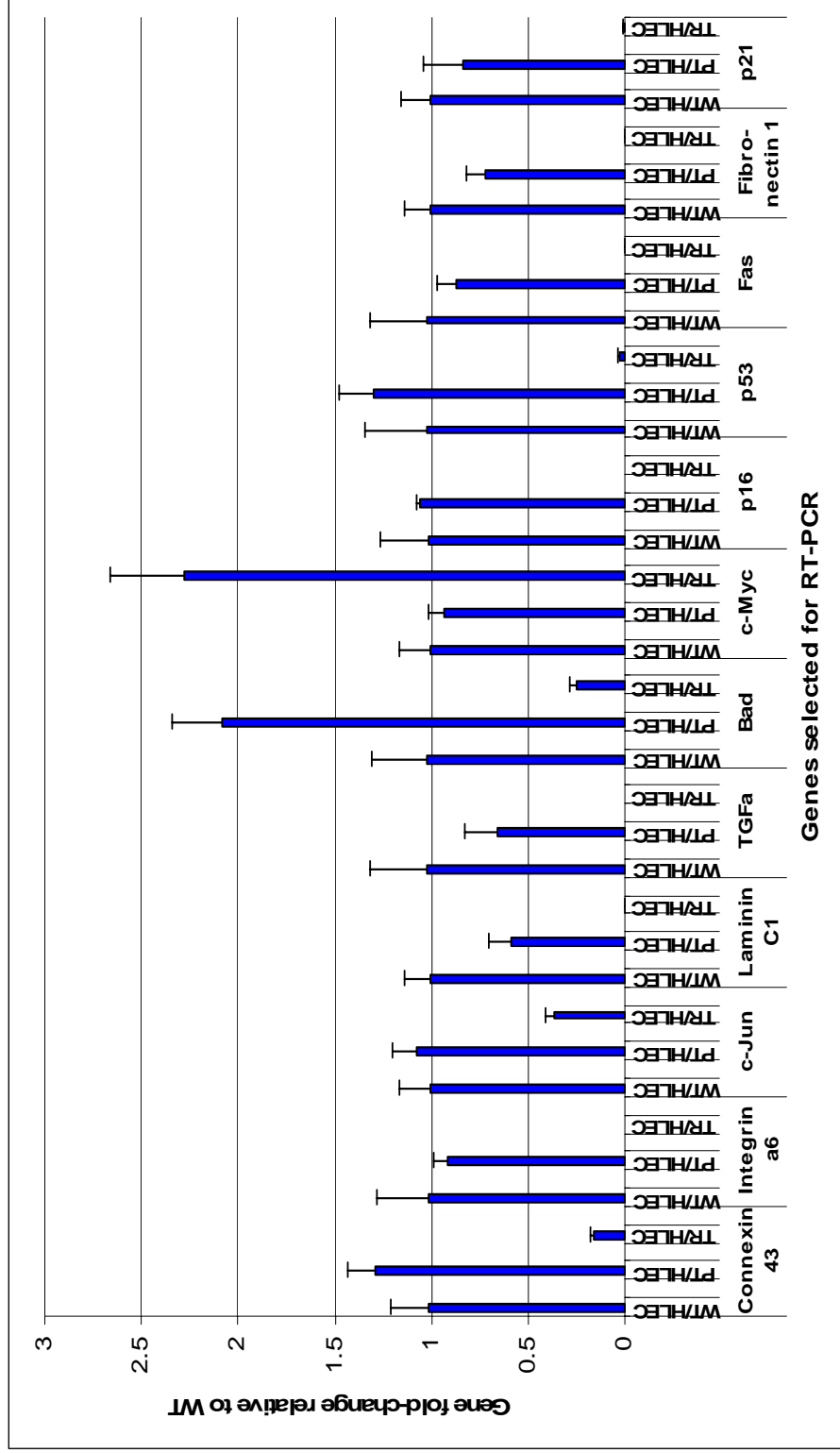
Figure 26: Fold-change in gene expression in HLE B-3 via quantitative RT-PCR. Values are normalized to WT cell values and to 18s ribosomal RNA concentration. n=2. PT = pTarget vector-transfected cells, TR = *hGSTA4*-transfected cells. Adapted from [1] with permission.

After observing positive results indicating significant modulation of gene expression in stably-transfected transformed HLE B-3 it was investigated whether similar changes in gene expression occur in *hGSTA4*-transfected RPE. Although it was observed that RPE did not undergo procarcinogenic transformation, it was possible that there were underlying genotypic changes which did not translate to a change in phenotype. Transiently-transfected RPE ($2x10^6$ in 10cm dishes) were harvested 24h post-transfection using RNAqueous-4PCR kit as described before and subjected to quantitative RT-PCR analysis in order to elucidate changes in gene expression for several genes known to be modulated in various cancer lines. Results of these studies revealed that RNA levels for investigated genes in transfected RPE cells did not change relative to WT or vector-transfected cells **(figure 27)**. This suggests that, consistent with morphological studies, these cells do not undergo a phenotypic transformation and that the reason for this lack of transformation secondary to HNE depletion is a lack of modulation of gene expression in pathways which may be necessary for such a transformation to occur. However this is not clear and it is possible that morphological changes occur before genomic changes. In the next chapter the issue of whether changes in gene expression occur before or after changes in morphology will be explored more directly.
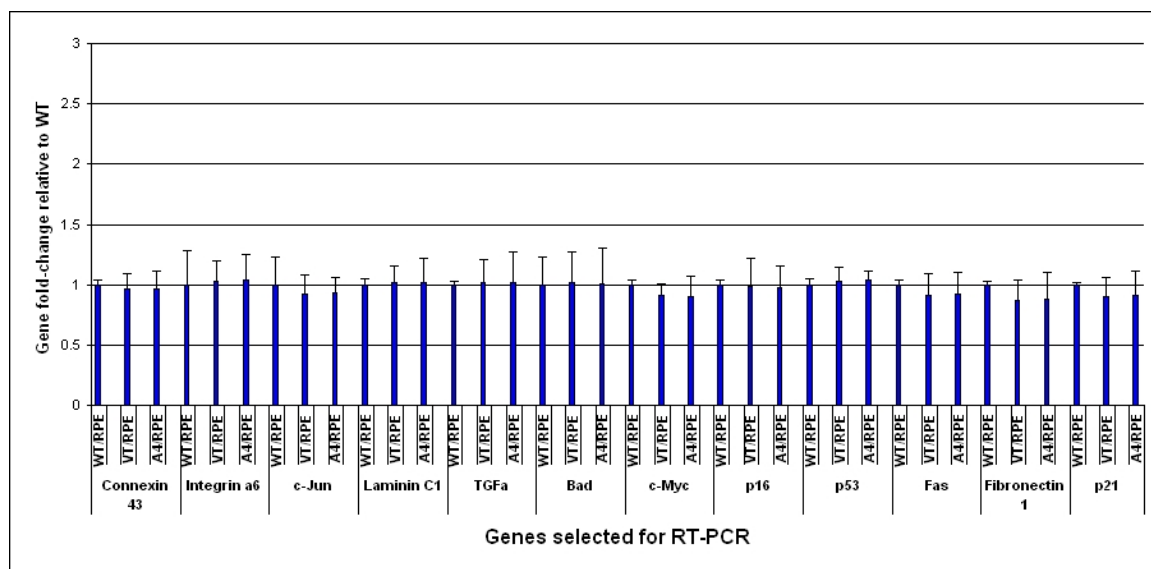
Figure 27: **Quantitative RT-PCR analysis of transiently-transfected RPE cells.** Values are normalized to WT and to 18s rRNA values. n=3.

Verification of translational modulation via Western blot: After examining the results of the quantitative RT-PCR performed on HLE B-3 cells and observing that those results obtained in the gene microarray do in fact reflect the changes in expression levels of the gene transcripts, we extended our investigation one step downstream to determine if these changes in transcription were accompanied by modulation of protein expression. This was important because transcriptional changes do not necessarily reflect translational changes, in a quantitative or even qualitative manner. As the Western blot technique is less expensive to perform than real-time qualitative RT-PCR, we included the genes of interest which were examined previously and whose expressions were modulated in the transformed cell line. These genes included Cyclin-dependent kinase 2 (CDK2) and Protein kinase C beta II (PKCβII), two proteins which have well-established roles in cell proliferation. WT, vector-transfected, and *hGSTA4*-transfected HLE B-3 cells (~$2x10^6$ in 10cm dishes) were harvested and lysates were sonicated on ice and

centrifuged at 22,000g for 30 minutes to clear insoluble material. Samples of supernatants containing between 20-60μg protein (depending on relative abundance of protein investigated) were loaded onto SDS-PAGE gels and run at 100V for ~1h, then immunoblotted onto PVDF membrane for ~3h at 35V. Results of Western blots showed that Laminin γ1, Connexin 43, Integrin α6, Fibronectin 1, Fas, Bad, p53, c-Jun, and p16 were all expressed in both WT and vector-transfected cells but either strongly downregulated or not detected in *hGSTA4*-transfected cells, while c-Myc, PKCβII, and CDK2 were all upregulated in *hGSTA4*-transfected cells relative to WT and vector-transfected cells **(figure 28)**. These qualitative results appear to correlate well with those of quantitative RT-PCR and gene microarray studies, and further suggest that phenotypic transformation of these cells is correlated with specific and substantial changes in gene expression.
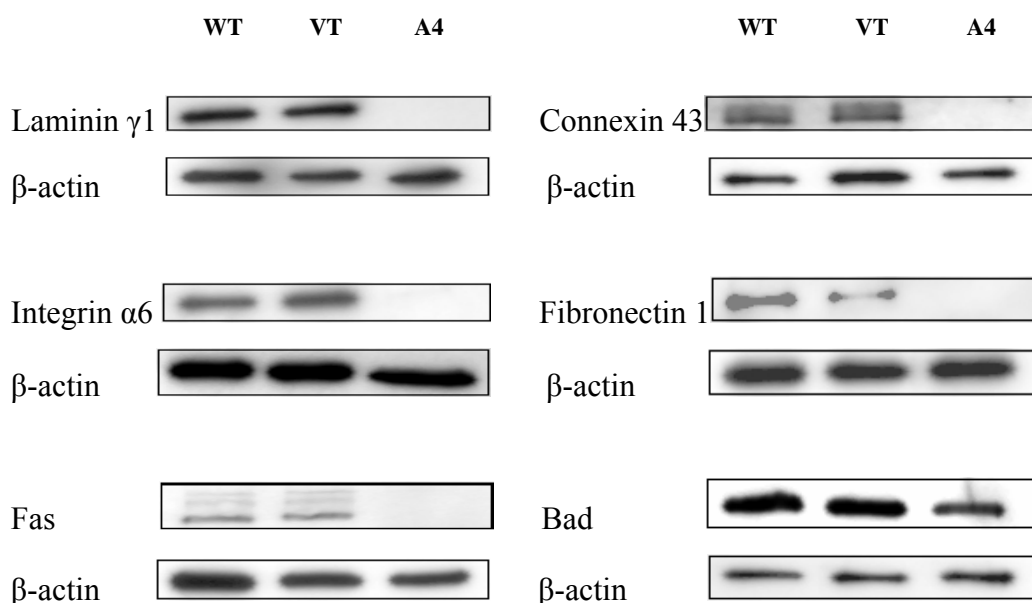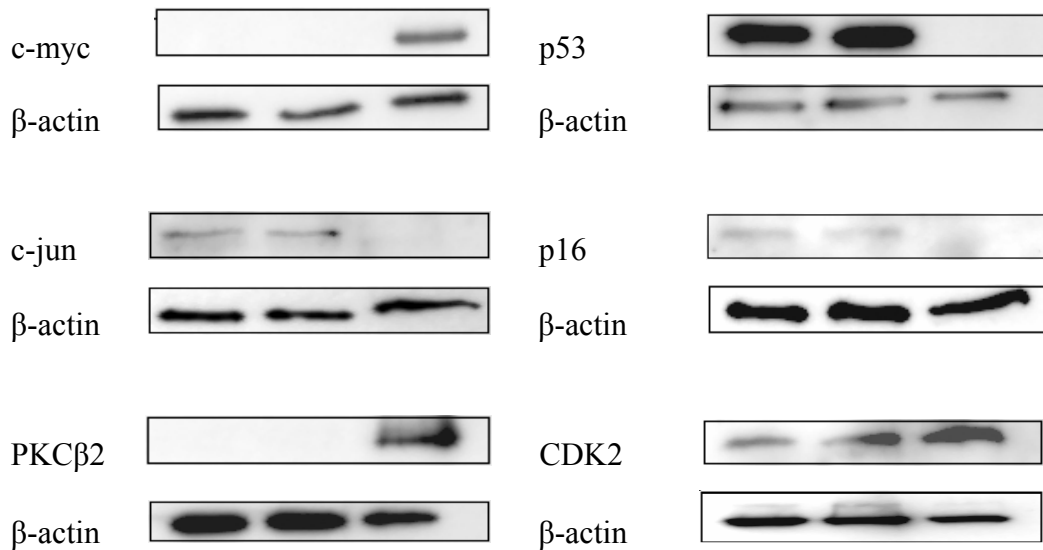
Figure 28: Changes in protein expression in HLE B-3 after transformation. Cells were grown in 100 or 150cm culture dishes and harvested in RIPA buffer on ice. Expression of genes of interest was measured via Western blot with β-actin used as loading control. Adapted from [1] with permission.

Alterations in cell cycle regulation protein expression: The results mirrored the transcriptional data well. The cell cycle regulatory genes of interest, p53 and p16, were both strongly down-regulated in the transformed cell line to nearly undetectable (p16) and below detectable (p53) from their levels in WT and vector-transfected (VT) cell lines. CDK2 was strongly upregulated in transformed cells from low levels found in WT and VT cells. PKCβII, while not generally classified as a cell cycle regulatory protein, has been implicated in proliferation of some cancer cell lines [356, 357] including colonic epithelial carcinoma where during the initial stages of carcinogenesis it is highly upregulated. This data fits well with what we observed in the transformed line in that cell division of this line is strongly increased, with less than 50% the WT population doubling time [173]. The near-loss of expression of p53, which as

100

discussed above regulates the slow and steady progression into cell division, as well as p21 which operates directly downstream of p53 to halt proliferation, and p16, which impedes division through inhibition of CDK4, explains well the strong observed increase in cell growth and division. There were problems encountered with both TGFα and p21, it proving impossible to show expression of these proteins in any of the three cell lines, possibly due to physiologically low protein expression levels in this cell line or cell cycle-dependent expression fluctuations.

Alterations in expression of proteins involved in regulation of survival/apoptosis: The cell survival/apoptotic control genes of interest, c-Jun, Bad, and Fas, were similarly found at much lower levels in the *hGSTA4*-transfected transformed line than in either the WT or the VT lines. c-Jun, while not normally strongly expressed in healthy cells, was found to be undetectable in transformed (Tr) cells. Fas, the TNF receptor family mediator of the extrinsic pathway of apoptosis, was expressed moderately in WT and VT cells but undetectable in transformed cells. This finding is interesting because it correlates HNE levels with Fas expression, which is known to be downregulated in cancer cell lines. Possible relationship between Fas expression and intracellular levels of HNE was further investigated and is described later in chapter V. The pro-apoptotic Bcl2 family mitochondrial-pathway regulator Bad, while strongly expressed in WT and VT lines, was only moderately expressed in transformed cells. The resistance of transformed cells to oxidative stress can be explained through the inhibition of these three mediators of apoptotic signaling, one through extrinsic pathway, one through mitochondrial pathway, and one as pro-apoptotic transcription factor (as AP-1) which in nontransformed cells are capable of producing cell death after such stresses.

Alterations in expression of proteins involved in cell adhesion/mobility: The cell adhesion/mobility genes of interest were modulated in transformed cells to a large degree as well. Integrin α6 was expressed well in WT and

101

VT cells, as might be expected for an attached, epithelioid cell line [353]. The same basal expression was found for the extracellular matrix proteins Laminin γ1 and Fibronectin 1, and the gap junction protein Connexin 43. While expressed fairly strongly in both WT and VT HLE B-3, these proteins were downregulated to the point of being essentially undetected by Western blot in HNE-decreased transformed cells.

Significance: These are significant findings and may serve to explain the loss of anchorage dependence which punctuates the WT phenotype of lens epithelial cells, since as explained above these proteins are integral to the function of the extracellular matrix and ability of cells to interact with it, in addition to their roles in cell-cell contact and adhesion, all of which is disturbed in metastasis. It should be noted however that anchorage-independent growth/migration/matrix invasion assays have either not yet been performed or not been included in these studies and therefore parallels to carcinogenic metastasis need to be experimentally elucidated to validate these comparisons. These *post hoc* studies investigated the phenomenon of transformation and identified several changes in transcription and translation of genes which involve members of the processes of cell cycle control, apoptosis, and cell adhesion, three processes which were shown to be altered in the physiology of the HNE-decreased cells. While the targets of our investigation were few in relation to the number of identified affected genes (less than 20 among almost 7000), those targets are *known key members* of the relevant processes. These studies were not intended to be exhaustive or all-inclusive, yet were designed to address the most likely effectors of the observed physiological changes via the three processes included in the experimental design. While we have identified those likely effectors and verified that their modulation correlates with phenotypic transformation, future studies involving specifically-targeted modulation of those genes will be necessary to determine whether these genes are necessary and/or sufficient to bring about some degree of transformation.

These global changes in gene expression observed in *hGSTA4*-transformed HLE B-3 are profound and consistent with what has been observed to occur at the level of cellular physiology after HNE depletion via overexpression of HNE-conjugating activity of hGSTA4-4. However, the question of whether morphological transformation is a cause or a consequence of gene expression modulation remains difficult to answer, particularly for the breadth of genes investigated. It may be possible that gene expression changes in HLE B-3 are a direct consequence of phenotypic transformation and not a direct consequence of the HNE depletion which follows overexpression of hGSTA4-4 activity. This may be because of the possibility that broad changes in gene expression are serving as a compensatory or adaptive response to broad changes in cell physiology. In order to determine more accurately the relationship between HNE depletion and expression of previously-investigated genes we have narrowed the scope of our investigation to focus on a single gene, Fas, which is well-established and prominent in regulation of apoptosis through the extrinsic pathway.

CHAPTER V – The role of 4-hydroxynonenal in regulation of the expression of Fas (CD95) and Fas-mediated signaling in HLE B-3 cells

Introduction

One of the key genes involved in the extrinsic pathway leading towards apoptosis in mammalian cells is Fas, otherwise known as CD95 or TNFα receptor family member 6. Fas, situated at and spanning the cellular membrane, is activated by the soluble protein FasL which stimulates activation and formation of the death inducing signaling complex (DISC) with FADD, TRADD, and procaspase 8 which ultimately leads to caspase 3,6, and 7 activation, JNK pathway activation, PARP fragmentation, and apoptosis [339]. Fas has been found to be downregulated or absent in several cancer cell lines [351, 352, 358] and its observed susceptibility to modulation after transformation makes it an interesting target of research leading to elucidation of its role in HNE-induced apoptosis as well as its possible causative role in phenotypic transformation of HLE B-3. Therefore we addressed whether or not downregulation of Fas expression in *hGSTA4*-transfected, HNE-decreased HLE B-3 cells precedes transformation and whether expression in *hGSTA4*-transfected cells is suppressed prior to transformation. To address this question we first addressed if there was a correlation between intracellular levels of HNE and the extent of Fas expression, with verification of *in vitro* results through utilization of an *in vivo* mouse model which exhibits superphysiological tissue levels of HNE. Next we studied the effect of a transient depletion of HNE on the expression of Fas in cells transiently-transfected with *hGSTA4* which show depletion of HNE but not transformation. In addition, we investigated the manner in which modulation of HNE levels affects Fas-mediated apoptotic signaling in HLE B-3 by determining the

involvement of two known mediators of Fas apoptotic pathway signaling, cleavage of PARP and activation of JNK.

Present studies:

Fas expression and intracellular HNE: It has been shown in the previous chapter that HNE depletion suppresses the expression of Fas in HLE B-3. In order to investigate a possible correlation between HNE levels and Fas expression, HLE B-3 cells were treated with a range of concentrations of HNE between 0 and 20 µM in medium for increasing time periods between 0 and 2h, and expression of Fas was measured by Western blot as follows. WT, vector-transfected, and *hGSTA4*-transfected HLE B-3 cells ($\sim 2 \times 10^6$ in 10cm dishes) were harvested and lysates were sonicated on ice and centrifuged at 22,000g for 30 minutes to clear insoluble material. Samples of supernatants containing 60µg protein were loaded onto SDS-PAGE gels and run at 100V for ~1h, then immunoblotted onto PVDF membrane for ~3h at 35V and detected with anti-Fas/anti-β-actin antibodies. Results of these experiments showed both an increase of Fas expression in WT cells with increasing HNE dosage, and an increase of Fas expression with time in WT and vector-transfected cells which was not seen in *hGSTA4*-transfected cells. This implies that cells respond to HNE insult by upregulating Fas in both a time- and concentration-dependent manner. This increase in Fas expression after HNE insult can be seen after two hours, an endpoint shown to cause caspase activation in this and similar cell lines **(figure 21)**. This upregulation was only present in VT cells, as transformed HLE B-3 appear to have lost their ability to upregulate Fas in response to a rise in HNE level up to and including a lethal dose **(figure 29)**. It is interesting to note that in WT cells Fas is upregulated after even a 0.1µM dose of HNE, which is in the physiological range of intracellular concentrations; this is, however, an exogenous addition to constitutive amounts already present in cells and therefore their

concentrations are likely to be additive and therefore might explain a stress response. These results indicated a somewhat direct influence on Fas expression by the intracellular levels of HNE.
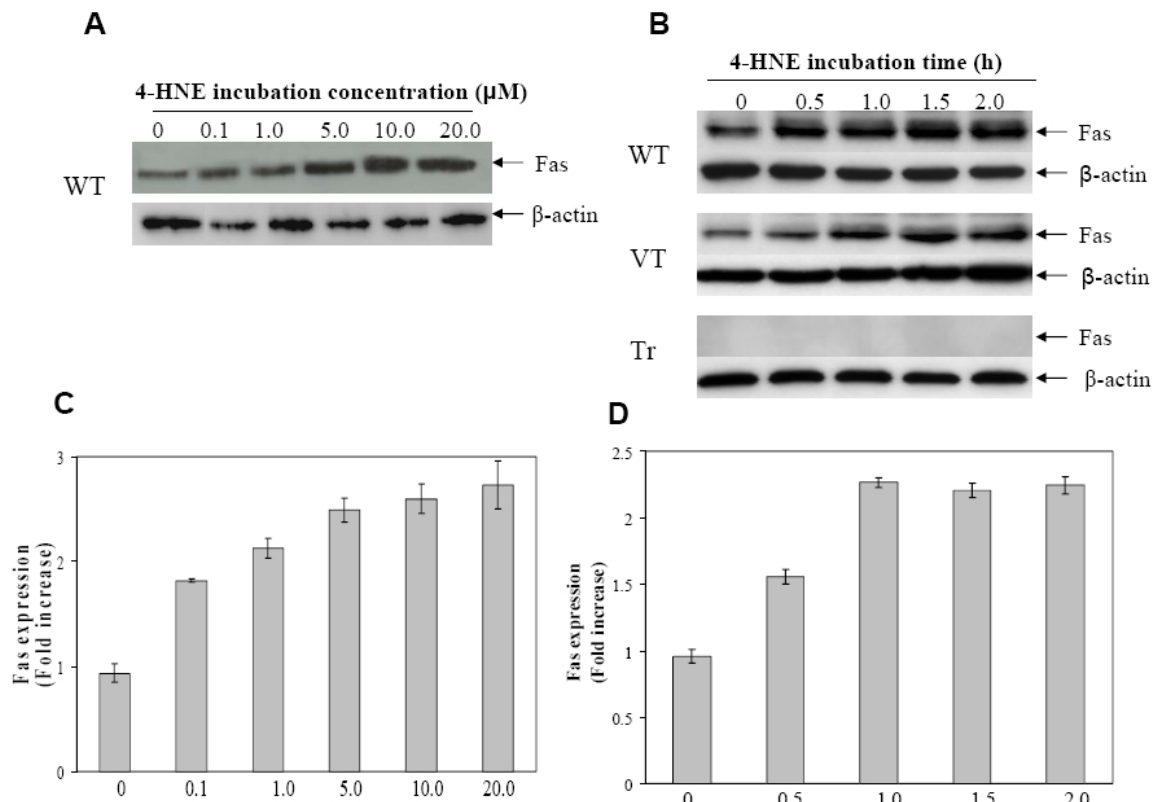
Figure 29: Time- and concentration-dependent induction of Fas expression by HNE in HLE B-3 cells. A, Cells were incubated with 0-20μM HNE in serum-free medium for 2h in 10cm dishes. **B,** Cells were incubated with 20mM HNE for 0-2h in 10cm dishes. **C and D,** densitometry of data from **A** and **B**, respectively. WT=wild-type, VT=vector-transfected, Tr=hGSTA4-transfecgted. Adapted from [156] with permission.

Such results were mirrored in immunofluorescence studies. In these studies, which were performed to verify Western blot studies and to visualize protein localization, empty vector- and *hGSTA4*-transfected HLE B-3 were grown on chamber slides, treated with 20 μM HNE for 0-2h and subsequently fixed, incubated with Fas-specific FITC-

106

conjugated antibodies. Results showed that there was an increase in Fas expression in HNE-treated WT cells over 2h treatment but no increase of expression in *hGSTA4-*transfected cells.   This implies that in stably-transfected transformed cells (which previously lost expression of Fas), increasing HNE had no inductive effect on Fas expression **(figure 30)**. Because the loss of Fas expression in transformed cells cannot be rescued by increasing HNE, such loss may be a permanent and unchangeable phenomenon in the transformed cells.
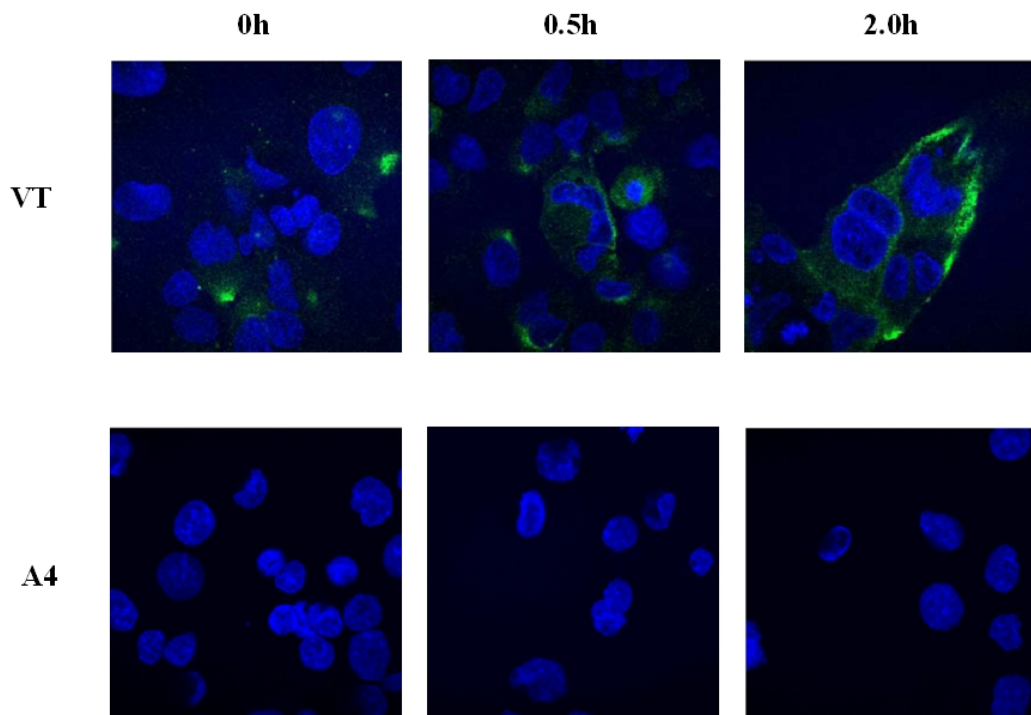
Figure 30: Immunofluorescence localization of Fas expression in HLE B-3 after HNE induction. VT and *hGSTA4*-transformed cells were grown in chamber slides and treated with 20μM HNE for 0 to 2h. Fluorescence was measured for nuclei (DAPI, blue) and Fas expression (FITC, green). Adapted from [156] with permission.

Effect of HNE on Fas expression *in vivo*: In order to determine whether Fas expression is correlated to intracellular HNE levels *in vivo* as it was observed to be *in vitro*, we employed a mouse model which has been selectively bred with a knockout of the *mGSTA4* gene, a mouse cytosolic Alpha-class GST which, like its human homolog *hGSTA4*, codes for its counterpart protein with strong catalytic efficiency for conjugation of HNE. This *mGsta4* null mouse model has been previously characterized in 129/Sv strain of mice [359] although this genotype is available in C57/BL6 which were developed by us and used for these studies. These mice have complete lack of expression of this gene as detected in several tissues, leading to much lower HNE-metabolizing activity (between 23-64% of WT values depending on tissue type) and significantly higher steady-state levels of HNE in tissues. Previously-harvested and frozen samples of these tissues containing 30μg protein from WT, heterozygous (offspring from knockout mice bred with WT mice, with one functional copy of the *mGTSA4* gene), and *mGSTA4*-null mice were loaded and run on SDS-PAGE gels and immunoblotted for expression of Fas via Western blot. Results showed that Fas is highly overexpressed in all tissues investigated except for lung in knockout mice, and similarly highly overexpressed in all tissues except for lung in heterozygous mice, with respect to expression levels seen in WT mice **(figure 31)**. These results show that expression of Fas *in vivo* in mice is correlated, at least in several tissues, with expression of HNE-conjugating activity, and this implies that just as overexpression of HNE-metabolizing activity and thereby depletion of HNE in HLE B-3 leads to decreased Fas expression, disruption of HNE-metabolizing activity and thereby increase of HNE in tissues leads to an increase in Fas expression.

To further substantiate this correlation between Fas expression and expression of HNE-metabolizing activity seen *in vivo*, Fas expression was visualized in wild-type, heterozygous, and *mGSTA4* knockout mouse tissues using immunofluorescence

techniques. Tissues harvested from mice were embedded in parafilm and sectioned at the Histopathology Core facility at UTMB, where the sections were mounted onto slides. The paraffin was removed and the sections prepared, and treated with Fas monoclonal antibodies with FITC-conjugated secondary antibodies.
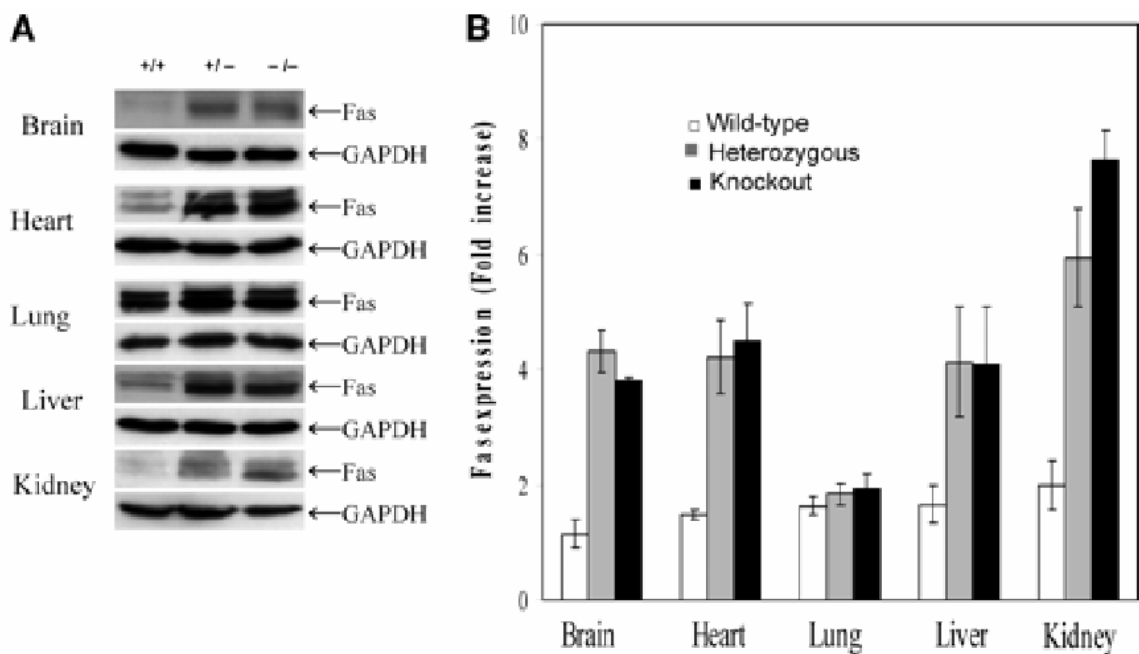
Figure 31: Expression of Fas in WT, +/-, and mGSTA4 -/- tissues. Tissue samples were harvested from mice and lysed in RIPA buffer and subjected to Western blot analysis with GAPDH as loading control. **A,** +/+ is WT, +/- is heterozygous, -/- is *mGSTA4* knockout. **B,** Densitometry from Western blot data, n=3. Adapted from [156] with permission.

Results of these studies showed a detectable level of physiological Fas expression in WT mouse tissues with much higher physiological expression in *mGSTA4*-null mouse tissues. This confirmed the previous Western blot studies and further showed that Fas expression in *mGSTA4* knockout tissues with less steady-state HNE conjugating activity is higher than in the counterpart WT mouse tissues **(figure 32)**, with some variation in the

magnitude of those differences by tissue type. Such variation (as seen in brain tissue) is difficult to explain and may be due to problems with tissue-specific fixation methods or possibly to intra-organ localization not displayed in the tissue sections prepared for microscopy (as the Western blots were performed on organ lysates).
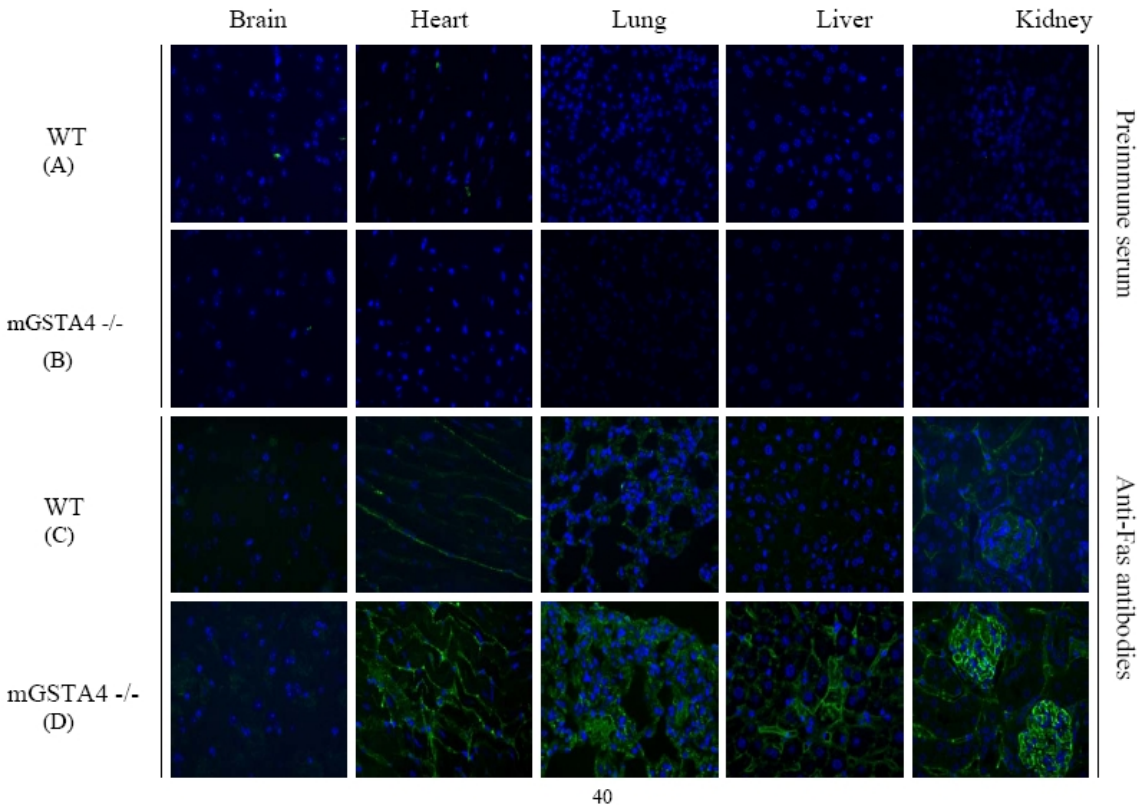
Figure 32: Immunohistochemical localization of Fas expression in WT and mGSTA4-/- mouse brain, heart, lung, liver, and kidney tissues. Tissues from WT and *mGSTA4 -/-* mice were embedded in paraffin and mounted on slides, and assayed for Fas expression with monoclonal antibodies. Fluorescence was measured for cell nuclei (DAPI, blue) and Fas (FITC, green). Adapted from [156] with permission.

Transient transfection studies:

110

Timing of Fas suppression in HNE depletion: To elucidate the correlation between overexpression of HNE-conjugating activity, the depletion of intracellular HNE levels, and expression of Fas in HLE B-3, cultures in 10cm dishes containing 1×10^6 cells were subjected to transient transfection of active *hGSTA4* using the same protocol as for stable transfection, which allowed all three of these parameters to be observed over time. Cells were harvested 48, 72, and 240h post-transfection and samples containing 30μg protein were loaded and run on SDS-PAGE gels and immunoblotted against anti-hGSTA4-4, anti-Fas, and anti-GAPDH antibodies as performed previously.   Results showed that while WT and VT cells did not express hGSTA4-4 protein at a detectable level, *hGSTA4*-transfected cells expressed protein until up to 72h post-transfection and such overexpression was lost by 240h **(figure 33)**. Coincident with overexpression of *hGSTA4* was depletion of intracellular HNE levels to between approximately 40-45% of WT levels up to 72h and by 240h, as *hGSTA4* expression decreased, post-transfection these levels returned to pre-transfection values. Interestingly, while WT and VT cells continued to express Fas normally throughout transfection, *hGSTA4*-transfected cells lost Fas expression at 48h. Loss of Fas expression continued at 72h and was restored to pre-transfection levels at 240h. This is an important finding and implies that expression of Fas is strongly influenced by intracellular HNE levels as modulated by metabolizing activity of overexpressed hGSTA4-4 protein. The fact that these events occur within a timeframe of a few days, when placed in context of the grand changes in cell morphology associated with morphological transformation beginning at least weeks later, strongly imply that, at least in the case of Fas, changes in gene expression are prior to and therefore likely contribute to the many possible causes of the observed transformation which remain to be determined.

JNK activation: Fas-mediated apoptotic signaling is known to be regulated through the JNK pathway, which involves phosphorylation and thereby activation of JNK, which activates c-Jun, which along with c-Fos form the AP-1 transcription factor

111

and bind to stress-response gene promoter elements [360], ultimately leading to activation of downstream apoptotic machinery. Therefore studies were included to measure JNK expression and phosphorylation in HLE B-3 and determine if incubation with HNE, which is sufficient to upregulate Fas expression, elicits activation of JNK. Vector- and *hGSTA4*-transfected cells ($2x10^5$) were treated in 6cm dishes with 20μM
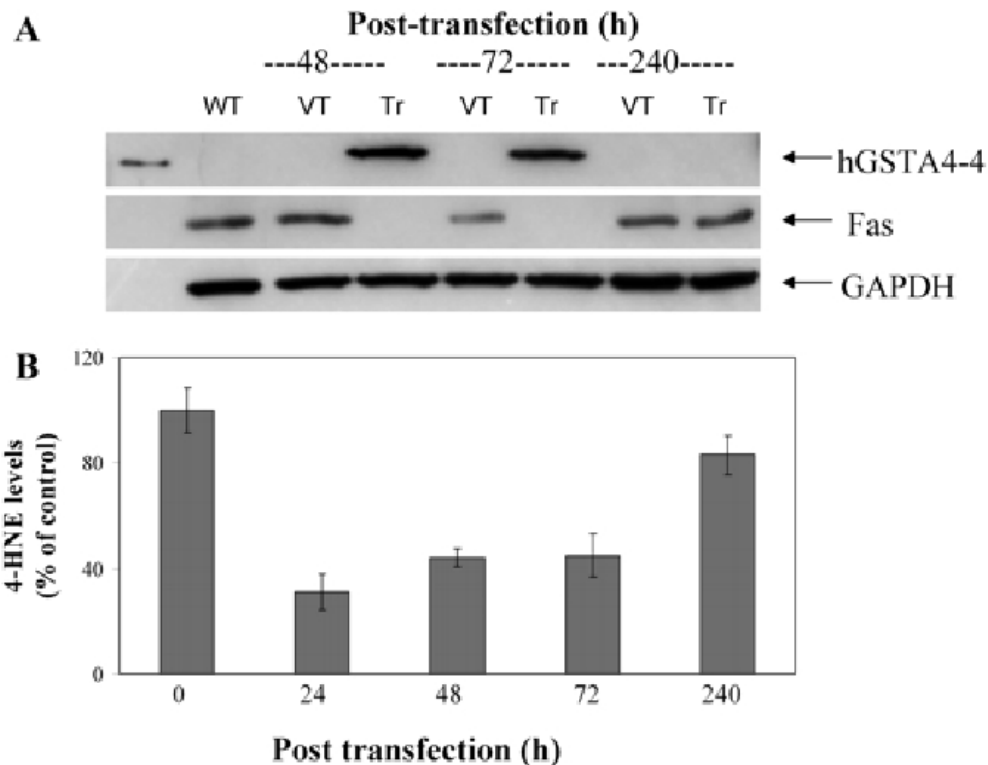
Figure 33: Expression of Fas in HLE B-3 after transient hGSTA4 transfection and correlation with decrease in intracellular HNE concentration. A, cells were transiently transfected with *hGSTA4* and harvested after 48, 72, and 240h, and assayed for expression hGSTA4-4 and Fas, with GAPDH used as loading control. **B,** cells were transfected and HNE concentration was determined via HPLC from lysate after extraction and normalized to protein concentration. Adapted from [156] with permission.

HNE for 2h, a previously-characterized toxic dose, and cells were harvested. Samples containing 30μg protein were loaded and run on SDS-PAGE gels and assayed by Western blot with both anti-JNK and anti-phosphorylated JNK antibodies to visualize

and quantify JNK expression and activation. Results showed an increase in phosphorylated JNK by 0.5h and up to 2h after HNE incubation in vector-transfected cells, but in *hGSTA4*-transfected cells there was no change in pJNK expression This implies that JNK is activated in a time-dependent manner **(figure 34)** after HNE exposure, which is coincident with Fas upregulation in these cells **(figure 29)**. These results correlate HNE levels to JNK activation, which elucidates the path by which HNE exerts downstream effects on these cells.
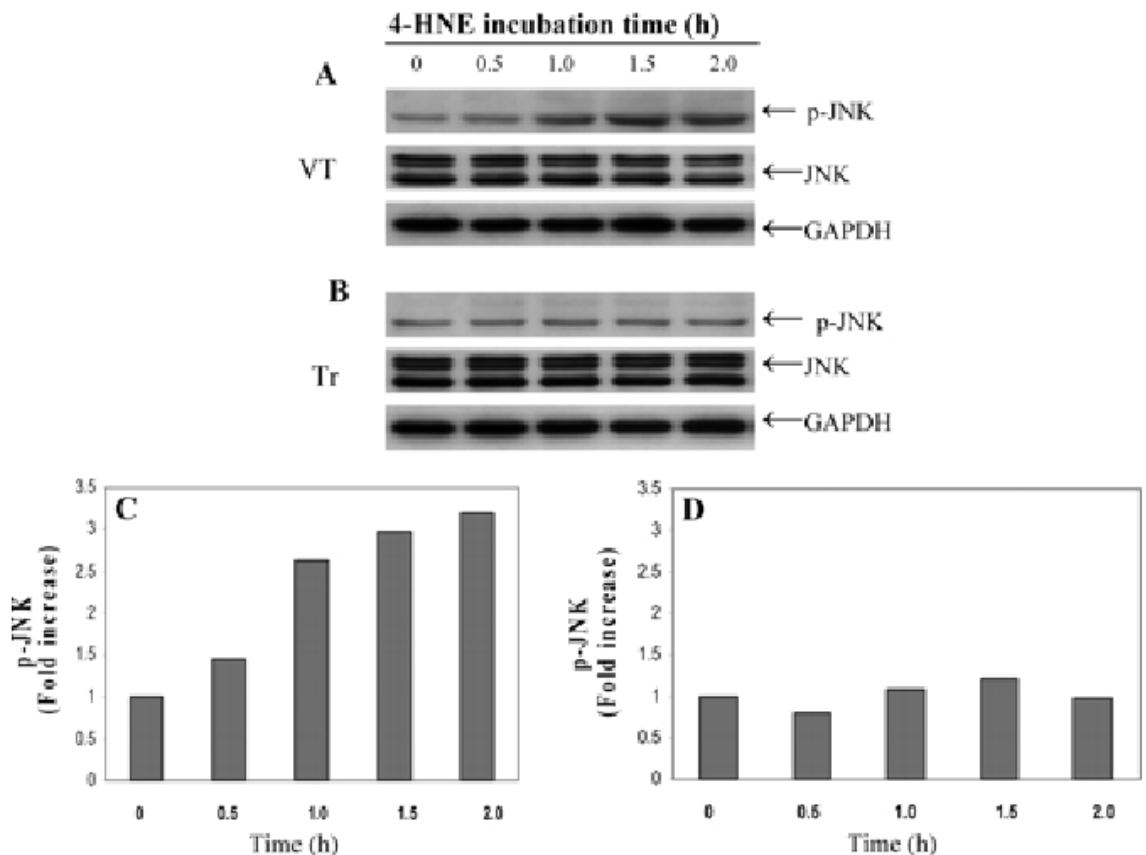
Figure 34: Protection of hGSTA4-transformed HLE B-3 from HNE-induced JNK activation. A, VT and **B,** *hGSTA4*-transformed cells were grown in 10cm dishes and treated with 20μM HNE for 0 to 2h and

assayed via Western blot for JNK and pJNK expression. **C,** Densitometry of Western blot data for VT cells shown in **A**. **D,** Densitometry of Western blot data for transformed cells shown in **B**. Adapted from [156] with permission.

Along with studies performed with HLE B-3 cells, JNK expression and phosphorylation in knockout mice was investigated. Samples of tissues containing 30μg protein were loaded and run on SDS-PAGE gels and transferred to PVDF membranes, and immunoblotted against anti-JNK, anti-phosphorylated JNK, and anti-GAPDH antibodies. Results of these studies showed a strong expression of both JNK and phosphorylated JNK in *mGSTA4*-null mouse tissues in all investigated tissues of WT mice except for lung, while in WT mouse tissues except for lung, JNK was present and phosphorylated JNK was either undetected or detected at low levels. Expression of phosphorylated JNK for heterozygous mouse tissues was between these levels for most tissues **(figure 35)**. These results of signaling effects in several tissues are not surprising when it is considered that mGSTA4-4 protein is expressed in most tissues assayed in C57BL/6 mice, and results are similar to and support results seen with HLE B-3 cells showing that increased JNK activation via phosphorylation is correlated with higher levels of HNE, with increased levels in cells due to exogenous treatment and increased levels *in vivo* due to lower HNE-metabolizing activity.

PARP cleavage: Cleavage of poly(ADP ribose) polymerase (PARP), a housekeeping gene, is an often-utilized marker of apoptosis in mammalian cells [361] downstream of caspase and JNK activation. Therefore studies were included to measure PARP cleavage in HLE B-3 in response to HNE treatment to determine if this pathway is involved in HNE-mediated apoptosis in this cell line, and if so to also determine whether

114

HNE depletion confers resistance against such signaling. Vector- and *hGSTA4*-transfected cells (2x10^5 in 6cm dishes) were treated with 20μM HNE for 0 to 2h and subsequently harvested and prepared for Western blot. Samples containing 30 μg protein were loaded and run on SDS-PAGE gels, transferred to PVDF membrane and immunoblotted with anti-PARP antibodies.
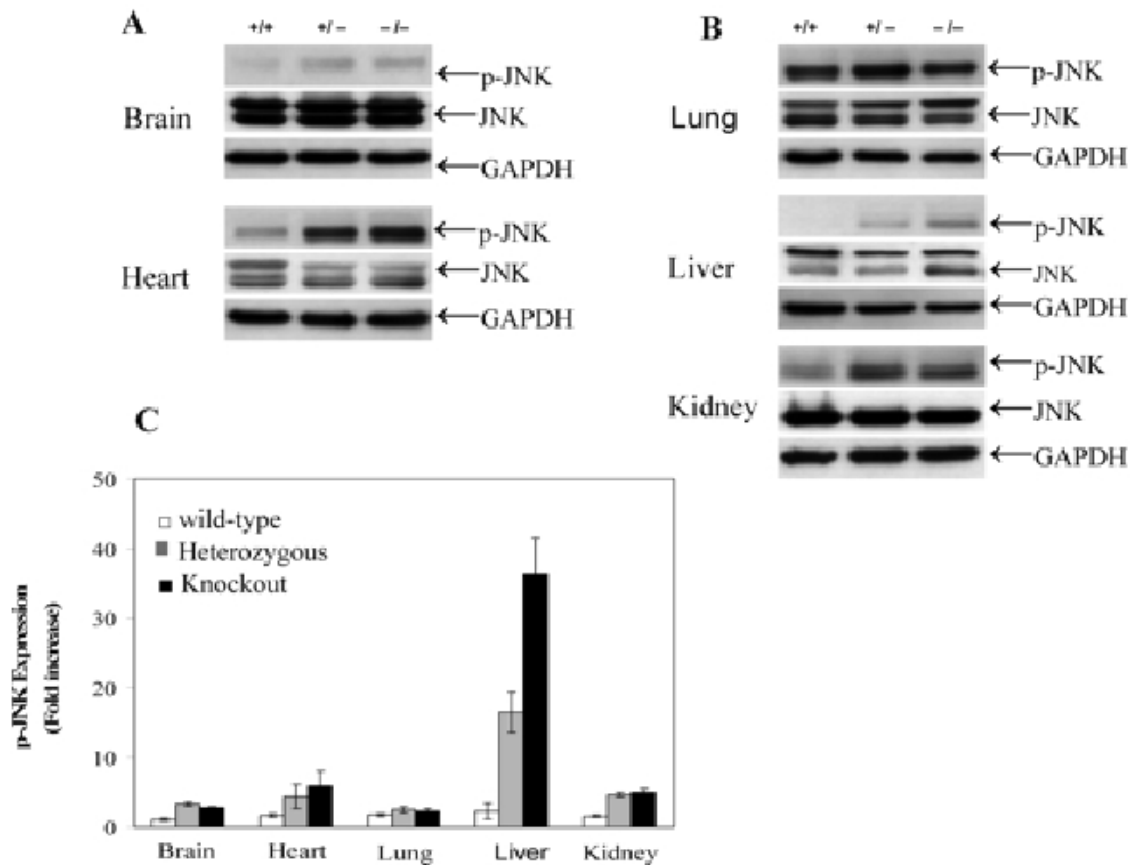
Figure 35:   Activation of JNK in mouse brain, heart, lung, liver, and kidney tissues of WT, heterozygous, and *mGSTA4*-null mice.   A and **B,** tissues were harvested from WT, +/-, and -/- mice and assayed for pJNK expression via Western blot. **C,** Densitometry of Western blot data was expressed as bar graph. Values are +/- SD, n=3. Adapted from [156] with permission.

Results of these studies showed an increase of cleaved PARP (89kDa band) at 1.5h and 2h incubation for vector-transfected cells and no such increase in cleaved PARP for *hGSTA4*-transfected cells. These results imply that while PARP fragmentation is involved in the HNE-mediated pathway (which includes both caspase and JNK activation) toward cell death, depletion of steady-state HNE levels is sufficient to block this step in HLE B-3.
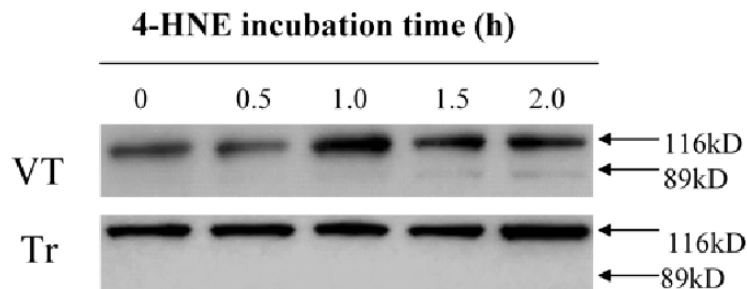
Figure 36: PARP cleavage in VT but not hGSTA4-transformed HLE B-3. VT and *hGSTA4*-transformed cells in 10cm dishes were treated with 20μM HNE for 0 to 2h and harvested. PARP cleavage was measured as expression of 89kDa band. Adapted from [156] with permission.

Significance: Unfortunately we cannot with confidence determine from studies performed whether the changes in gene expression observed secondary to overexpression of HNE-depleting activity in HLE B-3 is a causative event or a secondary event to phenotypic transformation. However it appears that since changes in Fas expression occur within 48h after transfection and concomitant with early HNE depletion events, and morphological transformation is not seen to occur until more than 8 weeks post-transfection with no obvious signs of such during the time frame of transient transfection, it is solidly implied that such changes in expression do occur prior to transformation. Therefore the implication is that these changes in gene expression are a possible cause of

116

phenotypic transformation and may affect relevant processes enough to allow cells to lose anchorage dependence and exist as suspended cells with a greatly increased proliferation, immortality, and augmented resistance to stress-mediated apoptosis.

Discussion:

From these studies it appears clear that depletion of HNE is an essential initial step in the progression of human lens epithelial (HLE B-3), as well as lung fibroblast (CCL-75) cells from attached cells with a limited lifespan and modest resistance to oxidative stress to an anchorage-independent cell lines with (as evidenced in HLE B-3) apparent unlimited lifespan and considerable stress resistance. Microinjection studies confirmed that increased activity against HNE is the required factor for transformation. These results were further illustrated by studies with hGSTA1-1 and hGSTP1-1 which show that GSTs unable to efficiently metabolize HNE are unable to elicit transformation. Some similarities in response to *hGSTA4* overexpression are apparent in human retinal pigment epithelial (RPE28 SV4) cells as evidenced by depletion of HNE, moderate alterations in cell morphology and increased protection against apoptotic stress. Since the mechanism(s) by which HNE depletion caused the observed profound changes in HLE B-3 is unknown, we investigated whether targets could be found which might better explain the manner in which HNE effects these changes.

To this end we examined global modulations in gene expression of genes relevant to the phenotypic alterations seen in HLE B-3 using well-established gene microarray techniques. Results of these studies showed a profound and global set of alterations in gene expression, numbering over 5000 significantly-modulated genes, including many

117

involved in pathways typically correlated with carcinogenesis and tumor metastasis. This is a substantial finding which illustrates the wide influence on intracellular signaling exerted by HNE. In order to both narrow the scope of our investigation and to verify these results we undertook quantitative RT-PCR studies using a subset of genes which were highly relevant to processes involved in transformation and which were identified by microarray studies to be highly-modulated in transformed cells. Results of these studies confirmed that these genes, involved in cell adhesion, cell cycle progression, and survival/apoptosis, were highly altered in *hGSTA4*-transfected, HNE-decreased transformed cells. This further implies that there is a necessary steady-state level of intracellular HNE in these cells which is critical for maintaining cell physiology through proper expression of critical genes. To further correlate changes in these previously-examined genes with phenotypic transformation we investigated whether the observed lack of procarcinogenic transformation in RPE was correlated with differences in gene modulations subsequent to HNE depletion. However we observed no changes in the expression of those genes previously investigated in HLE B-3 following *hGSTA4* overexpression, which implies that similar to vector-transfected HLE B-3, lack of profound alteration in gene expression in RPE was a likely cause of the lack of profound morphological transformation.

In order to determine more accurately the relationship between HNE depletion and expression of previously-investigated genes we further narrowed the scope of our investigation to investigate the relationship of *hGSTA4* overexpression, HNE depletion, Fas expression, and Fas-mediated apoptotic signaling. We investigated the manner in which HNE influences expression of Fas in HLE B-3 and results showed that there is a time- and concentration-dependent increase in expression in this cell line, which is consistent with previous studies correlating HNE depletion with decrease in Fas levels. These results were confirmed by immunocytochemistry, and correlated with *in vivo* studies using a previously-characterized *mGSTA4* knockout mouse model with superphysiological tissue levels of HNE, which showed increased Fas expression in most

tissues. We investigated the sequence of *hGSTA4* overexpression, HNE depletion, and Fas expression in transient transfection studies and results showed that Fas expression is lost simultaneously with HNE depletion 48h after *hGSTA4* transfection, and returns to physiological levels along with HNE several days later. These results strongly suggest a strong dependence of Fas expression levels on intracellular HNE levels. We also investigated the dependence of Fas-mediated apoptotic signaling on intracellular HNE levels. Results of these studies showed that activation of JNK in HLE B-3 is strongly influenced by depletion of HNE, and this was correlated with *in vivo* studies showing increase of activated JNK in mouse tissues expressing high levels of HNE. While these studies fall outside the timeframe of phenotypic transformation (occurring in the span of days rather than weeks required of transformation) the results indicate that alteration in intracellular HNE levels is sufficient to affect expression of Fas both *in vitro* and *in vivo* and to affect activity of Fas through downstream mediators of apoptosis.

Future studies in this area will likely include investigation into direct effects of HNE on Fas-specific transcriptional machinery as well as long-term studies of stably-transfected cells to determine a more illustrative timeline of modulation of previously-investigated genes during the process of transformation, using a larger scale to overcome the limitation of too small a population to perform necessary assays. In addition it may be prudent to investigate the extent of the phenotypic transformation of HLE B-3 through studies involving infecting an athymic mouse model to determine whether or not tumor formation occurs in these animals.

APPENDIX

Permissions were granted from the following publishers for reproduction rights in this dissertation:

[1] Blackwell Synergy, for reproduction of figures from:

Sharma, R.; Brown, D.; Awasthi, S.; Yang, Y.; Sharma, A.; Patrick, B.; Saini, M. K.; Singh, S. P.; Zimniak, P.; Awasthi, Y. C. Transfection with 4-hydroxynonenal-metabolizing glutathione S-transferase isozymes leads to phenotypic transformation and immortalization of adherent cells. *Euro J Biochem* **271:**1690-1701; 2004.

Permission was received via email on 1/19/2007 from Sally Byers, Permissions Assistant for Blackwell Publishing.

[2] Elsevier, for reproduction of figures and tables from:

Patrick, B.; Li, J.; Jeyabal, P. V.; Reddy, P. M.; Yang, Y.; Sharma, R.; Sinha, M.; Luxon, B.; Zimniak, P.; Awasthi, S.; Awasthi, Y. C. Depletion of 4-hydroxynonenal in hGSTA4-transfected HLE B-3 cells results in profound changes in gene expression. *Biochem Biophys Res Commun* **334:**425-432; 2005.

Permission was received via email on 1/18/2007 from Stephanie Smith, Rights Assistant for ACS Publications.

[3] American Chemical Society Publications, for reproduction of figures from:

Li, J.; Sharma, R.; Patrick, B.**;** Sharma, A.; Jeyabal, P. V. S.; Reddy, P. M. R. V.; Saini, M. K.; Dhanani, S.; Zimniak, P.; Awasthi, S.; Awasthi, Y. C. Regulation of CD95 (Fas) expression and Fas-mediated apoptotic signaling in HLE B-3 cells by 4-hydroxynonenal. *Biochemistry* **45:**12253-12264; 2006.

ACS Publications automatically permits reproduction of publications by their authors in theses and dissertations (http://pubs.acs.org/copyright/forms/dissertation.pdf).

REFERENCES

[1]   Patrick, B.; Li, J.; Jeyabal, P. V. S.; Reddy, P. M. R. V.; Yang, Y.; Sharma, R.; Sinha, M.; Luxon, B.; Zimniak, P.; Awasthi, S.; Awasthi, Y. C. Depletion of 4-hydroxynonenal in hGSTA4-transfected HLE B-3 cells results in profound changes in gene expression. *Biochemical and Biophysical Research Communications* **334:**425-432; 2005.

[2]   Marnett, L. J.; Riggins, J. N.; West, J. D. Endogenous generation of reactive oxidants and electrophiles and their reactions with DNA and protein. *J Clin Invest* **111:**583-593; 2003.

[3]   Kagi, J. H.; Schaffer, A. Biochemistry of metallothionein. *Biochemistry* **27:**8509-8515; 1988.

[4]   Thornalley, P. J.; Vasak, M. Possible role for metallothionein in protection against radiation-induced oxidative stress. Kinetics and mechanism of its reaction with superoxide and hydroxyl radicals. *Biochim Biophys Acta* **827:**36-44; 1985.

[5]   Hayes, J. D.; McLellan, L. I. Glutathione and glutathione-dependent enzymes represent a co-ordinately regulated defence against oxidative stress. *Free Radic Res* **31:**273-300; 1999.

[6]   Fenton, H. J. H. The oxidation of tartaric acid in presense of iron. *Proc Chem Soc* **9:**113; 1893.

[7]   King, M. M.; Lai, E. K.; McCay, P. B. Singlet oxygen production associated with enzyme-catalyzed lipid peroxidation in liver microsomes. *J Biol Chem* **250:**6496-6502; 1975.

[8]   Dix, T. A.; Aikens, J. Mechanisms and biological relevance of lipid peroxidation initiation. *Chem Res Toxicol* **6:**2-18; 1993.

[9]   Yang, Y.; Sharma, R.; Sharma, A.; Awasthi, S.; Awasthi, Y. C. Lipid peroxidation and cell cycle signaling: 4-hydroxynonenal, a key molecule in stress mediated signaling. *Acta Biochim Pol* **50:**319-336; 2003.

[10]   Guengerich, F. P. Common and uncommon cytochrome P450 reactions related to metabolism and chemical toxicity. *Chem Res Toxicol* **14:**611-650; 2001.

[11]   Zangar, R. C.; Davydov, D. R.; Verma, S. Mechanisms that regulate production of reactive oxygen species by cytochrome P450. *Toxicol Appl Pharmacol* **199:**316-331; 2004.

[12]   Gorsky, L. D.; Koop, D. R.; Coon, M. J. On the stoichiometry of the oxidase and monooxygenase reactions catalyzed by liver microsomal cytochrome P-450. Products of oxygen reduction. *J Biol Chem* **259:**6812-6817; 1984.

[13]   Kuthan, H.; Ullrich, V. Oxidase and oxygenase function of the microsomal cytochrome P450 monooxygenase system. *Eur J Biochem* **126:**583-588; 1982.

[14]   Gruenke, L. D.; Konopka, K.; Cadieu, M.; Waskell, L. The stoichiometry of the cytochrome P-450-catalyzed metabolism of methoxyflurane and benzphetamine in the presence and absence of cytochrome b5. *J Biol Chem* **270:**24707-24718; 1995.

[15]   White, R. E.; Coon, M. J. Oxygen Activation by Cytochrome P-4501. *Annu Rev Biochem* **49:**315-356; 1980.

[16]   Dai, Y.; Rashba-Step, J.; Cederbaum, A. I. Stable expression of human cytochrome P4502E1 in HepG2 cells: characterization of catalytic activities and production of reactive oxygen intermediates. *Biochemistry* **32:**6928-6937; 1993.

[17]   Armstead, W. M. Cyclooxygenase-2-dependent superoxide generation contributes to age-dependent impairment of G protein-mediated cerebrovasodilation. *Anesthesiology* **98:**1378-1383; 2003.

[18]   Schultz, B. E.; Chan, S. I. Structures and proton-pumping strategies of mitochondrial respiratory enzymes. *Annu Rev Biophys Biomol Struct* **30:**23-65; 2001.

[19]   Chance, B.; Sies, H.; Boveris, A. Hydroperoxide metabolism in mammalian organs. *Physiol Rev* **59:**527-605; 1979.

[20]   Knowles, R. G. Nitric oxide biochemistry. *Biochem Soc Trans* **25:**895-901; 1997.

[21]   Dixon, L. J.; Morgan, D. R.; Hughes, S. M.; McGrath, L. T.; El-Sherbeeny, N. A.; Plumb, R. D.; Devine, A.; Leahey, W.; Johnston, G. D.; McVeigh, G. E. Functional consequences of endothelial nitric oxide synthase uncoupling in congestive cardiac failure. *Circulation* **107:**1725-1728; 2003.

[22]	Zou, M. H.; Hou, X. Y.; Shi, C. M.; Nagata, D.; Walsh, K.; Cohen, R. A. Modulation by peroxynitrite of Akt- and AMP-activated kinase-dependent Ser1179 phosphorylation of endothelial nitric oxide synthase. *J Biol Chem* **277:**32552-32557; 2002.

[23]	Haruna, Y.; Morita, Y.; Komai, N.; Yada, T.; Sakuta, T.; Tomita, N.; Fox, D. A.; Kashihara, N. Endothelial dysfunction in rat adjuvant-induced arthritis: vascular superoxide production by NAD(P)H oxidase and uncoupled endothelial nitric oxide synthase. *Arthritis Rheum* **54:**1847-1855; 2006.

[24]	Osher, E.; Weisinger, G.; Limor, R.; Tordjman, K.; Stern, N. The 5 lipoxygenase system in the vasculature: Emerging role in health and disease. *Mol Cell Endocrin* **252:**201-206; 2006.

[25]	McCord, J. M.; Fridovich, I. The reduction of cytochrome c by milk xanthine oxidase. *J Biol Chem* **243:**5753-5760; 1968.

[26]	Algvere, P. V.; Marshall, J.; Seregard, S. Age-related maculopathy and the impact of blue light hazard. *Acta Opthalmol Scand* **84:**4-15; 2006.

[27]	Yang, Y.; Sharma, A.; Sharma, R.; Patrick, B.; Singhal, S. S.; Zimniak, P.; Awasthi, S.; Awasthi, Y. C. Cells preconditioned with mild, transient UVA irradiation acquire resistance to oxidative stress and UVA-induced apoptosis: Role of 4-hydroxynonenal in UVA-mediated signaling for apoptosis. *J Biol Chem* **278:**41380-41388; 2003.

[28]	Awasthi, Y. C.; Yang, Y.; Tiwari, N. K.; Patrick, B.; Sharma, A.; Li, J.; Awasthi, S. Regulation of 4-hydroxynonenal-mediated signaling by glutathione S-transferases. *Free Radical Biology and Medicine* **37:**607-619; 2004.

[29]	Chen, Y. R.; Wang, X.; Templeton, D.; Davis, R. J.; Tan, T. H. The role of c-Jun N-terminal kinase (JNK) in apoptosis induced by ultraviolet C and gamma radiation. Duration of JNK activation may determine cell death and proliferation. *J Biol Chem* **271:**31929-31936; 1996.

[30]	von Sonntag, C. *The chemical basis of radiation biology.* London: Taylor and Francis; 1987.

[31]	Borges, H. L.; Linden, R. Gamma irradiation leads to two waves of apoptosis in distinct cell populations of the retina of newborn rats. *J Cell Sci* **112 (Pt 23):**4315-4324; 1999.

[32]   Buttke, T. M.; Sandstrom, P. A. Oxidative stress as a mediator of apoptosis. *Immunology Today* **15:**7-10; 1994.

[33]   Ewing, D.; Jones, S. R. Superoxide removal and radiation protection in bacteria. *Arch Biochem Biophys* **254:**53-62; 1987.

[34]   Ansari, N. H.; Wang, L.; Srivastava, S. K. Role of lipid aldehydes in cataractogenesis: 4-hydroxynonenal-induced cataract. *Biochem Mol Med* **58:**25-30; 1996.

[35]   Dean, J. B.; Mulkey, D. K.; Henderson, R. A., III; Potter, S. J.; Putnam, R. W. Hyperoxia, reactive oxygen species, and hyperventilation: oxygen sensitivity of brain stem neurons. *J Appl Physiol* **96:**784-791; 2004.

[36]   Mantell, L. L.; Lee, P. J. Signal Transduction Pathways in Hyperoxia-Induced Lung Cell Death. *Mol Gen Metabol* **71:**359-370; 2000.

[37]   Duranteau, J.; Chandel, N. S.; Kulisz, A.; Shao, Z.; Schumacker, P. T. Intracellular Signaling by Reactive Oxygen Species during Hypoxia in Cardiomyocytes. *J Biol Chem* **273:**11619-11624; 1998.

[38]   Chandel, N. S.; Maltepe, E.; Goldwasser, E.; Mathieu, C. E.; Simon, M. C.; Schumacker, P. T. Mitochondrial reactive oxygen species trigger hypoxia-induced transcription. *Proc Natl Acad Sci U S A* **95:**11715-11720; 1998.

[39]   Ercal, N.; Gurer-Orhan, H.; Aykin-Burns, N. Toxic metals and oxidative stress part I: mechanisms involved in metal-induced oxidative damage. *Curr Top Med Chem* **1:**529-539; 2001.

[40]   Shafiq Ur, R. Lead-induced regional lipid peroxidation in brain. *Toxicol Lett* **21:**333-337; 1984.

[41]   Briede, J. J.; Godschalk, R. W.; Emans, M. T.; De Kok, T. M.; Van Agen, E.; Van Maanen, J.; Van Schooten, F. J.; Kleinjans, J. C. In vitro and in vivo studies on oxygen free radical and DNA adduct formation in rat lung and liver during benzo[a]pyrene metabolism. *Free Radic Res* **38:**995-1002; 2004.

[42]   Snyder, R.; Hedli, C. C. An Overview of Benzene Metabolism. *Environ Health Perspect* **104:**1165-1171; 1996.

[43]   Wu, D.; Cederbaum, A. I. Alcohol, oxidative stress, and free radical damage. *Alcohol Res Health* **27:**277-284; 2003.

[44]   Na, L.; Wartenberg, M.; Nau, H.; Hescheler, J.; Sauer, H. Anticonvulsant valproic acid inhibits cardiomyocyte differentiation of embryonic stem cells by increasing intracellular levels of reactive oxygen species. *Birth Defects Res A Clin Mol Teratol* **67:**174-180; 2003.

[45]   Winn, L. M.; Wells, P. G. Maternal administration of superoxide dismutase and catalase in phenytoin teratogenicity1. *Free Radic Biol Med* **26:**266-274; 1999.

[46]   Jaeschke, H.; Gores, G. J.; Cederbaum, A. I.; Hinson, J. A.; Pessayre, D.; Lemasters, J. J. Mechanisms of Hepatotoxicity. *Toxicol Sci* **65:**166-176; 2002.

[47]   Kloss, M. W.; Rosen, G. M.; Rauckman, E. J. Evidence of enhanced in vivo lipid peroxidation after acute cocaine administration. *Toxicology Letters* **15:**65-70; 1983.

[48]   Xu, B.; Wang, Z.; Li, G.; Li, B.; Lin, H.; Zheng, R.; Zheng, Q. Heroin-Administered Mice Involved in Oxidative Stress and Exogenous Antioxidant-Alleviated Withdrawal Syndrome. *Basic Clin Pharmacol Toxicol* **99:**153-161; 2006.

[49]   Montiel-Duarte, C.; Ansorena, E.; Lopez-Zabalza, M. J.; Cenarruzabeitia, E.; Iraburu, M. J. Role of reactive oxygen species, glutathione and NF-[kappa]B in apoptosis induced by 3,4-methylenedioxymethamphetamine ("Ecstasy") on hepatic stellate cells. *Biochem Pharmacol* **67:**1025-1033; 2004.

[50]   Joshi, G.; Sultana, R.; Tangpong, J.; Cole, M. P.; St Clair, D. K.; Vore, M.; Estus, S.; Butterfield, D. A. Free radical mediated oxidative stress and toxic side effects in brain induced by the anti cancer drug adriamycin: insight into chemobrain. *Free Radic Res* **39:**1147-1154; 2005.

[51]   Lee, J. E.; Nakagawa, T.; Kim, T. S.; Endo, T.; Shiga, A.; Iguchi, F.; Lee, S. H.; Ito, J. Role of reactive radicals in degeneration of the auditory system of mice following cisplatin treatment. *Acta Otolaryngol* **124:**1131-1135; 2004.

[52]   DeAtley, S. M.; Aksenov, M. Y.; Aksenova, M. V.; Harris, B.; Hadley, R.; Cole Harper, P.; Carney, J. M.; Butterfield, D. A. Antioxidants protect against reactive oxygen species associated with adriamycin-treated cardiomyocytes. *Cancer Lett* **136:**41-46; 1999.

[53]   Esterbauer, H.; Schaur, R. J.; Zollner, H. Chemistry and biochemistry of 4-hydroxynonenal, malonaldehyde and related aldehydes. *Free Radic Biol Med* **11:**81-128; 1991.

126

[54]   Frankel, E. N. Volatile lipid oxidation products. *Prog Lipid Res* **22:**1-33; 1983.

[55]   Benedetti, A.; Comporti, M.; Esterbauer, H. Identification of 4-hydroxynonenal as a cytotoxic product originating from the peroxidation of liver microsomal lipids. *Biochim Biophys Acta* **620:**281-296; 1980.

[56]   Schaur, R. J., Zollner, H., Esterbauer, H. In: Vigo-Pelfrey, C., ed. *Membrane Lipid Peroxidation*. Boca Raton: CRC; 1990: 141-163.

[57]   Pryor, W. A.; Porter, N. A. Suggested mechanisms for the production of 4-hydroxy-2-nonenal from the autoxidation of polyunsaturated fatty acids. *Free Radic Biol Med* **8:**541-543; 1990.

[58]   Schneider, C.; Tallman, K. A.; Porter, N. A.; Brash, A. R. Two Distinct Pathways of Formation of 4-Hydroxynonenal. Mechanisms of nonenzymatic transformation of the 9- and 13-hydroperoxides of linoleic acid to 4-hydroxyalkenals. *J Biol Chem* **276:**20831-20838; 2001.

[59]   Esterbauer, H.; Benedetti, A.; Lang, J.; Fulceri, R.; Fauler, G.; Comporti, M. Studies on the mechanism of formation of 4-hydroxynonenal during microsomal lipid peroxidation. *Biochim Biophys Acta* **876:**154-166; 1986.

[60]   Segall, H. J.; Wilson, D. W.; Dallas, J. L.; Haddon, W. F. trans-4-Hydroxy-2-hexenal: a reactive metabolite from the macrocyclic pyrrolizidine alkaloid senecionine. *Science* **229:**472-475; 1985.

[61]   Poli, G.; Dianzani, M. U.; Cheeseman, K. H.; Slater, T. F.; Lang, J.; Esterbauer, H. Separation and characterization of the aldehydic products of lipid peroxidation stimulated by carbon tetrachloride or ADP-iron in isolated rat hepatocytes and rat liver microsomal suspensions. *Biochem J* **227:**629-638; 1985.

[62]   Jungsuwadee, P.; Cole, M. P.; Sultana, R.; Joshi, G.; Tangpong, J.; Butterfield, D. A.; St Clair, D. K.; Vore, M. Increase in Mrp1 expression and 4-hydroxy-2-nonenal adduction in heart tissue of Adriamycin-treated C57BL/6 mice. *Mol Cancer Ther* **5:**2851-2860; 2006.

[63]   Sampey, B. P.; Korourian, S.; Ronis, M. J.; Badger, T. M.; Petersen, D. R. Immunohistochemical characterization of hepatic malondialdehyde and 4-hydroxynonenal modified proteins during early stages of ethanol-induced liver injury. *Alcohol Clin Exp Res* **27:**1015-1022; 2003.

[64]   Acworth, I. N.; McCabe, D. R.; Maher, T. J. The analysis of free radicals, their reaction products, and antioxidants. In: Baskin, S. I.; Salem, H., eds. *Oxidants, Antioxidants, and Free Radicals*. Washington, D.C.: Taylor and Francis; 1997: 23-77.

[65]   Foyer, C. H.; Lelandais, M.; Kunert, K. J. Photooxidative stress in plants. *Physiol Plant* **92:**696-717; 1994.

[66]   Diplock, A. T.; Xu, G. L.; Yeow, C. L.; Okikiola, M. Relationship of tocopherol structure to biological activity, tissue uptake, and prostaglandin biosynthesis. *Ann N Y Acad Sci* **570:**72-84; 1989.

[67]   Meister, A.; Anderson, M. E. Glutathione. *Annu Rev Biochem* **52:**711-760; 1983.

[68]   Waring, W. S. Uric acid: an important antioxidant in acute ischaemic stroke. *QJM* **95:**691-693; 2002.

[69]   Ames, B. N.; Cathcart, R.; Schwiers, E.; Hochstein, P. Uric Acid Provides an Antioxidant Defense in Humans against Oxidant- and Radical-Caused Aging and Cancer: A Hypothesis. *Proc Natl Acad Sci U S A* **78:**6858-6862; 1981.

[70]   Crane, F. L. Biochemical Functions of Coenzyme Q10. *J Am Coll Nutr* **20:**591-598; 2001.

[71]   Vieira, O.; Escargueil-Blanc, I.; Meilhac, O.; Basile, J.-P.; Laranjinha, J.; Almeida, L.; Salvayre, R.; Negre-Salvayre, A. Effect of dietary phenolic compounds on apoptosis of human cultured endothelial cells induced by oxidized LDL. *Br J Pharmacol* **123:**565-573; 1998.

[72]   Awasthi, S.; Srivatava, S. K.; Piper, J. T.; Singhal, S. S.; Chaubey, M.; Awasthi, Y. C. Curcumin protects against 4-hydroxy-2-trans-nonenal-induced cataract formation in rat lenses. *Am J Clin Nutr* **64:**761-766; 1996.

[73]   Kosower, N. S.; Kosower, E. M. The glutathione status of cells. *Int Rev Cytol* **54:**109-160; 1978.

[74]   McCord, J. M.; Fridovich, I. Superoxide Dismutase. An enzymatic function for erythrocuprein (hemocuprein). *J Biol Chem* **244:**6049-6055; 1969.

[75]   Gaetani, G. F.; Ferraris, A. M.; Rolfo, M.; Mangerini, R.; Arena, S.; Kirkman, H. N. Predominant role of catalase in the disposal of hydrogen peroxide within human erythrocytes. *Blood* **87:**1595-1599; 1996.

[76]   Carlberg, I.; Mannervik, B. Glutathione reductase. *Methods Enzymol* **113:**484-490; 1985.

[77]   Cosgrove, M. S.; Naylor, C.; Paludan, S.; Adams, M. J.; Levy, H. R. On the mechanism of the reaction catalyzed by glucose 6-phosphate dehydrogenase. *Biochemistry* **37:**2759-2767; 1998.

[78]   Nordberg, J.; Arner, E. S. J. Reactive oxygen species, antioxidants, and the mammalian thioredoxin system. *Free Radic Biol Med* **31:**1287-1312; 2001.

[79]   Chae, H. Z.; Kim, H. J.; Kang, S. W.; Rhee, S. G. Characterization of three isoforms of mammalian peroxiredoxin that reduce peroxides in the presence of thioredoxin. *Diabetes Res Clin Pract* **45:**101-112; 1999.

[80]   Srivastava, S.; Dixit, B. L.; Cai, J.; Sharma, S.; Hurst, H. E.; Bhatnagar, A.; Srivastava, S. K. Metabolism of lipid peroxidation product, 4-hydroxynonenal (HNE) in rat erythrocytes: role of aldose reductase. *Free Radic Biol Med* **29:**642-651; 2000.

[81]   Alary, J.; Gueraud, F.; Cravedi, J. P. Fate of 4-hydroxynonenal in vivo: disposition and metabolic pathways. *Mol Aspects Med* **24:**177-187; 2003.

[82]   Kaufmann, W. K.; Kaufman, D. G. Cell cycle control, DNA repair and initiation of carcinogenesis. *FASEB J* **7:**1188-1191; 1993.

[83]   Zhivotovsky, B.; Orrenius, S. Carcinogenesis and apoptosis: paradigms and paradoxes. *Carcinogenesis* **27:**1939-1945; 2006.

[84]   Hirohashi, S.; Kanai, Y. Cell adhesion system and human cancer morphogenesis. *Cancer Sci* **94:**575-581; 2003.

[85]   Manoharan, S.; Kolanjiappan, K.; Suresh, K.; Panjamurthy, K. Lipid peroxidation & antioxidants status in patients with oral squamous cell carcinoma. *Indian J Med Res* **122:**529-534; 2005.

[86]   Gonenc, A.; Erten, D.; Aslan, S.; Akinci, M.; Simsek, B.; Torun, M. Lipid peroxidation and antioxidant status in blood and tissue of malignant breast tumor and benign breast disease. *Cell Biol Int* **30:**376-380; 2006.

[87]   Czeczot, H.; Scibior, D.; Skrzycki, M.; Podsiad, M. Glutathione and GSH-dependent enzymes in patients with liver cirrhosis and hepatocellular carcinoma. *Acta Biochim Pol* **53:**237-242; 2006.

[88]   Aydin, A.; Arsova-Sarafinovska, Z.; Sayal, A.; Eken, A.; Erdem, O.; Erten, K.; Ozgok, Y.; Dimovski, A. Oxidative stress and antioxidant status in non-metastatic prostate cancer and benign prostatic hyperplasia. *Clin Biochem* **39:**176-179; 2006.

[89]   Zarkovic, K.; Juric, G.; Waeg, G.; Kolenc, D.; Zarkovic, N. Immunohistochemical appearance of HNE-protein conjugates in human astrocytomas. *Biofactors* **24:**33-40; 2005.

[90]   Dianzani, M. U. 4-hydroxynonenal from pathology to physiology. *Mol Aspects Med* **24:**263-272; 2003.

[91]   National Advisory Eye Council. Vision Research: A National Plan, 1999-2003. Bethesda, MD: United States Department of Health and Human Services, National Institutes of Health, National Eye Institute, 1998.

[92]   Simonelli, F.; Nesti, A.; Pensa, M.; Romano, L.; Savastano, S.; Rinaldi, E.; Auricchio, G. Lipid peroxidation and human cataractogenesis in diabetes and severe myopia. *Exp Eye Res* **49:**181-187; 1989.

[93]   Vinson, J. A. Oxidative stress in cataracts. *Pathophysiology* **13:**151-162; 2006.

[94]   Chylack, L. T., Jr. Mechanisms of senile cataract formation. *Ophthalmology* **91:**596-602; 1984.

[95]   Li, W. C.; Kuszak, J. R.; Dunn, K.; Wang, R. R.; Ma, W.; Wang, G. M.; Spector, A.; Leib, M.; Cotliar, A. M.; Weiss, M. Lens epithelial cell apoptosis appears to be a common cellular basis for non-congenital cataract development in humans and animals. *J Cell Biol* **130:**169-181; 1995.

[96]   Usha P. Andley, J. J.-N. L., M.F. Lou Biochemical Mechanisms of age-related cataract. In: D.M. Albert, F. A. J., ed. *Principle, Practices in Ophthalmology*. Philadelphia: Sanuders; 2000: 1428–1449.

[97]   Spector, A. Oxidative stress-induced cataract: mechanism of action. *FASEB J* **9:**1173-1182; 1995.

[98]   Li, W.-C.; Spector, A. Lens epithelial cell apoptosis is an early event in the development of UVB-induced cataract. *Free Radic Biol Med* **20:**301-311; 1996.

[99]   Babizhayev, M. A. Failure to withstand oxidative stress induced by phospholipid hydroperoxides as a possible cause of the lens opacities in systemic diseases and ageing. *Biochim Biophys Acta* **1315:**87-99; 1996.

[100]   Zigler, J. S., Jr.; Hess, H. H. Cataracts in the Royal College of Surgeons rat: evidence for initiation by lipid peroxidation products. *Exp Eye Res* **41:**67-76; 1985.

[101]   Srivastava, S. K.; Awasthi, S.; Wang, L.; Bhatnagar, A.; Awasthi, Y. C.; Ansari, N. H. Attenuation of 4-hydroxynonenal-induced cataractogenesis in rat lens by butylated hydroxytoluene. *Curr Eye Res* **15:**749-754; 1996.

[102]   Strauss, O. The Retinal Pigment Epithelium in Visual Function. *Physiol Rev* **85:**845-881; 2005.

[103]   Klein, R.; Klein, B. E. K.; Tomany, S. C.; Meuer, S. M.; Huang, G.-H. Ten-year incidence and progression of age-related maculopathy: The Beaver Dam eye study. *Ophthalmology* **109:**1767-1779; 2002.

[104]   Kopitz, J.; Holz, F. G.; Kaemmerer, E.; Schutt, F. Lipids and lipid peroxidation products in the pathogenesis of age-related macular degeneration. *Biochimie* **86:**825-831; 2004.

[105]   Beatty, S.; Koh, H.-H.; Phil, M.; Henson, D.; Boulton, M. The Role of Oxidative Stress in the Pathogenesis of Age-Related Macular Degeneration. *Survey of Ophthalmology* **45:**115-134; 2000.

[106]   Katz, M. L. Incomplete proteolysis may contribute to lipofuscin accumulation in the retinal pigment epithelium. *Adv Exp Med Biol* **266:**109-116; discussion 116-108; 1989.

[107]   Burcham, P. C.; Kuhan, Y. T. Diminished Susceptibility to Proteolysis after Protein Modification by the Lipid Peroxidation Product Malondialdehyde: Inhibitory Role for Crosslinked and Noncrosslinked Adducted Proteins. *Arch Biochem Biophys* **340:**331-337; 1997.

[108]   Schutt, F.; Bergmann, M.; Holz, F. G.; Kopitz, J. Proteins modified by malondialdehyde, 4-hydroxynonenal, or advanced glycation end products in lipofuscin of human retinal pigment epithelium. *Invest Ophthalmol Vis Sci* **44:**3663-3668; 2003.

[109]   Klein, R. Retinopathy in a population-based study. *Trans Am Ophthalmol Soc* **90:**561-594; 1992.

[110]   Ozdemir, G.; Ozden, M.; Maral, H.; Kuskay, S.; Cetinalp, P.; Tarkun, I. Malondialdehyde, glutathione, glutathione peroxidase and homocysteine levels in type 2 diabetic patients with and without microalbuminuria. *Ann Clin Biochem* **42:**99-104; 2005.

[111] Augustin, A. J.; Breipohl, W.; Boker, T.; Lutz, J.; Spitznas, M. Increased lipid peroxide levels and myeloperoxidase activity in the vitreous of patients suffering from proliferative diabetic retinopathy. *Graefes Arch Clin Exp Ophthalmol* **231:**647-650; 1993.

[112] Armstrong, D.; al-Awadi, F. Lipid peroxidation and retinopathy in streptozotocin-induced diabetes. *Free Radic Biol Med* **11:**433-436; 1991.

[113] Naseem H. Ansari, W. Z., Eva Fulep, Ahmad Mansour. Prevention of pericyte loss by trolox in diabetic rat retina. *Journal of Toxicology and Environmental Health Part A* **54:**467-475; 1998.

[114] Nguyen, Q. D.; Shah, S. M.; Van Anden, E.; Sung, J. U.; Vitale, S.; Campochiaro, P. A. Supplemental Oxygen Improves Diabetic Macular Edema: A Pilot Study. *Invest Ophthalmol Vis Sci* **45:**617-624; 2004.

[115] Cullen, P.; Rauterberg, J.; Lorkowski, S. The pathogenesis of atherosclerosis. *Handb Exp Pharmacol* **170:**3-70; 2005.

[116] Yang, Y.; Yang, Y.; Trent, M. B.; He, N.; Lick, S. D.; Zimniak, P.; Awasthi, Y. C.; Boor, P. J. Glutathione-S-transferase A4-4 modulates oxidative stress in endothelium: possible role in human atherosclerosis. *Atherosclerosis* **173:**211-221; 2004.

[117] Negre-Salvayre, A.; Vieira, O.; Escargueil-Blanc, I.; Salvayre, R. Oxidized LDL and 4-hydroxynonenal modulate tyrosine kinase receptor activity. *Mol Aspects Med* **24:**251-261; 2003.

[118] Hennig, B.; Chow, C. K. Lipid peroxidation and endothelial cell injury: implications in atherosclerosis. *Free Radic Biol Med* **4:**99-106; 1988.

[119] Henriksen, T.; Mahoney, E. M.; Steinberg, D. Enhanced macrophage degradation of biologically modified low density lipoprotein. *Arteriosclerosis* **3:**149-159; 1983.

[120] Jurgens, G.; Lang, J.; Esterbauer, H. Modification of human low-density lipoprotein by the lipid peroxidation product 4-hydroxynonenal. *Biochim Biophys Acta* **875:**103-114; 1986.

[121] Jessup, W.; Jurgens, G.; Lang, J.; Esterbauer, H.; Dean, R. T. Interaction of 4-hydroxynonenal-modified low-density lipoproteins with the fibroblast apolipoprotein B/E receptor. *Biochem J* **234:**245-248; 1986.

[122] Esterbauer, H.; Dieber-Rotheneder, M.; Waeg, G.; Striegl, G.; Jurgens, G. Biochemical, structural, and functional properties of oxidized low-density lipoprotein. *Chem Res Toxicol* **3:**77-92; 1990.

[123] Esterbauer, H.; Gebicki, J.; Puhl, H.; Jurgens, G. The role of lipid peroxidation and antioxidants in oxidative modification of LDL. *Free Radic Biol Med* **13:**341-390; 1992.

[124] Hoff, H. F.; O'Neil, J.; Chisolm, G. M., 3rd; Cole, T. B.; Quehenberger, O.; Esterbauer, H.; Jurgens, G. Modification of low density lipoprotein with 4-hydroxynonenal induces uptake by macrophages. *Arteriosclerosis* **9:**538-549; 1989.

[125] Uchida, K.; Toyokuni, S.; Nishikawa, K.; Kawakishi, S.; Oda, H.; Hiai, H.; Stadtman, E. R. Michael addition-type 4-hydroxy-2-nonenal adducts in modified low-density lipoproteins: markers for atherosclerosis. *Biochemistry* **33:**12487-12494; 1994.

[126] Sayre, L. M.; Zelasko, D. A.; Harris, P. L.; Perry, G.; Salomon, R. G.; Smith, M. A. 4-Hydroxynonenal-derived advanced lipid peroxidation end products are increased in Alzheimer's disease. *J Neurochem* **68:**2092-2097; 1997.

[127] Zarkovic, K. 4-hydroxynonenal and neurodegenerative diseases. *Mol Aspects Med* **24:**293-303; 2003.

[128] Lovell, M. A.; Ehmann, W. D.; Butler, S. M.; Markesbery, W. R. Elevated thiobarbituric acid-reactive substances and antioxidant enzyme activity in the brain in Alzheimer's disease. *Neurology* **45:**1594-1601; 1995.

[129] Mecocci, P.; MacGarvey, U.; Beal, M. F. Oxidative damage to mitochondrial DNA is increased in Alzheimer's disease. *Ann Neurol* **36:**747-751; 1994.

[130] Hensley, K.; Hall, N.; Subramaniam, R.; Cole, P.; Harris, M.; Aksenov, M.; Aksenova, M.; Gabbita, S. P.; Wu, J. F.; Carney, J. M.; et al. Brain regional correspondence between Alzheimer's disease histopathology and biomarkers of protein oxidation. *J Neurochem* **65:**2146-2156; 1995.

[131] Prasad, M. R.; Lovell, M. A.; Yatin, M.; Dhillon, H.; Markesbery, W. R. Regional membrane phospholipid alterations in Alzheimer's disease. *Neurochem Res* **23:**81-88; 1998.

[132] Bruce-Keller, A. J.; Li, Y. J.; Lovell, M. A.; Kraemer, P. J.; Gary, D. S.; Brown, R. R.; Markesbery, W. R.; Mattson, M. P. 4-Hydroxynonenal, a product of lipid

peroxidation, damages cholinergic neurons and impairs visuospatial memory in rats. *J Neuropathol Exp Neurol* **57:**257-267; 1998.

[133]   Kawaguchi-Niida, M.; Shibata, N.; Morikawa, S.; Uchida, K.; Yamamoto, T.; Sawada, T.; Kobayashi, M. Crotonaldehyde accumulates in glial cells of Alzheimer's disease brain. *Acta Neuropathol (Berl)* **111:**422-429; 2006.

[134]   Smith, J. L.; Xiong, S.; Lovell, M. A. 4-Hydroxynonenal disrupts zinc export in primary rat cortical cells. *Neurotoxicology* **27:**1-5; 2006.

[135]   Vigh, L.; Smith, R. G.; Soos, J.; Engelhardt, J. I.; Appel, S. H.; Siklos, L. Sublethal dose of 4-hydroxynonenal reduces intracellular calcium in surviving motor neurons in vivo. *Acta Neuropathol (Berl)* **109:**567-575; 2005.

[136]   Butterfield, D. A.; Reed, T.; Perluigi, M.; De Marco, C.; Coccia, R.; Cini, C.; Sultana, R. Elevated protein-bound levels of the lipid peroxidation product, 4-hydroxy-2-nonenal, in brain from persons with mild cognitive impairment. *Neurosci Lett* **397:**170-173; 2006.

[137]   Markesbery, W. R.; Kryscio, R. J.; Lovell, M. A.; Morrow, J. D. Lipid peroxidation is an early event in the brain in amnestic mild cognitive impairment. *Ann Neurol* **58:**730-735; 2005.

[138]   Yao, Y.; Clark, C. M.; Trojanowski, J. Q.; Lee, V. M.; Pratico, D. Elevation of 12/15 lipoxygenase products in AD and mild cognitive impairment. *Ann Neurol* **58:**623-626; 2005.

[139]   Hochstein, P.; Jain, S. K. Association of lipid peroxidation and polymerization of membrane proteins with erythrocyte aging. *Fed Proc* **40:**183-188; 1981.

[140]   Curzio, M.; Di Mauro, C.; Esterbauer, H.; Dianzani, M. U. Chemotactic activity of aldehydes. Structural requirements. Role in inflammatory process. *Biomed Pharmacother* **41:**304-314; 1987.

[141]   Zarkovic, N.; Ilic, Z.; Jurin, M.; Schaur, R. J.; Puhl, H.; Esterbauer, H. Stimulation of HeLa cell growth by physiological concentrations of 4-hydroxynonenal. *Cell Biochem Funct* **11:**279-286; 1993.

[142]   Leonarduzzi, G.; Arkan, M. C.; Basaga, H.; Chiarpotto, E.; Sevanian, A.; Poli, G. Lipid oxidation products in cell signaling. *Free Radic Biol Med* **28:**1370-1378; 2000.

[143]   Chiarpotto, E.; Domenicotti, C.; Paola, D.; Vitali, A.; Nitti, M.; Pronzato, M. A.; Biasi, F.; Cottalasso, D.; Marinari, U. M.; Dragonetti, A.; Cesaro, P.; Isidoro, C.; Poli, G. Regulation of rat hepatocyte protein kinase C beta isoenzymes by the lipid peroxidation product 4-hydroxy-2,3-nonenal: A signaling pathway to modulate vesicular transport of glycoproteins. *Hepatology* **29:**1565-1572; 1999.

[144]   Marinari, U. M.; Nitti, M.; Pronzato, M. A.; Domenicotti, C. Role of PKC-dependent pathways in HNE-induced cell protein transport and secretion. *Mol Aspects Med* **24:**205-211; 2003.

[145]   Parola, M.; Robino, G.; Marra, F.; Pinzani, M.; Bellomo, G.; Leonarduzzi, G.; Chiarugi, P.; Camandola, S.; Poli, G.; Waeg, G.; Gentilini, P.; Dianzani, M. U. HNE Interacts Directly with JNK Isoforms in Human Hepatic Stellate Cells. *J Clin Invest* **102:**1942-1950; 1998.

[146]   Uchida, K.; Shiraishi, M.; Naito, Y.; Torii, Y.; Nakamura, Y.; Osawa, T. Activation of Stress Signaling Pathways by the End Product of Lipid Peroxidation. 4-HYDROXY-2-NONENAL IS A POTENTIAL INDUCER OF INTRACELLULAR PEROXIDE PRODUCTION. *J Biol Chem* **274:**2234-2242; 1999.

[147]   Cheng, J. Z.; Singhal, S. S.; Sharma, A.; Saini, M.; Yang, Y.; Awasthi, S.; Zimniak, P.; Awasthi, Y. C. Transfection of mGSTA4 in HL-60 cells protects against 4-hydroxynonenal-induced apoptosis by inhibiting JNK-mediated signaling. *Arch Biochem Biophys* **392:**197-207; 2001.

[148]   Liu, W.; Kato, M.; Akhand, A. A.; Hayakawa, A.; Suzuki, H.; Miyata, T.; Kurokawa, K.; Hotta, Y.; Ishikawa, N.; Nakashima, I. 4-hydroxynonenal induces a cellular redox status-related activation of the caspase cascade for apoptotic cell death. *J Cell Sci* **113 (Pt 4):**635-641; 2000.

[149]   Cheng, J. Z.; Yang, Y.; Singh, S. P.; Singhal, S. S.; Awasthi, S.; Pan, S. S.; Singh, S. V.; Zimniak, P.; Awasthi, Y. C. Two distinct 4-hydroxynonenal metabolizing glutathione S-transferase isozymes are differentially expressed in human tissues. *Biochem Biophys Res Commun* **282:**1268-1274; 2001.

[150]   Awasthi, Y. C.; Yang, Y.; Tiwari, N. K.; Patrick, B.; Sharma, A.; Li, J.; Awasthi, S. Regulation of 4-hydroxynonenal-mediated signaling by glutathione S-transferases. *Free Radic Biol Med* **37:**607-619; 2004.

[151]   Awasthi, Y. C.; Ansari, G. A. S.; Awasthi, S. Regulation of 4-Hydroxynonenal-Mediated Signaling By Glutathione S-Transferases. *Methods Enzymol* 379-407; 2005.

135

[152]   Dickinson, D. A.; Iles, K. E.; Watanabe, N.; Iwamoto, T.; Zhang, H.; Krzywanski, D. M.; Forman, H. J. 4-hydroxynonenal induces glutamate cysteine ligase through JNK in HBE1 cells. *Free Radic Biol Med* **33:**974-987; 2002.

[153]   Barrera, G.; Pizzimenti, S.; Dianzani, M. U. 4-hydroxynonenal and regulation of cell cycle: effects on the pRb/E2F pathway. *Free Radic Biol Med* **37:**597-606; 2004.

[154]   Yang, Y.; Cheng, J.-Z.; Singhal, S. S.; Saini, M.; Pandya, U.; Awasthi, S.; Awasthi, Y. C. Role of Glutathione S-Transferases in Protection against Lipid Peroxidation. Overexpression of hGSTA2-2 in K562 cells protects against hydrogen peroxide-induced apoptosis and inhibits JNK and caspase 3 activation. *J Biol Chem* **276:**19220-19230; 2001.

[155]   Cheng, J.-Z.; Sharma, R.; Yang, Y.; Singhal, S. S.; Sharma, A.; Saini, M. K.; Singh, S. V.; Zimniak, P.; Awasthi, S.; Awasthi, Y. C. Accelerated Metabolism and Exclusion of 4-Hydroxynonenal through Induction of RLIP76 and hGST5.8 Is an Early Adaptive Response of Cells to Heat and Oxidative Stress. *J Biol Chem* **276:**41213-41223; 2001.

[156]   Li, J.; Sharma, R.; Patrick, B.; Sharma, A.; Jeyabal, P. V. S.; Reddy, P. M. R. V.; Saini, M. K.; Dwivedi, S.; Dhanani, S.; Ansari, N. H.; Zimniak, P.; Awasthi, S.; Awasthi, Y. C. Regulation of CD95 (Fas) Expression and Fas-Mediated Apoptotic Signaling in HLE B-3 Cells by 4-Hydroxynonenal. *Biochemistry* **45:**12253-12264; 2006.

[157]   Camandola, S.; Scavazza, A.; Leonarduzzi, G.; Biasi, F.; Chiarpotto, E.; Azzi, A.; Poli, G. Biogenic 4-hydroxy-2-nonenal activates transcription factor AP-1 but not NF-kappa B in cells of the macrophage lineage. *Biofactors* **6:**173-179; 1997.

[158]   Ramana, K. V.; Bhatnagar, A.; Srivastava, S.; Yadav, U. C.; Awasthi, S.; Awasthi, Y. C.; Srivastava, S. K. Mitogenic responses of vascular smooth muscle cells to lipid peroxidation-derived aldehyde 4-hydroxy-trans-2-nonenal (HNE): role of aldose reductase-catalyzed reduction of the HNE-glutathione conjugates in regulating cell growth. *J Biol Chem* **281:**17652-17660; 2006.

[159]   Camandola, S.; Poli, G.; Mattson, M. P. The lipid peroxidation product 4-hydroxy-2,3-nonenal increases AP-1-binding activity through caspase activation in neurons. *J Neurochem* **74:**159-168; 2000.

[160]   Parola, M.; Robino, G.; Marra, F.; Pinzani, M.; Bellomo, G.; Leonarduzzi, G.; Chiarugi, P.; Camandola, S.; Poli, G.; Waeg, G.; Gentilini, P.; Dianzani, M. U. HNE interacts directly with JNK isoforms in human hepatic stellate cells. *J Clin Invest* **102:**1942-1950; 1998.

[161] Paradisi, L.; Panagini, C.; Parola, M.; Barrera, G.; Dianzani, M. U. Effects of 4-hydroxynonenal on adenylate cyclase and 5'-nucleotidase activities in rat liver plasma membranes. *Chem Biol Interact* **53:**209-217; 1985.

[162] Leonarduzzi, G.; Scavazza, A.; Biasi, F.; Chiarpotto, E.; Camandola, S.; Vogel, S.; Dargel, R.; Poli, G. The lipid peroxidation end product 4-hydroxy-2,3-nonenal up-regulates transforming growth factor beta1 expression in the macrophage lineage: a link between oxidative injury and fibrosclerosis. *FASEB J* **11:**851-857; 1997.

[163] Cajone, F.; Bernelli-Zazzera, A. The action of 4-hydroxynonenal on heat shock gene expression in cultured hepatoma cells. *Free Radic Res Commun* **7:**189-194; 1989.

[164] Carbone, D. L.; Doorn, J. A.; Kiebler, Z.; Sampey, B. P.; Petersen, D. R. Inhibition of Hsp72-mediated protein refolding by 4-hydroxy-2-nonenal. *Chem Res Toxicol* **17:**1459-1467; 2004.

[165] Carbone, D. L.; Doorn, J. A.; Kiebler, Z.; Ickes, B. R.; Petersen, D. R. Modification of heat shock protein 90 by 4-hydroxynonenal in a rat model of chronic alcoholic liver disease. *J Pharmacol Exp Ther* **315:**8-15; 2005.

[166] Fazio, V. M.; Barrera, G.; Martinotti, S.; Farace, M. G.; Giglioni, B.; Frati, L.; Manzari, V.; Dianzani, M. U. 4-Hydroxynonenal, a product of cellular lipid peroxidation, which modulates c-myc and globin gene expression in K562 erythroleukemic cells. *Cancer Res* **52:**4866-4871; 1992.

[167] Barrera, G.; Pizzimenti, S.; Serra, A.; Ferretti, C.; Fazio, V. M.; Saglio, G.; Dianzani, M. U. 4-hydroxynonenal specifically inhibits c-myb but does not affect c-fos expressions in HL-60 cells. *Biochem Biophys Res Commun* **227:**589-593; 1996.

[168] Barrera, G.; Di Mauro, C.; Muraca, R.; Ferrero, D.; Cavalli, G.; Fazio, V. M.; Paradisi, L.; Dianzani, M. U. Induction of differentiation in human HL-60 cells by 4-hydroxynonenal, a product of lipid peroxidation. *Exp Cell Res* **197:**148-152; 1991.

[169] Kreuzer, T.; Grube, R.; Wutte, A.; Zarkovic, N.; Schaur, R. J. 4-Hydroxynonenal Modifies the Effects of Serum Growth Factors on the Expression of the c-fos Proto-Oncogene and the Proliferation of HeLa Carcinoma Cells. *Free Radic Biol Med* **25:**42-49; 1998.

[170] Ruef, J.; Rao, G. N.; Li, F.; Bode, C.; Patterson, C.; Bhatnagar, A.; Runge, M. S. Induction of rat aortic smooth muscle cell growth by the lipid peroxidation product 4-hydroxy-2-nonenal. *Circulation* **97:**1071-1078; 1998.

[171] Cheng, J.-Z.; Singhal, S. S.; Saini, M.; Singhal, J.; Piper, J. T.; Van Kuijk, F. J. G. M.; Zimniak, P.; Awasthi, Y. C.; Awasthi, S. Effects of mGST A4 Transfection on 4-Hydroxynonenal-Mediated Apoptosis and Differentiation of K562 Human Erythroleukemia Cells. *Arch Biochem Biophys* **372:**29-36; 1999.

[172] Kruman, I.; Bruce-Keller, A. J.; Bredesen, D.; Waeg, G.; Mattson, M. P. Evidence that 4-hydroxynonenal mediates oxidative stress-induced neuronal apoptosis. *J Neurosci* **17:**5089-5100; 1997.

[173] Sharma, R.; Brown, D.; Awasthi, S.; Yang, Y.; Sharma, A.; Patrick, B.; Saini, M. K.; Singh, S. P.; Zimniak, P.; Singh, S. V.; Awasthi, Y. C. Transfection with 4-hydroxynonenal-metabolizing glutathione S-transferase isozymes leads to phenotypic transformation and immortalization of adherent cells. *Eur J Biochem* **271:**1690-1701; 2004.

[174] Patrick, B.; Li, J.; Jeyabal, P. V.; Reddy, P. M.; Yang, Y.; Sharma, R.; Sinha, M.; Luxon, B.; Zimniak, P.; Awasthi, S.; Awasthi, Y. C. Depletion of 4-hydroxynonenal in hGSTA4-transfected HLE B-3 cells results in profound changes in gene expression. *Biochem Biophys Res Commun* **334:**425-432; 2005.

[175] Awasthi, Y. C.; Sharma, R.; Cheng, J. Z.; Yang, Y.; Sharma, A.; Singhal, S. S.; Awasthi, S. Role of 4-hydroxynonenal in stress-mediated apoptosis signaling. *Mol Aspects Med* **24:**219-230; 2003.

[176] Schaur, R. J. Basic aspects of the biochemical reactivity of 4-hydroxynonenal. *Mol Aspects Med* **24:**149-159; 2003.

[177] Siems, W.; Grune, T. Intracellular metabolism of 4-hydroxynonenal. *Mol Aspects Med* **24:**167-175; 2003.

[178] Alary, J.; Debrauwer, L.; Fernandez, Y.; Cravedi, J. P.; Rao, D.; Bories, G. 1,4-Dihydroxynonene mercapturic acid, the major end metabolite of exogenous 4-hydroxy-2-nonenal, is a physiological component of rat and human urine. *Chem Res Toxicol* **11:**130-135; 1998.

[179] de Zwart, L. L.; Hermanns, R. C.; Meerman, J. H.; Commandeur, J. N.; Vermeulen, N. P. Disposition in rat of [2-3H]-trans-4-hydroxy-2,3-nonenal, a product of lipid peroxidation. *Xenobiotica* **26:**1087-1100; 1996.

[180] Awasthi, S.; Sharma, R.; Yang, Y.; Singhal, S. S.; Pikula, S.; Bandorowicz-Pikula, J.; Singh, S. V.; Zimniak, P.; Awasthi, Y. C. Transport functions and

physiological significance of 76 kDa Ral-binding GTPase activating protein (RLIP76). *Acta Biochim Pol* **49:**855-867; 2002.

[181]   Sharma, R.; Singhal, S. S.; Cheng, J.; Yang, Y.; Sharma, A.; Zimniak, P.; Awasthi, S.; Awasthi, Y. C. RLIP76 Is the Major ATP-Dependent Transporter of Glutathione-Conjugates and Doxorubicin in Human Erythrocytes. *Arch Biochem Biophys* **391:**171-179; 2001.

[182]   Hayes, J. D.; Flanagan, J. U.; Jowsey, I. R. Glutathione transferases. *Annu Rev Pharmacol Toxicol* **45:**51-88; 2005.

[183]   Sharma, R.; Ansari, G. A.; Awasthi, Y. C. Physiological Substrates of Glutathione S-Transferases. In: Awasthi, Y. C., ed. *Toxicology of Glutathione Transferases*. Boca Raton, FL: Taylor & Francis; 2007: 179-204.

[184]   Hayes, J. D.; Pulford, D. J. The glutathione S-transferase supergene family: regulation of GST and the contribution of the isoenzymes to cancer chemoprotection and drug resistance. *Crit Rev Biochem Mol Biol* **30:**445-600; 1995.

[185]   Mannervik, B.; Alin, P.; Guthenberg, C.; Jensson, H.; Tahir, M. K.; Warholm, M.; Jornvall, H. Identification of three classes of cytosolic glutathione transferase common to several mammalian species: correlation between structural data and enzymatic properties. *Proc Natl Acad Sci U S A* **82:**7202-7206; 1985.

[186]   Sundberg, A. G.; Nilsson, R.; Appelkvist, E. L.; Dallner, G. Immunohistochemical localization of alpha and pi class glutathione transferases in normal human tissues. *Pharmacol Toxicol* **72:**321-331; 1993.

[187]   Robin, M. A.; Prabu, S. K.; Raza, H.; Anandatheerthavarada, H. K.; Avadhani, N. G. Phosphorylation enhances mitochondrial targeting of GSTA4-4 through increased affinity for binding to cytoplasmic Hsp70. *J Biol Chem* **278:**18960-18970; 2003.

[188]   Harris, J. M.; Meyer, D. J.; Coles, B.; Ketterer, B. A novel glutathione transferase (13-13) isolated from the matrix of rat liver mitochondria having structural similarity to class theta enzymes. *Biochem J* **278 (Pt 1):**137-141; 1991.

[189]   Raza, H.; Robin, M. A.; Fang, J. K.; Avadhani, N. G. Multiple isoforms of mitochondrial glutathione S-transferases and their differential induction under oxidative stress. *Biochem J* **366:**45-55; 2002.

[190]   Bhagwat, S. V.; Mullick, J.; Avadhani, N. G.; Raza, H. Differential response of cytosolic, microsomal, and mitochondrial glutathione S-transferases to xenobiotic inducers. *Int J Oncol* **13:**281-288; 1998.

[191]   Prabhu, K. S.; Reddy, P. V.; Gumpricht, E.; Hildenbrandt, G. R.; Scholz, R. W.; Sordillo, L. M.; Reddy, C. C. Microsomal glutathione S-transferase A1-1 with glutathione peroxidase activity from sheep liver: molecular cloning, expression and characterization. *Biochem J* **360:**345-354; 2001.

[192]   Singh, S. P.; Janecki, A. J.; Srivastava, S. K.; Awasthi, S.; Awasthi, Y. C.; Xia, S. J.; Zimniak, P. Membrane association of glutathione S-transferase mGSTA4-4, an enzyme that metabolizes lipid peroxidation products. *J Biol Chem* **277:**4232-4239; 2002.

[193]   Jakobsson, P. J.; Morgenstern, R.; Mancini, J.; Ford-Hutchinson, A.; Persson, B. Common structural features of MAPEG -- a widespread superfamily of membrane associated proteins with highly divergent functions in eicosanoid and glutathione metabolism. *Protein Sci* **8:**689-692; 1999.

[194]   Morel, F.; Rauch, C.; Petit, E.; Piton, A.; Theret, N.; Coles, B.; Guillouzo, A. Gene and Protein Characterization of the Human Glutathione S-Transferase Kappa and Evidence for a Peroxisomal Localization. *J Biol Chem* **279:**16246-16253; 2004.

[195]   Ladner, J. E.; Parsons, J. F.; Rife, C. L.; Gilliland, G. L.; Armstrong, R. N. Parallel Evolutionary Pathways for Glutathione Transferases: Structure and Mechanism of the Mitochondrial Class Kappa Enzyme rGSTK1-1. *Biochemistry* **43:**352-361; 2004.

[196]   Robinson, A.; Huttley, G. A.; Booth, H. S.; Board, P. G. Modelling and bioinformatics studies of the human Kappa-class glutathione transferase predict a novel third glutathione transferase family with similarity to prokaryotic 2-hydroxychromene-2-carboxylate isomerases. *Biochem J* **379:**541-552; 2004.

[197]   Nebert, D. W.; Vasiliou, V. Analysis of the glutathione S-transferase (GST) gene family. *Hum Genomics* **1:**460-464; 2004.

[198]   Mannervik, B.; Awasthi, Y. C.; Board, P. G.; Hayes, J. D.; Di Ilio, C.; Ketterer, B.; Listowsky, I.; Morgenstern, R.; Muramatsu, M.; Pearson, W. R.; et al. Nomenclature for human glutathione transferases. *Biochem J* **282 (Pt 1):**305-306; 1992.

[199]   Mannervik, B.; Board, P. G.; Hayes, J. D.; Listowsky, I.; Pearson, W. R. Nomenclature for mammalian soluble glutathione transferases. *Methods Enzymol* **401:**1-8; 2005.

[200]   Hayes, J. D.; Chanas, S. A.; Henderson, C. J.; McMahon, M.; Sun, C.; Moffat, G. J.; Wolf, C. R.; Yamamoto, M. The Nrf2 transcription factor contributes both to the basal expression of glutathione S-transferases in mouse liver and to their induction by the chemopreventive synthetic antioxidants, butylated hydroxyanisole and ethoxyquin. *Biochem Soc Trans* **28:**33-41; 2000.

[201]   Prestera, T.; Holtzclaw, W. D.; Zhang, Y.; Talalay, P. Chemical and molecular regulation of enzymes that detoxify carcinogens. *Proc Natl Acad Sci U S A* **90:**2965-2969; 1993.

[202]   Wasserman, W. W.; Fahl, W. E. Functional antioxidant responsive elements. *Proc Natl Acad Sci U S A* **94:**5361-5366; 1997.

[203]   Awasthi, Y. C.; Sharma, R.; Singhal, S. S. Human glutathione S-transferases. *Int J Biochem* **26:**295-308; 1994.

[204]   Hayes, J. D.; Strange, R. C. Potential contribution of the glutathione S-transferase supergene family to resistance to oxidative stress. *Free Radic Res* **22:**193-207; 1995.

[205]   Rushmore, T. H.; Morton, M. R.; Pickett, C. B. The antioxidant responsive element. Activation by oxidative stress and identification of the DNA consensus sequence required for functional activity. *J Biol Chem* **266:**11632-11639; 1991.

[206]   Ishii, T.; Itoh, K.; Yamamoto, M. Roles of Nrf2 in activation of antioxidant enzyme genes via antioxidant responsive elements. *Methods Enzymol* **348:**182-190; 2002.

[207]   Sharma, R.; Yang, Y.; Sharma, A.; Dwivedi, S.; Popov, V. L.; Boor, P. J.; Singhal, S. S.; Awasthi, S.; Awasthi, Y. C. Mechanisms and Physiological Significance of the Transport of the Glutathione Conjugate of 4-Hydroxynonenal in Human Lens Epithelial Cells. *Invest Ophthalmol Vis Sci* **44:**3438-3449; 2003.

[208]   Nikawa, T.; Schuch, G.; Wagner, G.; Sies, H. Interaction of ebselen with glutathione S-transferase and papain in vitro. *Biochem Pharmacol* **47:**1007-1012; 1994.

[209]   Kostyuk, V. A.; Potapovich, A. I. Antiradical and chelating effects in flavonoid protection against silica-induced cell injury. *Arch Biochem Biophys* **355:**43-48; 1998.

[210]   Aveldano, M. I. Phospholipid solubilization during detergent extraction of rhodopsin from photoreceptor disk membranes. *Arch Biochem Biophys* **324:**331-343; 1995.

[211]   Baumann E, P. C. Uber bromphenyl-mercaptursaure. *Ber Dtsch Chem Ges* **12:**806-810; 1879.

[212]   Jaffe, M. Uber die nach einfuhring von brombenzol und chlorbenzol im organismus entstehenden schwefelhaltigen sauren. *Ber Dtsch Chem Ges* **12:**1092-1098; 1879.

[213]   Barnes, M. M.; James, S. P.; Wood, P. B. The formation of mercapturic acids. 1. Formation of mercapturic acid and the levels of glutathione in tissues. *Biochem J* **71:**680-690; 1959.

[214]   Combes, B.; Stakelum, G. S. A liver enzyme that conjugates sulfobromophthalein sodium with glutathione. *J Clin Invest* **40:**981-988; 1961.

[215]   Booth, J.; Boyland, E.; Sims, P. An enzyme from rat liver catalysing conjugations with glutathione. *Biochem J* **79:**516-524; 1961.

[216]   Boyland, E.; Williams, K. An Enzyme Catalysing the Conjugation of Epoxides with Glutathione. *Biochem J* **94:**190-197; 1965.

[217]   Commandeur, J. N.; Stijntjes, G. J.; Vermeulen, N. P. Enzymes and transport systems involved in the formation and disposition of glutathione S-conjugates. Role in bioactivation and detoxication mechanisms of xenobiotics. *Pharmacol Rev* **47:**271-330; 1995.

[218]   Alary, J.; Bravais, F.; Cravedi, J. P.; Debrauwer, L.; Rao, D.; Bories, G. Mercapturic acid conjugates as urinary end metabolites of the lipid peroxidation product 4-hydroxy-2-nonenal in the rat. *Chem Res Toxicol* **8:**34-39; 1995.

[219]   Litwack, G.; Ketterer, B.; Arias, I. M. Ligandin: a hepatic protein which binds steroids, bilirubin, carcinogens and a number of exogenous organic anions. *Nature* **234:**466-467; 1971.

[220]   Habig, W. H.; Pabst, M. J.; Fleischner, G.; Gatmaitan, Z.; Arias, I. M.; Jakoby, W. B. The identity of glutathione S-transferase B with ligandin, a major binding protein of liver. *Proc Natl Acad Sci U S A* **71:**3879-3882; 1974.

[221]   Ketley, J. N.; Habig, W. H.; Jakoby, W. B. Binding of nonsubstrate ligands to the glutathione S-transferases. *J Biol Chem* **250:**8670-8673; 1975.

[222]   Mahajan, S.; Atkins, W. M. The chemistry and biology of inhibitors and pro-drugs targeted to glutathione S-transferases. *Cell Mol Life Sci* **62:**1221-1233; 2005.

142

[223]   Reyes, H.; Levi, A. J.; Gatmaitan, Z.; Arias, I. M. Organic anion-binding protein in rat liver: drug induction and its physiologic consequence. *Proc Natl Acad Sci U S A* **64:**168-170; 1969.

[224]   Hu, X.; Srivastava, S. K.; Xia, H.; Awasthi, Y. C.; Singh, S. V. An Alpha Class Mouse Glutathione S-Transferase with Exceptional Catalytic Efficiency in the Conjugation of Glutathione with 7beta ,8alpha -Dihydroxy-9alpha ,10alpha -oxy-7,8,9,10-tetrahydrobenzo(a)pyrene. *J Biol Chem* **271:**32684-32688; 1996.

[225]   Weng, M.-W.; Hsiao, Y.-M.; Chiou, H.-L.; Yang, S.-F.; Hsieh, Y.-S.; Cheng, Y.-W.; Yang, C.-H.; Ko, J.-L. Alleviation of benzo[a]pyrene-diolepoxide-DNA damage in human lung carcinoma by glutathione S-transferase M2. *DNA Repair* **4:**493-502; 2005.

[226]   Kushman, M. E.; Kabler, S. L.; Fleming, M. H.; Ravoori, S.; Gupta, R. C.; Doehmer, J.; Morrow, C. S.; Townsend, A. J. Expression of human glutathione S-transferase P1 confers resistance to benzo[a]pyrene or benzo[a]pyrene-7,8-dihydrodiol mutagenesis, macromolecular alkylation, and formation of stable N2-Gua-BPDE adducts in stably transfected V79MZ cells co-expressing hCYP1A1. *Carcinogenesis* **28:**207-214; 2006.

[227]   Sharma, A.; Patrick, B.; Li, J.; Sharma, R.; Jeyabal, P. V. S.; Reddy, P. M. R. V.; Awasthi, S.; Awasthi, Y. C. Glutathione S-transferases as antioxidant enzymes: Small cell lung cancer (H69) cells transfected with hGSTA1 resist doxorubicin-induced apoptosis. *Arch Biochem Biophys* **452:**165-173; 2006.

[228]   Depeille, P.; Cuq, P.; Mary, S.; Passagne, I.; Evrard, A.; Cupissol, D.; Vian, L. Glutathione S-Transferase M1 and Multidrug Resistance Protein 1 Act in Synergy to Protect Melanoma Cells from Vincristine Effects. *Mol Pharmacol* **65:**897-905; 2004.

[229]   Zhang, J.; Tian, Q.; Yung Chan, S.; Chuen Li, S.; Zhou, S.; Duan, W.; Zhu, Y. Z. Metabolism and transport of oxazaphosphorines and the clinical implications. *Drug Metab Rev* **37:**611-703; 2005.

[230]   Stuckler, D.; Singhal, J.; Singhal, S. S.; Yadav, S.; Awasthi, Y. C.; Awasthi, S. RLIP76 transports vinorelbine and mediates drug resistance in non-small cell lung cancer. *Cancer Res* **65:**991-998; 2005.

[231]   Singhal, S. S.; Yadav, S.; Singhal, J.; Zajac, E.; Awasthi, Y. C.; Awasthi, S. Depletion of RLIP76 sensitizes lung cancer cells to doxorubicin. *Biochem Pharmacol* **70:**481-488; 2005.

143

[232] Harbottle, A.; Daly, A. K.; Atherton, K.; Campbell, F. C. Role of glutathione S-transferase P1, P-glycoprotein and multidrug resistance-associated protein 1 in acquired doxorubicin resistance. *Int J Cancer* **92:**777-783; 2001.

[233] Saygili, E. I.; Akcay, T.; Konukoglu, D.; Papilla, C. Glutathione and Glutathione-Related Enzymes in Colorectal Cancer Patients. *J Toxicol Environ Health A* **66:**411-415; 2003.

[234] Morimura, S.; Suzuki, T.; Hochi, S.; Yuki, A.; Nomura, K.; Kitagawa, T.; Nagatsu, I.; Imagawa, M.; Muramatsu, M. Trans-Activation of Glutathione Transferase P Gene During Chemical Hepatocarcinogenesis of the Rat. *Proc Natl Acad Sci U S A* **90:**2065-2068; 1993.

[235] Prabhu, K. S.; Reddy, P. V.; Jones, E. C.; Liken, A. D.; Reddy, C. C. Characterization of a class alpha glutathione-S-transferase with glutathione peroxidase activity in human liver microsomes. *Arch Biochem Biophys* **424:**72-80; 2004.

[236] Hiratsuka, A.; Yamane, H.; Yamazaki, S.; Ozawa, N.; Watabe, T. Subunit Ya-specific Glutathione Peroxidase Activity toward Cholesterol 7-Hydroperoxides of Glutathione S-Transferases in Cytosols from Rat Liver and Skin. *J Biol Chem* **272:**4763-4769; 1997.

[237] Hubatsch, I.; Ridderstrom, M.; Mannervik, B. Human glutathione transferase A4-4: an alpha class enzyme with high catalytic efficiency in the conjugation of 4-hydroxynonenal and other genotoxic products of lipid peroxidation. *Biochem J* **330 (Pt 1):**175-179; 1998.

[238] Alin, P.; Danielson, U. H.; Mannervik, B. 4-Hydroxyalk-2-enals are substrates for glutathione transferase. *FEBS Lett* **179:**267-270; 1985.

[239] Singhal, S. S.; Zimniak, P.; Awasthi, S.; Piper, J. T.; He, N. G.; Teng, J. I.; Petersen, D. R.; Awasthi, Y. C. Several closely related glutathione S-transferase isozymes catalyzing conjugation of 4-hydroxynonenal are differentially expressed in human tissues. *Arch Biochem Biophys* **311:**242-250; 1994.

[240] Hartley, D. P.; Ruth, J. A.; Petersen, D. R. The hepatocellular metabolism of 4-hydroxynonenal by alcohol dehydrogenase, aldehyde dehydrogenase, and glutathione S-transferase. *Arch Biochem Biophys* **316:**197-205; 1995.

[241] Siems, W. G.; Zollner, H.; Grune, T.; Esterbauer, H. Metabolic fate of 4-hydroxynonenal in hepatocytes: 1,4-dihydroxynonene is not the main product. *J Lipid Res* **38:**612-622; 1997.

[242] Tjalkens, R. B.; Luckey, S. W.; Kroll, D. J.; Petersen, D. R. Alpha,beta-unsaturated aldehydes increase glutathione S-transferase mRNA and protein: correlation with activation of the antioxidant response element. *Arch Biochem Biophys* **359:**42-50; 1998.

[243] Hubatsch, I.; Mannervik, B. A Highly Acidic Tyrosine 9 and a Normally Titrating Tyrosine 212 Contribute to the Catalytic Mechanism of Human Glutathione Transferase A4-4. *Biochem Biophys Res Commun* **280:**878-882; 2001.

[244] Mannervik, B.; Danielson, U. H. Glutathione transferases--structure and catalytic activity. *CRC Crit Rev Biochem* **23:**283-337; 1988.

[245] Jakobsson, P. J.; Mancini, J. A.; Riendeau, D.; Ford-Hutchinson, A. W. Identification and characterization of a novel microsomal enzyme with glutathione-dependent transferase and peroxidase activities. *J Biol Chem* **272:**22934-22939; 1997.

[246] Lawrence, R. A.; Burk, R. F. Glutathione peroxidase activity in selenium-deficient rat liver. *Biochem Biophys Res Commun* **71:**952-958; 1976.

[247] Yang, Y.; Sharma, R.; Zimniak, P.; Awasthi, Y. C. Role of alpha class glutathione S-transferases as antioxidant enzymes in rodent tissues. *Toxicol Appl Pharmacol* **182:**105-115; 2002.

[248] Yang, Y.; Sharma, R.; Cheng, J.-Z.; Saini, M. K.; Ansari, N. H.; Andley, U. P.; Awasthi, S.; Awasthi, Y. C. Protection of HLE B-3 Cells against Hydrogen Peroxide- and Naphthalene-Induced Lipid Peroxidation and Apoptosis by Transfection with hGSTA1 and hGSTA2. *Invest Ophthalmol Vis Sci* **43:**434-445; 2002.

[249] Singhal, S. S.; Saxena, M.; Ahmad, H.; Awasthi, S.; Haque, A. K.; Awasthi, Y. C. Glutathione S-transferases of human lung: characterization and evaluation of the protective role of the alpha-class isozymes against lipid peroxidation. *Arch Biochem Biophys* **299:**232-241; 1992.

[250] Bhuyan, K. C.; Bhuyan, D. K. Molecular mechanism of cataractogenesis: III. Toxic metabolites of oxygen as initiators of lipid peroxidation and cataract. *Curr Eye Res* **3:**67-81; 1984.

[251] Coles, B.; Nowell, S. A.; MacLeod, S. L.; Sweeney, C.; Lang, N. P.; Kadlubar, F. F. The role of human glutathione S-transferases (hGSTs) in the detoxification of the food-derived carcinogen metabolite N-acetoxy-PhIP, and the effect of a polymorphism in hGSTA1 on colorectal cancer risk. *Mutat Res* **482:**3-10; 2001.

[252]   Satoh, K.; Kitahara, A.; Soma, Y.; Inaba, Y.; Hatayama, I.; Sato, K. Purification, induction, and distribution of placental glutathione transferase: a new marker enzyme for preneoplastic cells in the rat chemical hepatocarcinogenesis. *Proc Natl Acad Sci U S A* **82:**3964-3968; 1985.

[253]   Sugioka, Y.; Fujii-Kuriyama, Y.; Kitagawa, T.; Muramatsu, M. Changes in polypeptide pattern of rat liver cells during chemical hepatocarcinogenesis. *Cancer Res* **45:**365-378; 1985.

[254]   Satoh, K.; Hatayama, I.; Tateoka, N.; Tamai, K.; Shimizu, T.; Tatematsu, M.; Ito, N.; Sato, K. Transient induction of single GST-P positive hepatocytes by DEN. *Carcinogenesis* **10:**2107-2111; 1989.

[255]   Adler, V.; Yin, Z.; Fuchs, S. Y.; Benezra, M.; Rosario, L.; Tew, K. D.; Pincus, M. R.; Sardana, M.; Henderson, C. J.; Wolf, C. R.; Davis, R. J.; Ronai, Z. Regulation of JNK signaling by GSTp. *EMBO J* **18:**1321-1334; 1999.

[256]   Ruscoe, J. E.; Rosario, L. A.; Wang, T.; Gate, L.; Arifoglu, P.; Wolf, C. R.; Henderson, C. J.; Ronai, Z.; Tew, K. D. Pharmacologic or genetic manipulation of glutathione S-transferase P1-1 (GSTpi) influences cell proliferation pathways. *J Pharmacol Exp Ther* **298:**339-345; 2001.

[257]   Serrano, M.; Hannon, G. J.; Beach, D. A new regulatory motif in cell-cycle control causing specific inhibition of cyclin D/CDK4. *Nature* **366:**704-707; 1993.

[258]   Giono, L. E.; Manfredi, J. J. The p53 tumor suppressor participates in multiple cell cycle checkpoints. *J Cell Physiol* **209:**13-20; 2006.

[259]   Harris, S. L.; Levine, A. J. The p53 pathway: positive and negative feedback loops. *Oncogene* **24:**2899-2908; 2005.

[260]   Schafer, K. A. The cell cycle: a review. *Vet Pathol* **35:**461-478; 1998.

[261]   Lockshin, R. A.; Williams, C. M. Programmed Cell Death--I. Cytology of Degeneration in the Intersegmental Muscles of the Pernyi Silkmoth. *J Insect Physiol* **11:**123-133; 1965.

[262]   Berthold Huppertz, A. H. Regulation of proliferation and apoptosis during development of the preimplantation embryo and the placenta. *Birth Defects Research C: Embryo Today: Reviews* **75:**249-261; 2005.

[263]   Lolley, R. N. The rd gene defect triggers programmed rod cell death. The Proctor Lecture. *Invest Ophthalmol Vis Sci* **35:**4182-4191; 1994.

[264]   Wilson, S. E. Stimulus-specific and cell type-specific cascades: Emerging principles relating to control of apoptosis in the eye. *Exp Eye Res* **69:**255-266; 1999.

[265]   Yan, Q.; Liu, J. P.; Li, D. W. Apoptosis in lens development and pathology. *Differentiation* **74:**195-211; 2006.

[266]   Hengartner, M. O. The biochemistry of apoptosis. *Nature* **407:**770-776; 2000.

[267]   Riedl, S. J.; Shi, Y. Molecular mechanisms of caspase regulation during apoptosis. *Nat Rev Mol Cell Biol* **5:**897-907; 2004.

[268]   Nakashima, I.; Liu, W.; Akhand, A. A.; Takeda, K.; Kawamoto, Y.; Kato, M.; Suzuki, H. 4-Hydroxynonenal triggers multistep signal transduction cascades for suppression of cellular functions. *Mol Aspects Med* **24:**231-238; 2003.

[269]   Jiang, J.; Kini, V.; Belikova, N.; Serinkan, B. F.; Borisenko, G. G.; Tyurina, Y. Y.; Tyurin, V. A.; Kagan, V. E. Cytochrome c release is required for phosphatidylserine peroxidation during Fas-triggered apoptosis in lung epithelial A549 cells. *Lipids* **39:**1133-1142; 2004.

[270]   Hofmanova, J.; Vaculova, A.; Kozubik, A. Polyunsaturated fatty acids sensitize human colon adenocarcinoma HT-29 cells to death receptor-mediated apoptosis. *Cancer Lett* **218:**33-41; 2005.

[271]   Bellows, C. F.; Brain, J. D. Role of fibronectin in pancreatitis-associated lung injury. *Dig Dis Sci* **48:**1445-1452; 2003.

[272]   Hynes, R. O. Integrins: versatility, modulation, and signaling in cell adhesion. *Cell* **69:**11-25; 1992.

[273]   Martin, G. R.; Timpl, R. Laminin and other basement membrane components. *Annu Rev Cell Biol* **3:**57-85; 1987.

[274]   Carystinos, G. D.; Bier, A.; Batist, G. The role of connexin-mediated cell-cell communication in breast cancer metastasis. *J Mammary Gland Biol Neoplasia* **6:**431-440; 2001.

[275] Liotta, L. A.; Tryggvason, K.; Garbisa, S.; Hart, I.; Foltz, C. M.; Shafie, S. Metastatic potential correlates with enzymatic degradation of basement membrane collagen. *Nature* **284:**67-68; 1980.

[276] Debelle, L.; Tamburro, A. M. Elastin: molecular description and function. *Int J Biochem Cell Biol* **31:**261-272; 1999.

[277] Giancotti, F. G. Integrin signaling: specificity and control of cell survival and cell cycle progression. *Curr Opin Cell Biol* **9:**691-700; 1997.

[278] Burridge, K.; Chrzanowska-Wodnicka, M. Focal adhesions, contractility, and signaling. *Ann Rev Cell Devel Biol* **12:**463-519; 1996.

[279] Schwartz, M. A.; Schaller, M. D.; Ginsberg, M. H. Integrins: Emerging paradigms of signal transduction. *Ann Rev Cell Devel Biol* **11:**549-599; 1995.

[280] Albelda, S. M. Role of integrins and other cell adhesion molecules in tumor progression and metastasis. *Lab Invest* **68:**4-17; 1993.

[281] Zetter, B. R. Adhesion molecules in tumor metastasis. *Semin Cancer Biol* **4:**219-229; 1993.

[282] Meredith, J. E., Jr.; Fazeli, B.; Schwartz, M. A. The extracellular matrix as a cell survival factor. *Mol Biol Cell* **4:**953-961; 1993.

[283] Frisch, S. M.; Francis, H. Disruption of epithelial cell-matrix interactions induces apoptosis. *J Cell Biol* **124:**619-626; 1994.

[284] Boudreau, N.; Sympson, C. J.; Werb, Z.; Bissell, M. J. Suppression of ICE and apoptosis in mammary epithelial cells by extracellular matrix. *Science* **267:**891-893; 1995.

[285] Almeida, E. A. C.; Schlaepfer, D. D.; Dazin, P.; Aizawa, S.; Damsky, C. H. Extracellular Matrix Survival Signals Transduced by Focal Adhesion Kinase Suppress p53-mediated Apoptosis. *J Cell Biol* **143:**547-560; 1998.

[286] Sethi, T.; Rintoul, R. C.; Moore, S. M.; MacKinnon, A. C.; Salter, D.; Choo, C.; Chilvers, E. R.; Dransfield, I.; Donnelly, S. C.; Strieter, R.; Haslett, C. Extracellular matrix proteins protect small cell lung cancer cells against apoptosis: A mechanism for small cell lung cancer growth and drug resistance in vivo. *Nat Med* **5:**662-668; 1999.

[287]   Birnboim, H. C.; Doly, J. A rapid alkaline extraction procedure for screening recombinant plasmid DNA. *Nucleic Acids Res* **7:**1513-1523; 1979.

[288]   Bradford, M. M. A rapid and sensitive method for the quantitation of microgram quantities of protein utilizing the principle of protein-dye binding. *Anal Biochem* **72:**248-254; 1976.

[289]   Laemmli, U. K. Cleavage of structural proteins during the assembly of the head of bacteriophage T4. *Nature* **227:**680-685; 1970.

[290]   Singhal, S. S.; Godley, B. F.; Chandra, A.; Pandya, U.; Jin, G. F.; Saini, M. K.; Awasthi, S.; Awasthi, Y. C. Induction of glutathione S-transferase hGST 5.8 is an early response to oxidative stress in RPE cells. *Invest Ophthalmol Vis Sci* **40:**2652-2659; 1999.

[291]   Kozak, M. Point mutations define a sequence flanking the AUG initiator codon that modulates translation by eukaryotic ribosomes. *Cell* **44:**283-292; 1986.

[292]   Habig, W. H.; Pabst, M. J.; Jakoby, W. B. Glutathione S-transferases. The first enzymatic step in mercapturic acid formation. *J Biol Chem* **249:**7130-7139; 1974.

[293]   Beers, R. F., Jr.; Sizer, I. W. A spectrophotometric method for measuring the breakdown of hydrogen peroxide by catalase. *J Biol Chem* **195:**133-140; 1952.

[294]   Paoletti, F.; Mocali, A. Determination of superoxide dismutase activity by purely chemical system based on NAD(P)H oxidation. *Methods Enzymol* **186:**209-220; 1990.

[295]   Paglia, D. E.; Valentine, W. N. Studies on the quantitative and qualitative characterization of erythrocyte glutathione peroxidase. *J Lab Clin Med* **70:**158-169; 1967.

[296]   Awasthi, Y. C.; Beutler, E.; Srivastava, S. K. Purification and properties of human erythrocyte glutathione peroxidase. *J Biol Chem* **250:**5144-5149; 1975.

[297]   Beutler, E. *Red Cell Metabolism: A Manual of Biochemical Methods.* Orlando, FL: Grune and Stratton; 1984.

[298]   Andley, U. P.; Rhim, J. S.; Chylack, L. T., Jr.; Fleming, T. P. Propagation and immortalization of human lens epithelial cells in culture. *Invest Ophthalmol Vis Sci* **35:**3094-3102; 1994.

[299]   Andley, U. P.; Song, Z.; Mitchell, D. L. DNA repair and survival in human lens epithelial cells with extended lifespan. *Curr Eye Res* **18:**224-230; 1999.

[300]   Andley, U. P.; Patel, H. C.; Xi, J. H. The R116C mutation in alpha A-crystallin diminishes its protective ability against stress-induced lens epithelial cell apoptosis. *J Biol Chem* **277:**10178-10186; 2002.

[301]   Hosler, M. R.; Wang-Su, S. T.; Wagner, B. J. Targeted disruption of specific steps of the ubiquitin-proteasome pathway by oxidation in lens epithelial cells. *Int J Biochem Cell Biol* **35:**685-697; 2003.

[302]   Lee, D. H.; Cho, K. S.; Park, S. G.; Kim, E. K.; Joo, C. K. Cellular death mediated by nuclear factor kappa B (NF-kappaB) translocation in cultured human lens epithelial cells after ultraviolet-B irradiation. *J Cataract Refract Surg* **31:**614-619; 2005.

[303]   Huang, L.; Estrada, R.; Yappert, M. C.; Borchman, D. Oxidation-induced changes in human lens epithelial cells. 1. Phospholipids. *Free Radic Biol Med* **41:**1425-1432; 2006.

[304]   Sharma, R.; Yang, Y.; Sharma, A.; Dwivedi, S.; Popov, V. L.; Boor, P. J.; Singhal, S. S.; Awasthi, S.; Awasthi, Y. C. Mechanisms and Physiological Significance of the Transport of the Glutathione Conjugate of 4-Hydroxynonenal in Human Lens Epithelial Cells. *Invest Ophthalmol Vis Sci* **44:**3438-3449; 2003.

[305]   Liang, F. Q.; Godley, B. F. Oxidative stress-induced mitochondrial DNA damage in human retinal pigment epithelial cells: a possible mechanism for RPE aging and age-related macular degeneration. *Exp Eye Res* **76:**397-403; 2003.

[306]   Hurst, J. S.; Saini, M. K.; Jin, G. F.; Awasthi, Y. C.; van Kuijk, F. J. Toxicity of oxidized beta-carotene to cultured human cells. *Exp Eye Res* **81:**239-243; 2005.

[307]   Kannan, R.; Zhang, N.; Sreekumar, P. G.; Spee, C. K.; Rodriguez, A.; Barron, E.; Hinton, D. R. Stimulation of apical and basolateral VEGF-A and VEGF-C secretion by oxidative stress in polarized retinal pigment epithelial cells. *Mol Vis* **12:**1649-1659; 2006.

[308]   Qin, S.; McLaughlin, A. P.; De Vries, G. W. Protection of RPE cells from oxidative injury by 15-deoxy-delta12,14-prostaglandin J2 by augmenting GSH and activating MAPK. *Invest Ophthalmol Vis Sci* **47:**5098-5105; 2006.

[309]   Kaarniranta, K.; Ryhanen, T.; Karjalainen, H. M.; Lammi, M. J.; Suuronen, T.; Huhtala, A.; Kontkanen, M.; Terasvirta, M.; Uusitalo, H.; Salminen, A. Geldanamycin increases 4-hydroxynonenal (HNE)-induced cell death in human retinal pigment epithelial cells. *Neurosci Lett* **382:**185-190; 2005.

[310]   Choudhary, S.; Xiao, T.; Srivastava, S.; Zhang, W.; Chan, L. L.; Vergara, L. A.; Van Kuijk, F. J.; Ansari, N. H. Toxicity and detoxification of lipid-derived aldehydes in cultured retinal pigmented epithelial cells. *Toxicol Appl Pharmacol* **204:**122-134; 2005.

[311]   Gao, X.; Talalay, P. Induction of phase 2 genes by sulforaphane protects retinal pigment epithelial cells against photooxidative damage. *Proc Natl Acad Sci U S A* **101:**10446-10451; 2004.

[312]   Bruns, C. M.; Hubatsch, I.; Ridderstrom, M.; Mannervik, B.; Tainer, J. A. Human glutathione transferase A4-4 crystal structures and mutagenesis reveal the basis of high catalytic efficiency with toxic lipid peroxidation products. *J Mol Biol* **288:**427-439; 1999.

[313]   Allen, R. G.; Balin, A. K. Effects of oxygen on the antioxidant responses of normal and transformed cells. *Exp Cell Res* **289:**307-316; 2003.

[314]   Oh, S. H.; Lee, B. H.; Lim, S. C. Cadmium induces apoptotic cell death in WI 38 cells via caspase-dependent Bid cleavage and calpain-mediated mitochondrial Bax cleavage by Bcl-2-independent pathway. *Biochem Pharmacol* **68:**1845-1855; 2004.

[315]   Bartling, B.; Rehbein, G.; Silber, R. E.; Simm, A. Senescent fibroblasts induce moderate stress in lung epithelial cells in vitro. *Exp Gerontol* **41:**532-539; 2006.

[316]   Kang, K. A.; Lee, K. H.; Zhang, R.; Piao, M.; Chae, S.; Kim, K. N.; Jeon, Y. J.; Park, D. B.; You, H. J.; Kim, J. S.; Hyun, J. W. Caffeic acid protects hydrogen peroxide induced cell damage in WI-38 human lung fibroblast cells. *Biol Pharm Bull* **29:**1820-1824; 2006.

[317]   Zimniak, P.; Singhal, S. S.; Srivastava, S. K.; Awasthi, S.; Sharma, R.; Hayden, J. B.; Awasthi, Y. C. Estimation of genomic complexity, heterologous expression, and enzymatic characterization of mouse glutathione S-transferase mGSTA4-4 (GST 5.7). *J Biol Chem* **269:**992-1000; 1994.

[318]   Sawicki, R.; Singh, S. P.; Mondal, A. K.; Benes, H.; Zimniak, P. Cloning, expression and biochemical characterization of one Epsilon-class (GST-3) and ten Delta-class (GST-1) glutathione S-transferases from Drosophila melanogaster, and identification of additional nine members of the Epsilon class. *Biochem J* **370:**661-669; 2003.

[319]   Wang, Z. B.; Liu, Y. Q.; Cui, Y. F. Pathways to caspase activation. *Cell Biol Int* **29:**489-496; 2005.

151

[320] Xerri, L.; Palmerini, F.; Devilard, E.; Defrance, T.; Bouabdallah, R.; Hassoun, J.; Birg, F. Frequent nuclear localization of ICAD and cytoplasmic co-expression of caspase-8 and caspase-3 in human lymphomas. *J Pathol* **192:**194-202; 2000.

[321] Rodriguez-Nieto, S.; Zhivotovsky, B. Role of alterations in the apoptotic machinery in sensitivity of cancer cells to treatment. *Curr Pharm Des* **12:**4411-4425; 2006.

[322] Muris, J. J.; Meijer, C. J.; Ossenkoppele, G. J.; Vos, W.; Oudejans, J. J. Apoptosis resistance and response to chemotherapy in primary nodal diffuse large B-cell lymphoma. *Hematol Oncol* **24:**97-104; 2006.

[323] Maruyama, R.; Yamana, K.; Itoi, T.; Hara, N.; Bilim, V.; Nishiyama, T.; Takahashi, K.; Tomita, Y. Absence of Bcl-2 and Fas/CD95/APO-1 predicts the response to immunotherapy in metastatic renal cell carcinoma. *Br J Cancer* **95:**1244-1249; 2006.

[324] Zhao, Y.; Shen, S.; Guo, J.; Chen, H.; Greenblatt, D. Y.; Kleeff, J.; Liao, Q.; Chen, G.; Friess, H.; Leung, P. S. Mitogen-activated protein kinases and chemoresistance in pancreatic cancer cells. *J Surg Res* **136:**325-335; 2006.

[325] Johnson, J.; Lagowski, J.; Sundberg, A.; Kulesz-Martin, M. P53 family activities in development and cancer: relationship to melanocyte and keratinocyte carcinogenesis. *J Invest Dermatol* **125:**857-864; 2005.

[326] Soulitzis, N.; Karyotis, I.; Delakas, D.; Spandidos, D. A. Expression analysis of peptide growth factors VEGF, FGF2, TGFB1, EGF and IGF1 in prostate cancer and benign prostatic hyperplasia. *Int J Oncol* **29:**305-314; 2006.

[327] Said, T. K.; Medina, D. Cell cyclins and cyclin-dependent kinase activities in mouse mammary tumor development. *Carcinogenesis* **16:**823-830; 1995.

[328] Yu, W.; Murray, N. R.; Weems, C.; Chen, L.; Guo, H.; Ethridge, R.; Ceci, J. D.; Evers, B. M.; Thompson, E. A.; Fields, A. P. Role of cyclooxygenase 2 in protein kinase C beta II-mediated colon carcinogenesis. *J Biol Chem* **278:**11167-11174; 2003.

[329] Calviello, G.; Di Nicuolo, F.; Gragnoli, S.; Piccioni, E.; Serini, S.; Maggiano, N.; Tringali, G.; Navarra, P.; Ranelletti, F. O.; Palozza, P. n-3 PUFAs reduce VEGF expression in human colon cancer cells modulating the COX-2/PGE2 induced ERK-1 and -2 and HIF-1alpha induction pathway. *Carcinogenesis* **25:**2303-2310; 2004.

[330] Koo, E. H. The beta-amyloid precursor protein (APP) and Alzheimer's disease: does the tail wag the dog? *Traffic* **3:**763-770; 2002.

[331]   Haas, S.; Pierl, C.; Harth, V.; Pesch, B.; Rabstein, S.; Bruning, T.; Ko, Y.; Hamann, U.; Justenhoven, C.; Brauch, H.; Fischer, H. P. Expression of xenobiotic and steroid hormone metabolizing enzymes in human breast carcinomas. *Int J Cancer* **119:**1785-1791; 2006.

[332]   Sissung, T. M.; Price, D. K.; Sparreboom, A.; Figg, W. D. Pharmacogenetics and regulation of human cytochrome P450 1B1: implications in hormone-mediated tumor metabolism and a novel target for therapeutic intervention. *Mol Cancer Res* **4:**135-150; 2006.

[333]   Dimmeler, S.; Fleming, I.; Fisslthaler, B.; Hermann, C.; Busse, R.; Zeiher, A. M. Activation of nitric oxide synthase in endothelial cells by Akt-dependent phosphorylation. *Nature* **399:**601-605; 1999.

[334]   Wever, R. M. F.; Luscher, T. F.; Cosentino, F.; Rabelink, T. J. Atherosclerosis and the Two Faces of Endothelial Nitric Oxide Synthase. *Circulation* **97:** 108-112; 1998.

[335]   Marks, D. S.; Vita, J. A.; Folts, J. D.; Keaney, J. F., Jr.; Welch, G. N.; Loscalzo, J. Inhibition of neointimal proliferation in rabbits after vascular injury by a single treatment with a protein adduct of nitric oxide. *J Clin Invest* **96:**2630-2638; 1995.

[336]   Davenpeck, K. L.; Gauthier, T. W.; Lefer, A. M. Inhibition of endothelial-derived nitric oxide promotes P-selectin expression and actions in the rat microcirculation. *Gastroenterology* **107:**1050-1058; 1994.

[337]   Stott, F. J.; Bates, S.; James, M. C.; McConnell, B. B.; Starborg, M.; Brookes, S.; Palmero, I.; Ryan, K.; Hara, E.; Vousden, K. H.; Peters, G. The alternative product from the human CDKN2A locus, p14(ARF), participates in a regulatory feedback loop with p53 and MDM2. *EMBO J* **17:**5001-5014; 1998.

[338]   Hollstein, M.; Sidransky, D.; Vogelstein, B.; Harris, C. C. p53 mutations in human cancers. *Science* **253:**49-53; 1991.

[339]   Brunner, T.; Mogil, R. J.; LaFace, D.; Yoo, N. J.; Mahboubi, A.; Echeverri, F.; Martin, S. J.; Force, W. R.; Lynch, D. H.; Ware, C. F.; et al. Cell-autonomous Fas (CD95)/Fas-ligand interaction mediates activation-induced apoptosis in T-cell hybridomas. *Nature* **373:**441-444; 1995.

[340]   Lyons, R. M.; Moses, H. L. Transforming growth factors and the regulation of cell proliferation. *Eur J Biochem* **187:**467-473; 1990.

[341] Harper, J. W.; Adami, G. R.; Wei, N.; Keyomarsi, K.; Elledge, S. J. The p21 Cdk-interacting protein Cip1 is a potent inhibitor of G1 cyclin-dependent kinases. *Cell* **75:**805-816; 1993.

[342] Kuan, C. Y.; Yang, D. D.; Samanta Roy, D. R.; Davis, R. J.; Rakic, P.; Flavell, R. A. The Jnk1 and Jnk2 protein kinases are required for regional specific apoptosis during early brain development. *Neuron* **22:**667-676; 1999.

[343] Ranger, A. M.; Zha, J.; Harada, H.; Datta, S. R.; Danial, N. N.; Gilmore, A. P.; Kutok, J. L.; Le Beau, M. M.; Greenberg, M. E.; Korsmeyer, S. J. Bad-deficient mice develop diffuse large B cell lymphoma. *Proc Natl Acad Sci U S A* **100:**9324-9329; 2003.

[344] Evan, G. I.; Wyllie, A. H.; Gilbert, C. S.; Littlewood, T. D.; Land, H.; Brooks, M.; Waters, C. M.; Penn, L. Z.; Hancock, D. C. Induction of apoptosis in fibroblasts by c-myc protein. *Cell* **69:**119-128; 1992.

[345] Oren, M.; Levine, A. J. Molecular cloning of a cDNA specific for the murine p53 cellular tumor antigen. *Proc Natl Acad Sci U S A* **80:**56-59; 1983.

[346] Meijerink, J. P.; Mensink, E. J.; Wang, K.; Sedlak, T. W.; Sloetjes, A. W.; de Witte, T.; Waksman, G.; Korsmeyer, S. J. Hematopoietic malignancies demonstrate loss-of-function mutations of BAX. *Blood* **91:**2991-2997; 1998.

[347] Hogarth, L. A.; Hall, A. G. Increased BAX expression is associated with an increased risk of relapse in childhood acute lymphocytic leukemia. *Blood* **93:**2671-2678; 1999.

[348] Monni, O.; Franssila, K.; Joensuu, H.; Knuutila, S. BCL2 overexpression in diffuse large B-cell lymphoma. *Leuk Lymphoma* **34:**45-52; 1999.

[349] Sturm, I.; Stephan, C.; Gillissen, B.; Siebert, R.; Janz, M.; Radetzki, S.; Jung, K.; Loening, S.; Dorken, B.; Daniel, P. T. Loss of the tissue-specific proapoptotic BH3-only protein Nbk/Bik is a unifying feature of renal cell carcinoma. *Cell Death Differ* **13:**619-627; 2006.

[350] Kim, J. W.; Choi, E. J.; Joe, C. O. Activation of death-inducing signaling complex (DISC) by pro-apoptotic C-terminal fragment of RIP. *Oncogene* **19:**4491-4499; 2000.

[351] Bullani, R. R.; Wehrli, P.; Viard-Leveugle, I.; Rimoldi, D.; Cerottini, J. C.; Saurat, J. H.; Tschopp, J.; French, L. E. Frequent downregulation of Fas (CD95) expression and function in melanoma. *Melanoma Res* **12:**263-270; 2002.

[352]   Reichmann, E. The biological role of the Fas/FasL system during tumor formation and progression. *Semin Cancer Biol* **12:**309-315; 2002.

[353]   Tamura, R. N.; Rozzo, C.; Starr, L.; Chambers, J.; Reichardt, L. F.; Cooper, H. M.; Quaranta, V. Epithelial integrin alpha 6 beta 4: complete primary structure of alpha 6 and variant forms of beta 4. *J Cell Biol* **111:**1593-1604; 1990.

[354]   Bernards, R. Transcriptional regulation. Flipping the Myc switch. *Curr Biol* **5:**859-861; 1995.

[355]   de Nigris, F.; Sica, V.; Herrmann, J.; Condorelli, G.; Chade, A. R.; Tajana, G.; Lerman, A.; Lerman, L. O.; Napoli, C. c-Myc oncoprotein: cell cycle-related events and new therapeutic challenges in cancer and cardiovascular diseases. *Cell Cycle* **2:**325-328; 2003.

[356]   Craven, P. A.; DeRubertis, F. R. Alterations in protein kinase C in 1,2-dimethylhydrazine induced colonic carcinogenesis. *Cancer Res* **52:**2216-2221; 1992.

[357]   Murray, N. R.; Baumgardner, G. P.; Burns, D. J.; Fields, A. P. Protein kinase C isotypes in human erythroleukemia (K562) cell proliferation and differentiation. Evidence that beta II protein kinase C is required for proliferation. *J Biol Chem* **268:**15847-15853; 1993.

[358]   Algeciras-Schimnich, A.; Pietras, E. M.; Barnhart, B. C.; Legembre, P.; Vijayan, S.; Holbeck, S. L.; Peter, M. E. Two CD95 tumor classes with different sensitivities to antitumor drugs. *Proc Natl Acad Sci U S A* **100:**11445-11450; 2003.

[359]   Engle, M. R.; Singh, S. P.; Czernik, P. J.; Gaddy, D.; Montague, D. C.; Ceci, J. D.; Yang, Y.; Awasthi, S.; Awasthi, Y. C.; Zimniak, P. Physiological role of mGSTA4-4, a glutathione S-transferase metabolizing 4-hydroxynonenal: generation and analysis of mGsta4 null mouse. *Toxicol Appl Pharmacol* **194:**296-308; 2004.

[360]   Dempsey, P. W.; Doyle, S. E.; He, J. Q.; Cheng, G. The signaling adaptors and pathways activated by TNF superfamily. *Cytokine & Growth Factor Rev* **14:**193-209; 2003.

[361]   Koh, D. W.; Dawson, T. M.; Dawson, V. L. Mediation of cell death by poly(ADP-ribose) polymerase-1. *Pharmacol Res* **52:**5-14; 2005.

VITA

Brad Allen Patrick, the son of Andrew Patrick, M.D. and Sandra Patrick, R.N., was born in Metairie, Louisiana on May 9, 1979. He graduated from high school in 1997 and received his Bachelor of Science degree in the field of biochemistry with a minor in philosophy from Louisiana State University in Baton Rouge in May 2002 while receiving the full Tuition Opportunity Scholarship. Brad joined the Graduate School of Biomedical Sciences at the University of Texas Medical Branch in August 2002 and the Pharmacology and Toxicology graduate program in 2003. He acquired teaching experience as an instructor of the Texas A&M University at Galveston Survey of Toxicology course for three years and as mentor to an undergraduate student in the Summer Undergraduate Research Program. His mentor is professor Yogesh C. Awasthi. He is a member of the Society for Free Radical Biology and Medicine and the Association for Research in Vision and Ophthalmology. He has been named as an author of 7 published research articles including 1 first-author paper, and 6 meeting abstracts in Dr. Awasthi's laboratory, with one Young Investigator Award from the Society for Free Radical Biology and Medicine. Brad gained expertise in molecular toxicology as a trainee on a National Institute of Environmental Health Sciences Toxicology Training Grant.

Permanent Address:

4017 Deerfield Lane
Baton Rouge, LA 70816

This dissertation was typed by Brad A. Patrick.

Publications

A. Articles in peer-reviewed journals:

[1] Dwivedi, S.; Sharma, A.; **Patrick, B.;** Sharma, R.; Awasthi, Y. C. Role of HNE and its metabolites in signaling. *Redox Rep*. **12:**4-10; 2007.

[2] Li, J.; Sharma, R.; **Patrick**, **B.;** Sharma, A.; Jeyabal, P. V. S.; Reddy, P. M. R. V.; Saini, M. K.; Dhanani, S.; Zimniak, P.; Awasthi, S.; Awasthi, Y. C. Regulation of CD95 (Fas) expression and Fas-mediated apoptotic signaling in HLE B-3 cells by 4-hydroxynonenal. *Biochemistry*. **45:**12253-12264; 2006.

[3] Sharma, A.; **Patrick**, **B.;** Li, J.; Sharma, R.; Jeyabal, P. V. S.; Reddy, P. M. R. V.; Awasthi, S.; Awasthi, Y. C. Glutathione S-transferases as antioxidant enzymes: Small cell lung cancer (H69) cells transfected with hGSTA1 resist doxorubicin-induced apoptosis. *Arch. Biochem. Biophys*. **452:**165-173; 2006.

[4] **Patrick**, **B.;** Li, J.; Jeyabal, P. V.; Reddy, P. M.; Yang, Y.; Sharma, R.; Sinha, M.; Luxon, B.; Zimniak, P.; Awasthi, S.; Awasthi, Y. C. Depletion of 4-hydroxynonenal in hGSTA4-transfected HLE B-3 cells results in profound changes in gene expression. *Biochem Biophys Res Commun*. **334:**425-432; 2005.

[5] Awasthi, Y. C.; Yang, Y.; Tiwari, N. K.; **Patrick**, **B.;** Sharma, A.; Li, J.; Awasthi, S. Regulation of 4-hydroxynonenal mediated signaling by Glutathione S-transferases. *Free Rad. Biol. Med.* **37:**607-619; 2004.

[6] Sharma, R.; Brown, D.; Awasthi, S.; Yang, Y.; Sharma, A.; **Patrick**, **B.;** Saini, M. K.; Singh, S. P.; Zimniak, P.; Awasthi, Y. C. Transfection with 4-hydroxynonenal-metabolizing glutathione S-transferase isozymes leads to phenotypic transformation and immortalization of adherent cells. *Euro. J. Biochem.* **271:**1690-1701; 2004.

[7] Yang, Y.; Sharma, A.; Sharma, R.; **Patrick**, **B.;** Singhal, S. S.; Zimniak, P.; Awasthi, S.; Awasthi, Y. C. Cells Preconditioned with Mild, Transient UVA Irradiation Acquire Resistance to Oxidative Stress and UVA-induced Apoptosis: ROLE OF 4-HYDROXYNONENAL IN UVA-MEDIATED SIGNALING FOR APOPTOSIS. *J. Biol. Chem.* **278:**41380-41388; 2003.

B. Abstracts:

[1] Awasthi, Y.C.; Sharma, R.; Li, J.; **Patrick, B.**; Dwivedi, S.; Sharma, A. Regulation of the expression and functions of Fas (CD95) by 4-hydroxynonenal in human lens

epithelial (HLE B-3) cells. *Annual Meeting of Association for Research in Vision and Ophthalmology.* May 2007, Fort Lauderdale, FL.

[2] **Patrick**, **B.;** Sharma, R.; Li, J.; Sharma, A.; Dwivedi, S.; Zimniak, P.; Awasthi, S.; Awasthi, Y. C. Regulation of Fas (CD95) expression and Fas-mediated apoptotic signaling in HLE B-3 cells by 4-hydroxynonenal. *Society for Free Radical Biology and Medicine Annual Meeting*. November 2006, Denver, CO.

[3] Matthews, N.; **Patrick**, **B.;** Dwivedi, S.; Sharma, A.; Sharma, R.; Awasthi, Y. C. Human Glutathione S-transferase depletes 4-hydroxynonenal and modifies gene expression in eye epithelial cells. *UTMB Summer Undergraduate Research Program Presentation*. August 2006, Galveston, TX.

[4] **Patrick**, **B.;** Li, J.; Jeyabal, P. V. S.; Sharma, A.; Saini, M. K.; Awasthi, Y. C. Lowering of constitutive 4-hydroxynonenal levels in human lens epithelial cells leads to profound changes in gene expression. *Annual Meeting of Association for Research in Vision and Ophthalmology.* April 2005, Fort Lauderdale, FL.

[5] Li, J.; Jeyabal, P. V. S.; **Patrick**, **B.;** Sharma, R.; Yang, Y.; Sharma, A.; Saini, M. K.; Awasthi, Y. C. Analysis of gene expression in transformation and immortalization of adherent cells transfected with hGSTA4 using cDNA microarray. *ASBMB Annual Meeting.* April 2005, San Diego, CA.

[6] Awasthi, Y. C.; Sharma, R.; Brown, D.; Yang, Y.; Sharma, A.; **Patrick**, **B.;** Saini, M. K.; Singh, S. P.; Zimniak, P.; Singh, S. V.; Awasthi, S. Alteration in 4-hydroxynonenal homeostasis profoundly affects cell cycle signaling events. *2nd Meeting of the HNE Club.* July 2004, Berlin, Germany.

[7] Awasthi, Y. C.; Brown, D.; Sharma, R.; Yang, Y.; Sharma, A.; Tewari, N. K.; Saini, M. K.; **Patrick, B.** Alteration in 4-Hydroxynonenal Homeostasis in Human Lens Epithelial cell (HLE B-3) leads to their Phenotypic Transformation. *Annual Meeting of Association for Research in Vision and Ophthalmology.* May 2004, Fort Lauderdale, FL.